School of Science
Department of Mathematics and Statistics

A Study on the Behaviour of Microscopic Car-Following Models in Urban Settings

Sarah Peursum

This thesis is presented for the Degree of
Doctor of Philosophy
of
Curtin University

May 2015

Declaration

To the best of my knowledge and belief this thesis contains no material previously published by any other person except where due acknowledgement has been made.

This thesis contains no material which has been accepted for the award of any other degree or diploma in any university.

The research presented and reported in this thesis was conducted in accordance with the National Health and Medical Research Council National Statement on Ethical Conduct in Human Research (2007) updated March 2014. The proposed research study received human research ethics approval from the Curtin University Human Research Ethics Committee (EC00262), Approval Number SMEC-52-10.

Sarah Peursum

6 May 2015

Date

Contents

List of Figures

List of Tables

Acknowledgement

Wow, what an experience this has been! When I began this journey, I was not to know the trials and tribulations that I would have to face and overcome, nor how deep I would have to dig to find the fortitude to keep on travelling and in the right direction. I am glad I undertook this task, it has made me become an all-round better person, and for that I am grateful.

I would particularly like to thank my supervisors, Professor Yong Hong Wu and Associate Professor Volker Rehbock, for having the faith in me to take me on in the beginning, for showing admirable patience when dealing with my independence and stubborn streak, and for allowing me the freedom to explore the unknown. The support I got has been invaluable to me, and I appreciate this enormously.

I must also thank all the countless other PhD students whose theses I read, not only to contribute information for this thesis, but also for me to get an understanding of how to craft my own.

Finally, special thanks to the Australian Postgraduate Award (APA) for providing me with a scholarship without which I could not have continued to study.

Abstract

The study of traffic flow is concerned with the prevention of congestion, the maintenance of traffic stability, and the use of mathematical models to simulate real-world vehicular movement. One of the issues with imitating realistic traffic flow is that drivers are human and their complex behaviour is difficult to model accurately and efficiently. Thus many models have been developed to simulate traffic flow at different levels of detail, ranging from tracking each individual vehicle ('microscopic') to aggregating vehicles into one fluid-like entity ('macroscopic'), and in between where aspects of both are utilised ('mesoscopic').

This thesis focuses on microscopic driver models, which model traffic at the level of the individual driver. The objective is to investigate how well such models represent real traffic flow, and more specifically, the work aims to examine the detailed driver model behaviour as compared to human drivers, and to investigate the issues that arise when mixing different types of driver models to trade off accuracy with efficiency. The focus is on urban (stop-and-go) traffic flow rather than the more well-studied freeway flow. The driver models themselves do not take into account road network structures such as intersections or merge points, therefore a simulation has been designed in such a way that it can support analysis in such circumstances.

A detailed empirical analysis of everyday urban traffic scenarios is then carried out by using four common space-continuous microscopic models (as opposed to space-discrete microscopic models), both in comparison to each other and against the behaviour of human drivers in the same circumstances. The performances of these driver models are compared and situations are identified where the models respond unreasonably. The Intelligent Driver Model (IDM) comes out as the best performing model in these experiments, however, it was subsequently identified that the IDM is an unstable model when vehicles travel at the speed limit in a platoon. A variant of the IDM, called the speed-limit-stable IDM (SLS-IDM), is proposed and implemented which allows vehicles to travel at the speed limit whilst maintaining stable traffic flow.

The behaviour of a mix of different types of microscopic model within the same road

network was analysed. Most networks that have been studied are homogeneous in nature, that is, they simulate only one type of driver model. In practice, hybrids consisting of different types of macroscopic / microscopic models have been used to compromise between accuracy and efficiency in different sections of the network. This thesis extends the concept by implementing a continuous microscopic / discrete microscopic heterogeneous network using the SLS-IDM for the continuous sectors of the network and the simple but effective Nagel-Schreckenberg algorithm for the discrete segments of the network. Since both driver models are inherently stable, any instability in the system is due to the change-over in model, and it is found that a characteristic traffic density fluctuation occurs at this transition point. This distinctive density anomaly can be used to identify the switching of models from one to the other and is different from instability in traffic flow related to congestion.

Chapter 1

Introduction

1.1 Background and Motivation

Over the last 60 years there has been a marked increase in the number of vehicles on our roads. This has led to a corresponding increase in traffic congestion which is an undesirable condition that has an accumulative effect. As a consequence, the modelling of traffic flow has become an important analytical and decision-making tool to assist with alleviating the congestion often found on today's road networks. To effectively evaluate and make useful determinations, various mathematical models have been developed since the 1950's that aim to simulate the flow of traffic.

From a physical perspective, traffic flow can be broadly categorised into two groups: *free-way* flow and *stop-and-go* flow. The former type of flow typically includes progressive acceleration / deceleration and merging actions whilst the latter flow incorporates traffic control mechanisms such as intersections, where vehicles must react to by accelerating or decelerating relatively quickly.

From the standpoint of a mathematical model that seeks to represent vehicle behaviour, traffic flow can be evaluated at different levels of detail. At one end of the spectrum there are *macroscopic* models which view traffic flow as a homogeneous, fluid-like mass, where distinct vehicles are not taken into account. On the other end of this spectrum are *microscopic* models, which consider and track individual vehicles via equations to describe the actions of the driver. *Mesoscopic* models are those that exist between these two extremes, but have seen relatively little development since they tend to either aggregate microscopic information or perform fine-grained macroscopic-like approaches, and thus have similar strengths and weaknesses.

Traffic flow is inherently comprised of discrete elements (vehicles) that move by means

of physical configurations (roads and intersections) according to specified road rules, and due to the element of human decision-making, the movement does not always occur in the prescribed manner. Since macroscopic models simplify traffic flow behaviour with its aggregation of individual components, it is not analogous to the precise actions of distinct vehicles, and is thus commonly applied to freeway flow conditions where the assumption of fluid-like behaviour is more plausible. Conversely, microscopic driver models directly capture the behaviour of individual vehicles and so are equally applicable to both freeway and urban traffic, but tend to be more computationally expensive when many vehicles are being modelled. Additionally, microscopic models can provide more flexibility of choice as they can be further subdivided into *continuous* and *discrete* with respect to vehicle movement on a network.

Most research has focused on freeway flow analysis, and empirical studies involving both macroscopic and microscopic models have been applied to this situation. Urban stop-and-go flow investigation has seen less attention, and has largely been conducted using microscopic models. In both cases, research is mainly concentrated on the prevention of congestion and the detection of density fluctuations (Hoogendoorn and Bovy, 2001) which can indicate traffic flow instabilities caused by such features as poorly placed merge points or a series of intersections. However, although traffic flow arises from the behaviour of individual vehicles, very little work has been done on analysing the ability of mathematical models to accurately represent the detailed interactions between individual vehicles and its effect on measured density, especially within urban networks around intersections where vehicle movement is complex.

In addition, the road networks that provide the framework for the driver models to run simulations typically only show one granularity of detail, that is, they are either implemented using microscopic, macroscopic or mesoscopic principles. There has been some research into the viability of multi-scale microscopic / macroscopic hybrids (or heterogeneous networks) with emphasis on the benefits of utilising different models in different sections of road that they are most suited to (Burghout *et al.*, 2005; Newell, 2011). Previous work has shown that the main complication arises at the transition boundary between the two model types, and effort has focused on reducing the undesirable effects of the transition. However, this has not translated into a similar examination of microscopic / microscopic hybrid networks that mix continuous and discrete microscopic models which have their own relative merits.

This thesis investigates the performance of some widely-used continuous microscopic driver models in everyday traffic scenarios in an urban environment, and specifically examines the interaction of individual vehicles as they transit through intersections. Modifications to the most effective continuous microscopic model — the Intelligent Driver Model (Treiber *et al.*, 2000b) — are then proposed to resolve an issue not previously identified in the model which causes traffic flow to become unstable when vehicles travel at or near the speed limit. Finally, a heterogeneous network comprised of the best performing continuous microscopic model and a commonly used discrete microscopic model is constructed to capture the relative merits of each model type and to analyse the transition boundary where the models switch over to detect any instability in traffic flow. From this density changes in traffic flow at the transition boundary are examined to identify a characteristic fluctuation pattern in density, and methods for minimising this 'signature' of model switch-over are investigated.

1.2 Research Issues and Objectives

A relatively wide variety of continuous, and to a lesser extent discrete, microscopic models have been developed and refined over the last 60 years. The analysis of these microscopic models in stop-and-go traffic flow has mainly been dedicated to detecting traffic density fluctuations, examining traffic stability and determining when and how congestion occurs to enable possible prevention measures to be put in place (Ahn and Vadlamani, 2010; Pueboobpaphan and van Arem, 2010; Treiber and Kesting, 2012). As such, no significant empirical analysis has been carried out to study the detailed interactions between specific vehicles in stop-and-go traffic flow, particularly around intersections where traffic relations are complex.

This more detailed examination of a model, where well-defined scenarios can be specified and executed, will allow for a detailed view of where models may perform poorly in common traffic situations. Any subsequent documented deficiencies in a model can be used to make improvements to that model, which is a critical issue since the overall traffic flow, that is the focus of most analysis, arises from individual vehicle behaviours, and models which do not adequately represent real driver reactions cannot be anticipated to produce realistic traffic flow either.

Model analysis and testing typically focus on examining one particular model, thus road networks that support this analysis are built to accommodate only the one specific model. There are, however, a number of examples (Helbing *et al.*, 2002; Burghout *et al.*, 2005; Newell, 2011) where a hybrid of a microscopic and a macroscopic model are used, with the transition boundary where the two models meet being of particular importance. On the other hand, a hybrid comprised of a continuous microscopic model and a discrete microscopic model has not been methodically explored, including the testing of transition boundaries. Therefore this thesis constructs and analyses a heterogeneous model consisting of two different types of microscopic models.

Thus the specific objectives of this thesis are as follows.

Aim 1 To carry out an empirical analysis of several widely-used microscopic continuous car-following models and compare this against the behaviour of human drivers for the purposes of identifying scenarios that commonly occur in urban traffic flow where these models react poorly.

Aim 2 To select the continuous car-following model that performed most effectively in the investigation of Aim 1 and examine its mathematical properties such as stability, particularly with respect to situations that have not been covered by the original proposing authors or in any subsequent analyses.

Aim 3 To build a heterogeneous network that utilises a mix of the continuous microscopic model from Aim 1 and a well-known discrete microscopic model, analyse the behaviour of traffic flow at the transition boundaries to determine whether the density changes at this point are uniquely identifiable, and investigate methods to minimise the adverse effects of the transition on density.

To facilitate the objectives of this thesis, an urban road network is constructed which supports and simulates the continuous and discrete microscopic models investigated. The system is extended to incorporate a heterogeneous network that is comprised of a continuous microscopic model/discrete microscopic model hybrid.

The network consists of links (roads) and nodes (intersections), with the latter including

give-way rules. Short-term route planning effectively manages traffic flow through the intersections and provides feedback from vehicles and their movements.

1.3 Contributions and Significance

This thesis makes three main contributions to the field of traffic flow:

- A detailed empirical analysis of several popular continuous microscopic car-following models, with emphasis on analysing the specific behaviour of the models compared to a human driver, and identifying scenarios that – whilst common in urban traffic – produce unusual input parameters to the models that can cause unreasonable responses. This is important in identifying situations where the models are unrepresentative of real human drivers, since this would adversely impact the validity of any traffic flow and congestion results that arise from these models.

- The identification of a significant flaw in the formulation of the Intelligent Driver Model (IDM) (Treiber *et al.*, 2000b) which causes the model to fail to achieve the desired velocity (speed limit) except when headway approaches infinity. This thesis proposes a principled modification to the IDM, dubbed the 'speed-limit-stable IDM' (SLS-IDM) that resolves this flaw without causing any side-effects in the behaviour of the IDM.

- The construction and analysis of a heterogeneous network that mixes two distinct types of microscopic models within the same network. This is in contrast to existing heterogeneous networks which have focused on mixing microscopic with macroscopic models (multi-scale). Whilst such multi-scale models are clearly useful, there is also a benefit to mixing different types of microscopic models, and we specifically mix the high-precision continuous car-following IDM (Treiber *et al.*, 2000b) with the fast integer-based discrete cellular automata Nagel-Schreckenberg algorithm (Nagel and Schreckenberg, 1992). Another contribution is the detection of a distinct density fluctuation configuration at the boundary point of the two models where they switch over, which can be used in heterogeneous networks as an indicator of a change in models rather than a density variation of the model itself, and can thus be disregarded for the purposes of density analysis of the network's models.

1.3.1 Detailed Microscopic Car-Following Model Comparison

The first contribution to this thesis is the identification of areas in four commonly used continuous microscopic driver models where these models behave unrealistically when compared against the actions of real human drivers in an urban environment. Typical everyday traffic flow scenarios are constructed to pinpoint the shortcomings of each model, and their performance is compared to the expected responses of a human driver. Two sets of experiments are conducted, with the first focusing on the interaction between two vehicles in an urban situation (including intersections). This allows for testing the short-term reactions of each driver model independently and in isolation from any other activity. The second series of experiments take GPS data from real-world human drivers and compares this against each model in the exact same scenario. For the latter set of tests the vehicles interact with a controlled intersection where either the traffic light turns from red to green or green to red, thus the vehicle accelerates from standstill or comes to a stop.

The models selected for testing consist of the Optimal Velocity Model (OVM), the Full Velocity Difference Model (FVDM), the Full Velocity and Acceleration Difference Model (FVADM), and the Intelligent Driver Model (IDM). The OVM is the simplest model and is primarily used as a baseline that all the other models would be expected to outperform. It takes the current vehicle's position and velocity into account. Whilst the FVDM has the same foundation as the OVM, it adds in a velocity difference term between the following (current) vehicle and the leading (ahead) vehicle, a factor that is fairly standard in most models. The FVADM extends the FVDM by appending an acceleration difference term to determine whether the disparity in acceleration for the leading and following vehicles can improve accurately mimicking driver behaviour. The last model is the IDM, which is based on different premises to the other three included models, and attempts to balance acceleration versus braking tendencies by using velocity and headway ratios.

Models are analysed by selecting parameter inputs that stress-test the models and their behaviour, and though in their parameterisation they are seemingly unusual, they can be readily linked to very typical urban situations. Comparisons between the models and real-world drivers of acceleration and deceleration profiles over time around controlled intersections are used to clearly demonstrate the difference between how each of the models behaves as against a human. To our knowledge, these types of conditions have not been methodically studied and documented. Examining the detailed behaviour of the driver

models is important since if a driver model causes vehicles to behave unrealistically at times and thus is not representative of individual vehicle behaviour, it becomes questionable as to whether the aggregate traffic behaviour based on such a model can safely be assumed to be representative of the real traffic flow, and thus whether conclusions drawn from simulations using the model are applicable to real traffic.

The investigation shows that the IDM generally performs more realistically than the other models, although it is slightly conservative in its decision making at times — it is overall cautious about accelerating and yet postpones braking somewhat versus what would be expected of a real driver. There is one scenario, however, where the IDM accelerates slightly when it arguably should instead brake. The acceleration difference incorporated in the FVADM facilitates accuracy in some situations but hinders in others, and both this model and the FVDM produce a very peculiar braking profile where there is a constant alternation of braking-coasting-braking action. Finally, the OVM is the poorest performer overall, however it did surprisingly surpass the other more sophisticated models in one scenario where moderate acceleration was anticipated.

1.3.2 An Improved Intelligent Driver Model

Having performed most effectively in comparison to the other three models, further investigation of the IDM was carried out and highlighted a significant anomaly — at or near the speed limit in an open system where some vehicles have no lead vehicles ahead of them, the IDM produces instabilities in headway. Specifically, without the encumbrance of external factors (*eg:* traffic lights, congestion, or other obstacles) the IDM will stretch out the headway between vehicles towards infinity. This is an issue since it introduces a subtle type of instability given that the vehicle will never reach infinite headway, and consequently the IDM will never reach a stable velocity. Stable (equilibrium) traffic states for the IDM are discussed by Treiber *et al.* (2000a) but only for conditions when the velocity of the vehicles were significantly lower than the speed limit. The stability behaviour of the IDM when the velocity is near the speed limit was not touched on, and thus it has until now gone unrecognised that the IDM is unstable near the speed limit.

Examination of the IDM shows that the speed limit constant is in fact an absolute upper bound upon vehicle velocity, which is only reachable when headway grows towards infinity. Treiber *et al.* (2000a) in fact terms this constant the 'desired velocity' and makes no

mention of its specific meaning. Thus this thesis proposes to resolve the IDM's instability at the speed limit by splitting the speed limit and the upper bound, and redefining the upper bound in terms of a *desired headway gap* — the well-known 'two-second rule' gap between vehicles. This is dubbed the speed limit stable IDM (SLS-IDM) and ensures that the IDM is able to maintain an equilibrium velocity at the speed limit with the equilibrium headway gap converging to the desired 'two-second' gap, thereby achieving a stable model. Since the SLS-IDM only affects the definition of the upper bound velocity, a constant in the original IDM, the behaviour of the IDM below the speed limit remains unchanged and the analysis of stability by Treiber *et al.* (2000a) continues to hold.

1.3.3 Micro/Micro Heterogeneous Networks

Multi-scale macroscopic/microscopic hybrid networks have become relatively common over the last 15 years (Helbing *et al.*, 2002; Burghout *et al.*, 2005; Newell, 2011). During this time, however, there has been a paucity of continuous microscopic / discrete microscopic hybrid networks even though there are benefits in combining these models to take advantage of their strengths in different parts of a network, for example, continuous models provide precision whilst discrete ones offer computational speed.

As with their multi-scale counterparts, special attention must be paid to the boundary transitions between the two models since this is where anomalies in the density produced by the model switch-over arise, thus creating instability in the system. These variances are related to the different behaviours of each model and are not a reflection of any instability in either model.

Stability entails unchanging traffic density when all other factors are held constant and this requires constant spacing between vehicles, which implies constant headway and constant velocity between vehicles. A simple circuit road network was meticulously constructed to encompass the above constraint so as to ensure that density is perfectly uniform with no variation in density due to vehicle placement or velocity. This then allows for the ability to detect any deviations of density and unequivocally associate them as effects of the boundary transition. Analysis of this system provides a 'signature' traffic density fluctuation at the boundary transition where the models switch from continuous to discrete, showing a prominent spike-or-dip marker immediately succeeding each boundary point in what is otherwise the expected uniform density. Investigation reveals that the density anomalies

are generated due to rounding issues from the transition to a discrete model.

It is also shown that this characteristic density spike-or-dip anomaly also clearly occurs in even realistic networks where density is not strictly uniform due to rounding issues. To try and minimise the density irregularities, different cells sizes and rounding (up or down) are experimented with at the boundary transition point. Small cell sizes and nearest-rounding minimises the problem, but these will still produce a spike-or-dip signature due to rounding issues. Fortunately, the position of the density anomaly is predictably located immediately succeeding the boundary point, hence it could be possible to use this information to avoid including the anomaly in higher-order traffic flow or congestion analysis.

1.4 Structure of this Thesis

This thesis is organised as follows. In Chapter 2 a review of the related work in the area of traffic flow stability is presented, followed by synopsis of macroscopic models including some widely-used examples. Then various types of microscopic models are discussed in detail, with examples provided and the relative merits of each examined. Then a brief outline of mesoscopic models is given together with discussion on where they fit in with respect to macroscopic and microscopic models. The advantages and disadvantages of using a macroscopic model versus a microscopic model and versus a mesoscopic perspective, when analysing traffic situations, are discussed. Then multi-scale (hybrid) networks are reviewed, including macro-simulation packages.

Chapter 3 describes the road network environment used for simulating traffic flow for the different models in experiments. The network is constructed using nodes to mimic intersections and links to mimic roads, and these can be interchanged to build different network configurations as desired. Intersections include throughways (no change in direction of traffic flow), t-junctions (give a choice of two directions to take) and fourways (provide the option of three directions to take). The roads include continuous microscopic and discrete microscopic implementations to allow for a heterogeneous network to be developed. A short-term route planning strategy is incorporated to enable vehicles to transit through intersections without causing collisions with other vehicles, since this is not taken into account by the driver models themselves. The simulation is run on a predict-update cycle to keep track of all vehicle positions and to detect collisions.

Chapter 4 presents the empirical behaviour of four continuous microscopic models, namely the OVM, FVDM, FVADM and IDM, in common urban scenarios. Two sets of experiments are conducted, both of which compare the models against the behaviour of a human driver. The first investigation looks at the behaviour of the models in urban situations where two vehicles interact whilst the second one compares the driver models to real human driver data captured by GPS. Traffic situations where the driver models have unreasonable responses are identified.

The contributions of Chapter 5 are threefold: First, it is shown that the IDM is in fact unstable when vehicles travel at or near the nominal speed limit v_0, and introduce a variant of the IDM that resolves the instability without altering its stable behaviour at lower speeds. This is done by re-interpreting v_0 as an upper bound on velocity and shifting the focus to appropriately setting v_0 as a function of the '2-second-rule' headway gap and the true speed limit. The resultant speed-limit-stable IDM (SLSIDM) allows vehicles to converge to the speed limit in a stable manner. Second, although the SLS-IDM and N-S models are both stable on their own, when they are mixed within the same road network, instabilities are generated at the boundary of their transition points due to rounding issues. However, the choice of rounding (up or down) produces different effects and we conclude that rounding up is the better alternative. Finally, we show that these model-caused instabilities produce a characteristic 'fingerprint' effect on measures of density and headway, and find that this fingerprint remains identifiable even in more realistic networks. Stability in the heterogeneous network is investigated by constructing a simple 'circuit' network with alternating continuous and discrete road links. Detailed analysis of the heterogeneous link behaviour shows that stability can be correlated with density in such a circuit. The parameters that affect stability in the heterogeneous system are identified and experiments are run to analyse the effect of varying these parameters. It is shown that mixing continuous microscopic and discrete microscopic models in a network creates instabilities at the model transition points unless very strict conditions can be satisfied. Fortunately, it is also shown that the system re-stabilises itself quickly due to the inherent stability of the underlying vehicle models, hence the instability caused by the junctions is not likely to propagate significantly except in the sections of a network containing clusters of short heterogeneous links.

Chapter 2

Literature Review

Traffic is a commonplace phenomenon in our society today, an activity most of us participate in on a daily basis. Traffic movement can not only be experienced but also be mathematically represented by its constituent components to get a better understanding of its dynamics. The basic underlying elements that have been defined in traffic are velocity, density and flow rate, with some adjunct factors including position, instant in time and headway. Flow is described as being the number of vehicles passing a specified point over a unit of time and can be calculated by the equation shown in Equation (2.1). Another way to specify flow is by its inverse of headway (see Section 2.4). Density represents the number of vehicles per unit length of roadway, and velocity is denoted as the distance covered in unit time, usually written in terms of m/s or km/h.

$$flow = density \times velocity \tag{2.1}$$

The modelling of traffic is an active area of research and includes the simulation of traffic to assist in road policy decision-making (intersection placement, analysing merging issues, preventing congestion, determining traffic densities on roads, etc) (Papageorgiou *et al.*, 2003; Treiber and Kesting, 2012).

Traffic flow models are used to describe, understand and predict the behaviour of traffic flow. The common element in the study of traffic flow is a relationship between the different constituents that make up this flow, depending on the level of detail that is being modelled. This relation was coined the 'fundamental relation' by Greenshields (1934) and was originally depicted as being between headway (*ie:* the distance between the front of a particular vehicle and the front of the vehicle behind it, see Figure 2.1) and vehicle velocity. However, it can also be characterised using density (average number of vehicles per length of road) and flow (average number of vehicles per unit of time) (van Wageningen-Kessels *et al.*, 2014). These variables can then be used in different combinations to create

fundamental diagrams, in essence showing a 2D 'slice' of the relationship between the two chosen variables *eg:* it is possible to examine the density-flow plane, density-velocity plane, flow-velocity plane, headway-velocity plane, etc. These graphs will all have different shapes and serve different purposes for different investigations (van Wageningen-Kessels *et al.*, 2014). del Castillo (2012) proposed some properties and guidelines to produce a reliable fundamental relation, and work has been continued to this day (Helbing, 2009; Treiber *et al.*, 2010; Gayah and Daganzo, 2011; Geroliminis and Sun, 2011; Keyvan-Ekbatani *et al.*, 2012; Knoop *et al.*, 2012; Kerner, 2013).

The interaction of headway versus vehicle velocity or density versus flow over time can be described in different levels of detail, ranging from a very fine-grained level of detail where individual vehicles are considered, through to a coarse level of detail where vehicles are considered collectively as one moving mass, with a mixture of the two in between (Bellemans *et al.*, 2002). Microscopic, macroscopic and mesoscopic models have been developed from these levels of perspective respectively, and it is presumed that all traffic flow models are in some type of state described by the elements that encompass the fundamental relation, or are tending towards it (van Wageningen-Kessels *et al.*, 2014).

Macroscopic models are based on the physical properties of fluid dynamics (Hoogendoorn and Bovy, 2001) and therefore represent traffic dynamics as the flow of a whole entity rather than its discrete constituents, hence giving the lowest level of detail. In contrast, microscopic models track the movement and behaviour of individual vehicles within the traffic flow and thus provide the highest level of detail. Mesoscopic models exist between these two extreme perspectives of granularity, giving a medium level of detail.

Macroscopic models do not consider individual vehicles in their calculations, rather they describe the aggregate behaviour of traffic flow characteristics, and as such use various analogies to illustrate traffic flow, *eg:* fluid flow, heat flow and gas flow. Since they are assumed to correspond to physical flows which have actual measured physical properties and laws governing their behaviour, it is assumed that these laws can also be applied to traffic. Specifically, the Law of Conservation pertaining to vehicles (see Section 2.2) is used to obtain a limited number of equations that are complex enough to adequately describe traffic flow. The resultant differential equations are typically used to model these types of movements, and traffic flow characteristics such as velocity, density and flow are employed in their calculations.

Microscopic models on the other hand derive their data from taking into account individual vehicles, and thus all vehicles in the system are tracked. A car-following strategy is used to calculate the position and velocity of each vehicle, so that each vehicle also references the vehicle in front of it. If there is no other vehicle in front of the current vehicle or if that vehicle is far away enough so as not to affect the current vehicle, then vehicles are propagated at default parameters *ie:* travel at the speed limit with constant velocity. These types of models are broadly categorised into two different types: *continuous* and *discrete*.

Mesoscopic models fall between these two extremes by modelling vehicles en masse (macroscopic) using individual vehicle behaviours (microscopic), and are often statistical in nature. For instance, a cluster of vehicles will be treated as a distinct entity from other clusters of vehicles, so in essence the groups are viewed as two independent 'vehicles'. Some of the models are based on gas-kinetic theory whilst others are derived via clustering or headway properties.

These mathematical models can be used for different types of simulations such as modelling human driver behaviour (Treiber *et al.*, 2006), predictive control (Hegyi *et al.*, 2005; Bellemans *et al.*, 2006), adaptive cruise control (Marsden *et al.*, 2001; van Arem *et al.*, 2006; Kesting *et al.*, 2008), agent-based modelling (Horni *et al.*, 2009), handling emergency situations (Hoogendoorn *et al.*, 2013).

In the physical world traffic flow can be either free flow or stop-and-go flow or a combination of the two depending on the environment being simulated (*ie:* freeway or urban driving respectively). The question is, which model fits which type of flow best? And if there is a mixture of the two, which combination of models can give optimal results? These questions have not been definitively answered in the literature, although more recent research has included the use of either type of model for both types of traffic flows (Knospe *et al.*, 2000; van den Berg *et al.*, 2003, 2004; Daganzo, 2007; Flötteröd and Rohde, 2011). These questions will be investigated in this thesis. The rest of this chapter will review topics highly relevant to this research, including stability of traffic flows, various important classes of traffic flow models, simulation packages, as well as empirical analysis of driver models. Some critical comments and discussion will also be presented.

2.1 Stability in Traffic Flow

A central theme for traffic models is *stability*. Stability in a traffic flow network means that there are no unaccountable fluctuations, and any changes in flow do not unreasonably magnify downstream, thereby reflecting real-world driver behaviour. The concept of stability is a major objective of driver models for traffic simulations. A traffic-flow system in a state of equilibrium is deemed to be stable if, after a perturbation, the system returns to an equilibrium state (Pueboobpaphan and van Arem, 2010). Three distinct types of stability have been defined for traffic flow — *local* stability, *platoon* (or string) stability and *overall* (traffic-flow) stability (Holland, 1998).

Local stability is related to the spacing (headway) between successive vehicles. This spacing can become irregular (for example, due to vehicles braking for a traffic light), causing disturbances in traffic flow. If this occurs, a stable system will decrease the magnitude of the perturbance over time, otherwise the system is unstable. Platoon stability is concerned with the spreading of a disturbance from one vehicle to other vehicles within a cluster of vehicles. Platoon stability is achieved if the magnitude of the propagation of the perturbance reduces downstream and the platoon once again stabilises. If the size of this disturbance increases as it propagates downstream through the platoon, then the system is said to be unstable (Pueboobpaphan and van Arem, 2010). Finally the notion of overall (traffic flow) stability is poorly defined, as it encompasses all aspects of stability in a network (of which local and platoon stability are merely the most easily-defined aspects), including considerations such as the gaps between platoons, the distribution of platoons in the network and how this changes over time.

2.2 Macroscopic Models

The basic fundamental variables used in macroscopic models are flow rate, density and average velocity, where:

- The *flow rate* q is the number of vehicles N passing a specific point on the road over a time period T, usually given in vehicles per hour *ie:* $q = N/T$ (Papageorgiou *et al.*, 1983; van Wageningen-Kessels, 2013). An alternative is to view the total number of

passed vehicles during the specified time period as equal to the sum of the individual time headways of the vehicles. From this it can be derived that flow rate is equal to the inverse of the average time headway h_t so that $q = 1/h_t$.

- The *density* k relates to the number of vehicles passing a specific point on the road in time over a spatial distance L, which is usually given in vehicles per kilometre *ie:* $k = N/L$ (Papageorgiou *et al.*, 1983; van Wageningen-Kessels, 2013). Similarly to the flow rate, the total number of vehicles passing over the spatial distance in time is equal to the sum of the individual space headways. From here the density can be derived as being the inverse of the average space headway h_s so that $k = 1/h_s$.

- The *average velocity* v is given as either mean velocity of vehicles at a specific point or over a section of road. The mean velocity over a specific point is calculated by taking the arithmetic mean of observed vehicle velocities at a point *ie:* $v_t = \frac{1}{N}\sum_{i-1}^{N} v_i$. The mean velocity over a given space is determined by dividing the distance of the space by the average time the vehicles take to cover this distance *ie:* $v_s = \frac{L}{\frac{1}{N}\sum_i T_i}$ (Papageorgiou *et al.*, 1983; van Wageningen-Kessels, 2013).

The relationship between these three variables is termed a *fundamental equation*, and it states that the flow rate is the product of density and average velocity *ie:* $q = v_s k$.

Macroscopic models describe traffic as a continuous fluid flow travelling down a channel that does not distinguish between its constituent elements (vehicles). Characteristics such as density, velocity and flow rate are used to denote traffic flow and these models are most commonly governed by partial differential equations (PDEs) (Hoogendoorn and Bovy, 2001). This type of model can be computationally efficient since individual vehicles are not considered. This approach also simplifies the modelling of merging and splitting traffic because lane-changing is not specifically enumerated in the system, making freeway flow ideally suited to this type of modelling since there are no stop-and-go situations as occurs in urban environments due to intersections and traffic lights where vehicles potentially have to give-way to oncoming traffic.

One of the earliest macroscopic PDE models is the Lighthill-Whitham-Richards (LWR) model which was developed independently in the 1950's by Lighthill and Whitham (1955) and Richards (1956). It is a first order model with only one state variable which is traffic density and the model assumes that the Law of Conservation of flow holds for traffic (Bellemans *et al.*, 2002). The advantage of the model is that it produces simple linear

equations for the traffic density at any position x and time t. However, a unique solution is not always guaranteed, for example in the case where two different velocity flows meet, namely an accelerating flow colliding with a decelerating flow, leading to the concept of a shockwave. The LWR was modified to handle shockwaves and stop-and-go flow in congested traffic conditions by Newell (1993).

Another extension to the LWR is the Payne model introduced by Peng *et al.* (1971), which implements a system of two PDEs rather than just the one. It is thus a second order model with two state variables: traffic density, as found in the LWR model, as well as average velocity (Hoogendoorn and Bovy, 2001).

A further model was proposed by Helbing (1996), which has three state variables, namely traffic density, average velocity (similar to the Payne model) as well as variance on velocity. A less commonly used macroscopic model is the Aw and Rascle model (Aw and Rascle, 2000) which is also based on the LWR model and was developed to resolve some of the issues of its predecessor.

2.2.1 Lighthill-Whitham-Richards (LWR) Model

One of the earliest macroscopic PDE models is the Lighthill-Whitham-Richards (LWR) Model, developed in the 1950's by two independent sets of authors, Lighthill and Whitham (1955) and Richards (1956). The model is based on fluid flow and assumes that the Law of Conservation of flow (Equation (2.2)), a principle that has been utilised successfully in other areas such as heat transfer and fluid dynamics, holds for traffic. This means that no vehicle can appear, disappear or jump within a section of road – in other words, in order to move from a point a to another point b on a section of road, a vehicle must travel over time through every point in between. The advantage of the model is that it produces simple linear equations when solving for flow q and density ρ at any position x and time t. However, a unique solution is not always guaranteed, leading to the concept of a *shockwave*, which is the point where two different solutions meet.

$$\frac{\delta \rho}{\delta t} + \frac{\delta q}{\delta x} = 0 \tag{2.2}$$

The LWR model is a first order model that incorporates only one partial differential

equation (see Equation (2.3) and corresponding fundamental relation (2.4)). The standard LWR model is shown in Equation (2.3), and a multi-lane version is shown in Equation (2.5) (Bellemans *et al.*, 2002). In both equations the first term is related to traffic density and the second term is related to traffic flow.

$$\frac{\delta\rho(x,t)}{\delta t} + \frac{\delta q(x,t)}{\delta x} = 0 \tag{2.3}$$

$$q = q(\rho) \tag{2.4}$$

$$\frac{n(x)\delta\rho(x,t)}{\delta t} + \frac{\delta q(x,t)}{\delta x} = 0 \tag{2.5}$$

Since differential equations are used in the model, it is very difficult or even impossible to find an analytical solution of the equations for a full road network, thus in practice the model is discretised in space and time (Papageorgiou *et al.*, 1983; Bellemans *et al.*, 2002). Discretisation in space is achieved by dividing the road network into sections Δx, with each segment usually being $500 - 1000m$ in length.

The flow from discrete section $j-1$ to section j can be defined as the minimum of the outflow of section $j-1$ (the supply) and the maximal possible inflow of section j (the demand). A simulation would thus show the traffic density, average velocity and traffic in each of these sections (Bellemans *et al.*, 2002), and discretisation of the model to allow for computer simulation has to provide for flow from one section to another section. To facilitate this, the distinct traffic components of density, velocity and flow must be calculated separately from the original differential equation for each section.

In each section the traffic density is measured in the time interval $k+1$, which is derived by adding the traffic density of the preceding time interval k to the change in traffic density due to net inflow in that section (see Equation (2.6)). $\rho(k)$ in this case denotes the average traffic density in section j and over period k, with ℓ_j being the length of the particular section, n_j the number of lanes in the section and Δt is the timestep used (Bellemans *et al.*, 2002).

$$\rho_j(k+1) = \rho_j(k) + \frac{\Delta t}{\ell_j, n_j}[q_{in,j}(k) - q_{out,j}(k)] \tag{2.6}$$

Equation (2.7) show the calculation for the average velocity in section j, where V^e is the average velocity in equilibrium, v_f is the traffic flow velocity, α and β are parameters which have been fitted to traffic data, and ρ_{jam} is the traffic density at which the average velocity of vehicles becomes zero (ie: vehicles are not moving) (Bellemans *et al.*, 2002).

$$v_j(k) = V^e(\rho_j(k)) \triangleq v_f \left[1 - \left[\frac{\rho_j(k)}{\rho_{jam}}\right]^\alpha\right]^\beta \tag{2.7}$$

Traffic flow for each section can now be determined by putting together Equations (2.6) and (2.7) plus taking into account the number of lanes to obtain Equation (2.8).

$$q_j(k) = \rho_j(k) v_j(k) n_j \tag{2.8}$$

By dividing the road network into sections and applying Equations (2.6)–(2.8) to every section, a computer can simulate traffic flow using macroscopic definitions.

Note that there may be more than one solution to Equation (2.3), due to differing densities along the road section. The LWR resolves this by introducing the concept of a *shockwave*, where a discontinuity in density is introduced along the line where the differing densities intersect. This reflects a real phenomenon in traffic flow where sudden changes in flow causes a density wave to propagate backwards through the traffic, such as where vehicles 'pile up' as they approach a red traffic light.

The LWR model has been popular in the literature due to its simplicity and ability to reproduce some essential features of traffic flow including the formation and propagation of traffic disturbances, and continues to be further developed today (Wong and Wong, 2002; Bourrel and Lesort, 2003; Donat and Mulet, 2008; Lu *et al.*, 2008; Li *et al.*, 2012; Tang *et al.*, 2012; Jin, 2013). However, it does have some shortcomings (Daganzo, 1995; van Wageningen-Kessels, 2013), in particular:

- Problems with exhibiting infinite acceleration behaviour with changes in traffic state, where the model assumes that a new equilibrium velocity will be attained immediately after the event. This is mitigated by the development of higher order models (Peng *et al.*, 1971; Aw and Rascle, 2000) and is also addressed by (Lebacque, 2002; Leclercq, 2007) who impose an upper bound on acceleration.
- Issues with traffic flow switching from free-flow to congestion, where this transition continually seems to occur at a particular density, and furthermore does so without a capacity drop or hysteresis (van Wageningen-Kessels *et al.*, 2014). Different approaches have been used to try to resolve this, including (Daganzo *et al.*, 1997; Laval and C, 2006; Jin, 2010) where a discretised version of the LWR uses lane changing maneouvres; a proposal to use various stochastic kinematic wave models where probabilities are used to reproduce fundamental diagrams (Jabari and HX, 2012, 2013); and an investigation into whether free-flow to congestion changeovers can potentially occur at distinct rather than similar densities (Hoogendoorn *et al.*, 2009).

2.2.2 Payne Model

The Payne model extends the LWR model with the addition of a traffic acceleration term, thus the equation is a system of two partial differential equations (PDEs) rather than just one (Peng *et al.*, 1971; Helbing, 1996), as shown in Equation (2.9). In this model, there are three elements that influence the average velocity in each section of road network: *relaxation*, *convection* and *anticipation* (Bellemans *et al.*, 2002).

Convection Vehicles travelling from one section of the road network to another section may need to change velocity (either accelerate or decelerate) as they cross the boundary between the sections since there there is a possibility that there is an average velocity differential between the two sections. Convection takes into account the average velocity difference between two adjacent sections, allowing vehicles to smoothly transition between sections with differing average velocities. This is accomplished by having vehicles either accelerate or decelerate until their velocity matches the average velocity of the section, thus ensuring that vehicles all travel as close as possible to the desired velocity V^e. The larger the velocity difference between the adjacent sections, the longer it takes vehicles to reach their desired velocity.

Relaxation Relaxation is concerned with how the drivers reach their desired velocity. For this attribute, the larger the difference in actual versus desired velocity V^e, the greater the driver's response to this difference, and thus the relaxation term will be larger. A time constant τ that guides the driver's reaction time, thus the slower the driver's response time to a change in velocity, the larger τ will be and the smaller the relaxation term.

Anticipation In real world traffic situations, drivers look ahead and anticipate possible scenarios that may eventuate, *ie:* if traffic is more dense ahead drivers will slow down (this corresponds to the sign in Equation (2.10) for the anticipation term) and if traffic ahead is more sparse drivers will speed up, unless they are already at the desired velocity. The anticipation constant v_a is proportional to the relative density difference between adjacent sections, τ is once again a time constant as for the relaxation term, and v_a and κ are used for tuning the anticipation term.

Note that since both the LWR and Payne models are based on continuous modelling principles, there are times when there is no analytical solution to these models and a numerical solution needs to be derived. Singh (2006) gives one way to do this by discretising parts of the system (semi-discrete and discrete macroscopic flow models). This simplifies the macroscopic PDE into a set of ordinary differential equations (ODEs), which markedly reduces the computational time required for their solution.

$$\frac{\delta v}{\delta t} + \underbrace{v\frac{\delta v}{\delta x}} = \underbrace{\frac{v^e(\rho) - v}{t_{relax}}} - \underbrace{\frac{c_0^2}{\rho}\frac{\delta \rho}{\delta x}} \tag{2.9}$$

Here v^e relates to the average velocity in equilibrium, c_0 is an anticipation constant and t_{relax} is a relaxation constant. This equation replaces Equation (2.7) in the LWR. In order to simulate the model using a computer, the equation also needs to be discretised in a similar manner as the LWR model ((Papageorgiou *et al.*, 1990a)), resulting in the following equation:

$$v_j(k{+}1) = v_j(k) + \underbrace{\frac{\Delta t}{\ell_j} v_j(k)[v_{j-1}(k) - v_j(k)]} + \underbrace{\frac{\Delta t}{\tau}[V(\rho_j(k)) - v_j(k)]} - \underbrace{\frac{v_a \Delta t[\rho_{j+1}(k)] - \rho_j(k)]}{\tau \ell_j[\rho_j(k) + \kappa]}} \tag{2.10}$$

Note that each grouped element in Equation (2.9) relates to the corresponding grouped discretised component in Equation (2.10).

In general for the Payne model, the velocity in section j at time interval $k+1$ equals the velocity in section j at time interval k in addition to a correction for convection, relaxation and anticipation. In this equation τ is a time constant, v_a is an anticipation constant, κ is a tuning parameter and $\rho j(k)$ is average density in equilibrium. All of these terms must be calibrated against actual driver behaviour in traffic.

Some improvements to the Payne model were made by (Papageorgiou *et al.*, 1990a,b), including the addition of a merging term to deal with traffic flow that converges with the mainstream traffic flow from an on / off ramp situation, a concept called *weaving*. Weaving sections are small but crucial areas of a road network that allow smooth transitioning of traffic flow when two lanes come together without the intervention of traffic control devices.

There are several different methods of analysing weaving sections and lane-changing maneouvres, with the most widely used based on the Highway Capacity Manual (HCM), an authoritative publication that is released on a regular basis (most recently in 2010) by the National Research Council in Washington DC and provides state-of-the-art methods for evaluating transportation services (Roess and Ulerio, 2000; Zegeer *et al.*, 2008). Other common approaches include the Leisch method (Leisch, 1979) and the Level D Method (Windover and May, 1994). Weaving and lane-changing research continues to this day (Jin, 2010; Skabardonis and Christofa, 2011).

Helbing (1996) extends the initial Payne model by adding another condition to the two existing states of traffic density and average velocity in each section. This third state tracks the variance on the average velocity of vehicles in a section. For example, in two traffic scenarios with identical traffic density and equivalent average traffic velocity in a section but with differing variances on velocity the resultant disturbance on traffic flow will contrast. With a small variance in velocity, all vehicles will converge to travelling at a similar velocity, resulting in smooth flowing traffic. On the other hand, with a large variance in velocity, traffic flow will be more chaotic (Bellemans *et al.*, 2002).

2.2.3 Aw and Rascle Model

The Aw and Rascle model is another macroscopic model which is based on the LWR model (Aw and Rascle, 2000) and is one of the higher order models that addresses the problems discussed by (Daganzo, 1995) by proposing to use a different velocity equation to the one used in the Payne model (van Wageningen-Kessels, 2013):

$$\frac{\delta}{\delta t}\left(v + p(\rho)\right) + v\frac{\delta}{\delta x}\left(v + p(\rho)\right) = 0 \tag{2.11}$$

where $p(\rho)$ is termed a 'pressure' component and is defined as $p(\rho) = \rho^c$ for some constant $c > 0$ that is determined via calibration against real world traffic.

Further work has been done on the Aw and Rascle model, with the introduction of multiple lanes by Klar *et al.* (0003), a multi-class version was presented by Bagnerini and Rascle (2003), and a hybrid model was developed by Aw *et al.* (2002) and Moutari and Rascle (2007) that combines the original Aw and Rascle model with a microscopic equivalent.

2.2.4 Discussion

Helbing (1995) specifies that macroscopic models have been found to be suitable for:

- Short-term traffic flow predictions.
- The development of systems for optimisation of traffic flow.
- Evaluation of averages for vehicle statistics in driving conditions such as travel times, fuel consumption and vehicle emissions.

However, these models do exhibit some inherent deficiencies due to the fact that they use the notion of a continuous fluid to represent traffic. For example since it is a continuous fluid, vehicles will not only react to the leading vehicle but also to the following vehicle, thus a vehicle (portions of the fluid) may actually end up driving backwards as a result (Daganzo, 1995). Variants have been established independently over the years to try and

address some of these documented shortcomings (Papageorgiou, 1998; Kotsialos *et al.*, 2002; Wang *et al.*, 2006; Lebacque, 2002; Leclercq, 2007).

2.3 Mesoscopic Models

Mesoscopic models take input from individual vehicles and then model their collective behaviour, for instance grouping vehicles with similar characteristics and modelling the group's behaviour as a single entity rather than the individual vehicles within the group. They attempt to combine the benefits of the macroscopic and microscopic models by retaining details on a micro-scale whilst maintaining scalability to larger networks (macro-scale). There are several broad classifications of different types of models within the mesoscopic area: *headway distribution* models, *cluster* models, and *gas-kinetic* models.

2.3.1 Headway Distribution Models

These models measure the difference in the passage of time between two successive vehicles. It is assumed that the time-headways are identically distributed independent random variables (which means that all vehicles follow the same headway pattern) and the model seeks to describe the overall distribution of the headways of all vehicles. However, individual vehicle are not considered separately (Hoogendoorn and Bovy, 2001).

2.3.2 Cluster Models

Here, vehicles are grouped in clusters usually based on similarity in position, speed and / or vehicle size, making clusters homogeneous in these properties (Hoogendoorn and Bovy, 2001). Then the behaviour of the clusters is considered rather than the individual vehicles making up the cluster, thus any differences of velocity or headways within the cluster are not modelled.

2.3.3 Gas-Kinetic Models

These type of models are based on the phase-state density for gas-kinetic flow theory from statistical physics and were first introduced by (Prigogine and Andrews, 1960, 1961) with the following partial differential equation:

$$\frac{\delta\tilde{\rho}}{\delta t} + v\frac{\delta\tilde{\rho}}{\delta x} = \left(\frac{\delta\tilde{\rho}}{\delta t}\right)_{acceleration} + \left(\frac{\delta\tilde{\rho}}{\delta t}\right)_{interaction} \tag{2.12}$$

where $\tilde{\rho}$ is the reduced phase-space density element. The left hand side of the equation consists of two terms — the first term $\frac{\delta\tilde{\rho}}{\delta t}$ is a time derivative whilst the second term $v\frac{\delta\tilde{\rho}}{\delta x}$ depicts the propagation of the phase-space density for vehicle velocity and is called the advection term. The right hand side of the equation has an acceleration term $\left(\frac{\delta\tilde{\rho}}{\delta t}\right)_{acceleration}$ which illustrates vehicle flow acceleration towards an equilibrium velocity, as well as an interaction term $\left(\frac{\delta\tilde{\rho}}{\delta t}\right)_{interaction}$ (also known as a collision term) which describes the interaction between vehicles in the vicinity of each other (van Wageningen-Kessels, 2013).

Macroscopic-like principles are applied in the way where a gas is used to approximate discrete vehicular flow, similar to the fluid-based approach of macroscopic models. However, it differs in that it models the velocities of individual particles (vehicles) in the gas, rather than modelling aggregate density as macroscopic models do (Hoogendoorn and Bovy, 2001).

Since the original work of Prigogine and Andrews (1960, 1961), several extensions and improvements have been made, with the models regaining some popularity in the 1990's Helbing and Tilch (1997).

An interesting note is that gas-kinetic models are not generally applied directly to simulations, however a continuum traffic model is developed from the gas-kinetic model and simulations are run using this derivation (*ie:* a gas-kinetic continuum model) (van Wageningen-Kessels, 2013). Since these models include a description of vehicle velocity dynamics, they tend to be categorised as higher-order macroscopic models, with some investigation done in this area (Treiber and Helbing, 1999; Hoogendoorn, 1999; Helbing, 2001; Tampere *et al.*, 2003).

2.4 Microscopic Models

Microscopic models depict the longitudinal (car-following) and in some cases the lateral (lane-changing) behaviour of individual vehicles (van Wageningen-Kessels *et al.*, 2014), and are based on the interactions between a leading and following vehicle pair. Parameters such as headway (the distance between the leading vehicle and the following vehicle) and the differences in both velocity and acceleration of this vehicle pair are used to determine the acceleration/deceleration action that the following vehicle should take (Hoogendoorn and Bovy, 2001). The concept of headway can be further delineated by *time* headway and *distance* headway. Time headway is the time that elapses between the i^{th} (following) vehicle and the $(i+1)^{th}$ (leading) vehicle. Distance headway corresponds to the spacing between the leading and following vehicles and this is defined as the centre-to-centre distance between the two vehicles.

Microscopic models can be further classified as being either *continuous* or *discrete* in nature. In the former instance this means that the road is viewed as a continuous space where vehicles can be located at any particular point, and the calculations can be very precise in placing vehicles in exact positions. These will be referred to in this thesis as *continuous car-following* models. In the latter case, the road is divided into equally-sized units (or cells) and each cell can either be empty or occupied by a vehicle (some approaches also allow a cell to be occupied by only part of a vehicle). Even though the mechanics of moving vehicles from one cell to another relies on car-following methodologies, these will be referred to as *discrete cellular-automata* models in this thesis. Thus depending on the type of microscopic model used, the length of road and the vehicle state (position, velocity etc) can be either continuous or discrete in nature.

Another consideration when using microscopic models is that every vehicle is tracked individually, and so for every timestep the simulation must take the current position and velocity of each vehicle and calculate its acceleration, making it computationally expensive.

In general, microscopic models are organised such that:

- i is the current vehicle under consideration
- $i-1$ is the vehicle behind i *ie:* the following vehicle

- $i+1$ is the vehicle ahead of i *ie:* the leading vehicle

It stands to reason that i is the leading vehicle for $i-1$ and the following vehicle for $i+1$.

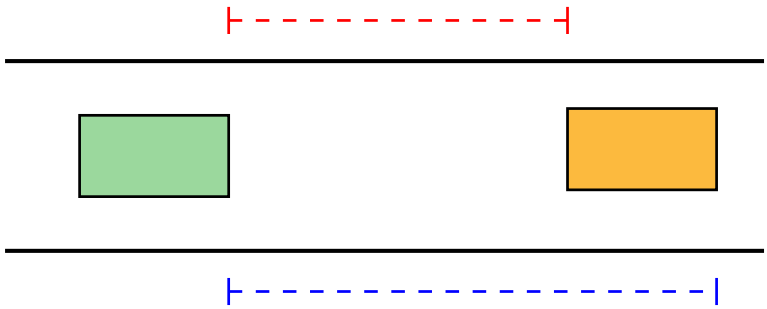

Figure 2.1: Leading vehicle represented by gold box. Following vehicle represented by green box. Red dotted line shows gap distance between leading and following vehicles. Blue dotted line shows headway distance between leading and following vehicles.

2.4.1 Continuous Car-Following Models

Continuous car-following models, also known as follow-the-leader models (Hoogendoorn and Bovy, 2001), track the interactions of a single vehicle on a single lane with the vehicle in front of it and then apply this logic to all vehicle pairs in a continuum space. Overtaking maneouvres are not taken into account. The vehicle in front is often referred to as the *leading* vehicle and the vehicle behind this leading vehicle is generally called the *following* vehicle. Special cases are where a vehicle has no leading vehicle (*ie:* it is the first vehicle or the vehicle in front of it is too far away to have any impact) or where the vehicle will have no following vehicle (*ie:* it is the last vehicle).

Continuous car-following models are amongst the earliest approaches for modelling traffic and still see active development due to their focus on modelling and tracking individual vehicle behaviour in a precise manner. As such, there is a very large body of research in the field of car-following models, covered in a detailed survey by Brackstone and McDonald (1999); Hoogendoorn and Bovy (2001); van Wageningen-Kessels (2013). Car-following models can be divided into the following general categories:

- Safe-distance models, also knowns as collision avoidance models.

- Stimulus-response models.
- Action point models, also known as psycho-physical models.
- Fuzzy logic models.

The following notation will be used in this chapter and subsequent chapters for each of the continuous car-following models discussed:

$x_i(t)$ = position of vehicle i at time t, $x_i(t) > 0$

$x_{i-1}(t)$ = position of vehicle $i-1$ at time t, $x_{i-1}(t) > 0$

$s_i(t)$ = size and headway of vehicle i *ie:* the distance between the front of the following vehicle i to the front of the leading vehicle $i+1$ at standstill at time t

$s_{i-1}(t)$ = size and headway of vehicle $i-1$ *ie:* the distance between the front of the following vehicle $i-1$ to the front of the leading vehicle i at standstill at time t

$v_i(t)$ = velocity of vehicle i at time t, $v_i(t) > 0$

$a_i(t)$ = acceleration of vehicle i at time t

$\Delta v_i(t)$ = difference of the leading and the following vehicle velocities at time t

$\Delta a_i(t)$ = difference of the leading and the following vehicle accelerations at time t

τ = reaction or delay time, constant for all vehicles and identical to the simulation timestep

a_{max} = maximum acceleration for vehicle i

a_{min} = maximum deceleration for vehicle i where $a_{max} < 0$

v_{max} = desired or maximum velocity of vehicle i

2.4.1.1 Safe-Distance Models

Safe-distance models attempt to keep all vehicles at a certain distance (or headway) from each other by choosing a velocity in such a way that the vehicle can safely stop if the leading vehicle acts in an upredictable manner. Models in this category include initial relatively simple methods such as Pipes' model, with more recently developed and more sophisticated

approaches including Gipps' and Newell's models that continue to be employed today (Wilson, 2001; Bevrani and Chung, 2011).

Pipes' Model

A relatively simple early safe-distance model was put forward by Pipes in 1953 (Brackstone and McDonald, 1999; Hoogendoorn and Bovy, 2001; van Wageningen-Kessels, 2013) who suggested that the position of the following vehicle can be determined by the position of the leading vehicle:

$$x_{i+1} = x_i + s + Tv_i + \ell_{i+1} \tag{2.13}$$

with x_i being the position of vehicle i, s being the distance between the two vehicles at a standstill, Tv_i denoted as the 'legal distance' between the following and leading vehicles and ℓ_{n-1} defined as the length of the leading vehicle. This model, however, does not consider unpredictable behaviour on the part of the leading vehicle.

A more complex model was proposed by Kometani and Sasaki (1959), who developed a car-following model from the basic Newtonian equations of motion. Here collisions can still be avoided even with erratic behaviour of the leading vehicle by having a velocity-dependent term and a time delay τ incorporated into the model (Brackstone and McDonald, 1999).

Newell's Model

Another early car-following model is Newell's model, originally proposed in Newell (1961) with a later refinement in Newell (2002). The model applies a time delay τ to the following vehicle's reactions according to the equation (Newell, 2002):

$$x_i(t + \tau_i) = x_{i+1}(t) - s_i \tag{2.14}$$

where τ is the reaction time delay and s_i is the headway for vehicle i.

The model assumes that the spacing and velocity of vehicles are linearly related when there are no lane-changing actions and uses the trajectory of the leading vehicle to decide the following vehicle's preferred headway and velocity. Thus the trajectory for both vehicles

is identical except for a translation in space and time. This highly simplified approach to traffic modelling is surprisingly useful, and has been empirically validated in several works (Ahn *et al.*, 2004; Chiabaut *et al.*, 2009, 2010). Subsequent developments of the model includes the macroscopically equivalent models (Bourrel and Lesort, 2003; Leclercq *et al.*, 2007). A similar car-following model to Equation (2.14) was also put forward by Laval and Leclercq (2010) who extended it to include differences in 'tentative' and 'aggressive' drivers.

However, one of the issues is that it assumes the following vehicle derives its behaviour directly from how the leading vehicle behaved when it had reached the position that the follower now occupies. This is a somewhat feasible assumption in a freeway situation where the 'chain' of traffic is unbroken at all times. However, it can become invalid in urban situations where intersections interrupt the flow of traffic — a leading vehicle may be able to cross an intersection whereas the following vehicle may be forced to give way to oncoming traffic. Moreover, although the model has relatively few parameters and is thus easy to implement, Hoogendoorn *et al.* (2006) showed that Newell's model cannot predict the detailed microscopic behaviour of following vehicles as accurately as more elaborate models.

Gipps' Model

One of the earliest models that produced demonstrably acceptable traffic behaviour was developed by Gipps (1981). It uses ratios of the relative velocities and relative positions of the leading and following vehicles to determine the velocity of the following vehicle. The model switches between a free flowing state, where the vehicle can accelerate freely to the desired velocity, and a car-following or restricted state where a following vehicle maintains a velocity which will allow it to avoid a collision with its corresponding leading vehicle (or any other type of obstacle). The model is relatively accurate but also relatively complicated to configure due to the number of parameters it consists of (Olstam, 2005):

1) Free driving situation:

$$v_i^a(t+\tau) = v_i(t) + 2.5 a_{max} \tau \left(1 - \frac{v_i(t)}{v_{max}}\right) \sqrt{0.025 + \frac{v_i(t)}{V_i}} \tag{2.15}$$

where τ is again a reaction time delay and v_{max} is the maximum acceleration.

2) Restricted (car-following) situation:

$$v_i^d(t+\tau) = a_{min}\tau + \sqrt{a_{min}^2\tau^2 - a_{min}\left[2(x_{i-1}(t) - x_i(t) - s_{i-1}) - v_i(t)\tau - \frac{(v_{i-1}(t))^2}{b}\right]} \tag{2.16}$$

where a_{min} is maximum deceleration and s_i is the front-to-front spacing between two stationary vehicles.

3) Resultant Gipps' model:

$$v_i(t+\tau) = min\left(v_i^a(t+\tau), v_i^d(t+\tau)\right) \tag{2.17}$$

To enable switching between the two states, the model calculates both velocities for each of the following and leading vehicles respectively for each timestep: a velocity v_i^f for the free driving situation (*ie:* unrestricted by a leading vehicle or obstacle) given by Equation (2.15) and a velocity v_i^r for the car-following situation (*ie:* restricted by a leading vehicle or obstacle), given by Equation (2.16). Taking the minimum value between these two velocities results in the actual desired velocity of the following vehicle.

A thorough mathematical analysis of Gipps' model was undertaken by Wilson (2001), an important work since Gipps' model is also used in different commercial microsimulation packages such as SISTM and PARAMICS (Wilson, 2001) as well as AIMSUN2 (developed by Transport Simulation Systems 2010) (Bevrani and Chung, 2011).

Whilst most models try to simplify their equations and reduce the number of parameters as much as possible, Gipps' model tries to be as expansive as it can, thereby markedly increasing the complexity and number of parameters. This tends to make Gipps' model more realistic in terms of mimicking driver behaviour than other similar models. However, this does make it difficult to predict how the model will behave in situations it has not been calibrated for. In addition it is unclear how certain parameters relate to traffic flow (since there are so many parameters), and repeating the simulation at many points in the parameter space is computationally expensive.

Discussion

Safe-distance models are based on simple premises and are relatively straightforward, with some (*ie:* Newell's model) having few parameters which are easily implemented. Though

the models are clear-cut, they have however been successfully utilised with other traffic flow methods in commercial simulations. For example, Gipps' model underpins AIMSUN2 (Bevrani and Chung, 2011), SISTM and PARAMICS (Wilson, 2001) whilst Pipes' model is used in CORSIM (Rakha and Crowther, 2002). On the other hand, these type of models only consider the safety margin between vehicles which can be rather a simplistic solution for capturing the complexities of traffic flow, including factors such as the difference in velocities between vehicles and human driver behaviour, which all affect decision making on the road.

2.4.1.2 Stimulus-Response Models

A refinement on the safe-distance concept are *stimulus-response models*, which take into account more information about the dynamics between the following and leading vehicles by incorporating a sensitivity (or urgency) of the reaction of the following vehicle to the leading vehicle's actions. In general, different stimuli require different levels of reaction (sensitivity) according to the following principle (Hoogendoorn and Bovy, 2001):

$$response = sensitivity \times stimulus \tag{2.18}$$

The *response* is the braking or acceleration of the following vehicle and the *stimulus* is defined by the velocity difference between the leading and following vehicles. For example, if the leading vehicle brakes suddenly, the sensitivity should be high to respond quickly and avoid an accident. On the other hand, only low sensitivity should be required for acceleration or a lane change to another lane (Hawas, 2007).

These models assume that a vehicle accelerates or decelerates as a response to three stimuli (van Wageningen-Kessels *et al.*, 2014):

- The velocity of the current vehicle n *ie:* $v_i = \frac{dx_i}{dt}$
- The headway spacing between the current vehicle and the vehicle ahead of it *ie:* $s_i = x_{i-1} - x_i$
- The relative velocity between the current vehicle and the vehicle ahead of it *ie:*

$\dot{s}_i = \frac{ds_i}{dt} = v_{i-1} - v_i$, although some simpler models such as the OVM will not consider this stimulus

A relatively large volume of research was produced in the 1950s and 1960s with respect to stimulus-response models, and as such there has been a corresponding amount of effort in calibrating and validating these early models (van Wageningen-Kessels, 2013). Other types of models subsequently took precedence, and it was not until the mid 1990s that there was a resurgence of new stimulus-response models, which has continued to this day (Bando *et al.*, 1995; Helbing and Tilch, 1998; Brackstone and McDonald, 1999; Treiber *et al.*, 2004; van Wageningen-Kessels *et al.*, 2014).

Other contributions of stimulus-response models are based on three-phase traffic theory proposed by Kerner and Rehborn (1996) and later extended by Kerner (2009). The classic theories are based on the fundamental diagram of traffic flow, which is comprised of two phases: free flow and congested flow. In Kerner's three phase theory, congested flow is divided into two components: synchronised flow and wide moving jam, where wide refers to the length of the traffic jam. A stochastic car-following model was produced by Kerner and Klenov (2002) and an acceleration delay model subsequently followed (Kerner and Klenov, 2006).

Gazis-Herman-Rothery Model

Early work on stimulus-response models was done as part of a General Motors initiative (van Wageningen-Kessels *et al.*, 2014). These endeavours culminated in the inception of the notable Gazis-Herman-Rothery (GHR) model and is named after Gazis *et al.* (1961). Enhancements and additional refinements continue to this day, such as work by Bevrani *et al.* (2012).

The equation for the basic GHR model is as follows:

$$a_i(t) = \gamma \frac{(v_{i-1}(t))_1^c}{(s_i(t-\tau))_2^c} \dot{s}_i(t-\tau) \tag{2.19}$$

where $\gamma \frac{(v_{i-1}(t))_1^c}{(s_i(t-\tau))_2^c}$ is the sensitivity of vehicle n (and as such all vehicles have the same sensitivity), $\dot{s}_i(t-\tau)$ is the stimulus term, the resultant acceleration $a_i(t)$ is the response component, γ is the sensitivity parameter, and constants c_1 and c_2 are calibration constants. τ is again a reaction time delay of the vehicle driver.

Limitations of the GHR model have been documented (Hae, 2009) and include:

- An arbitrary small change in the relative velocity may cause a significant reaction by the following vehicle.
- Even with large headways where there should not realistically be a response, the following vehicle is still affected by the leading vehicle's actions.

An interesting side note is that a macroscopic version of the GHR model has been derived by integrating the car-following equation and obtaining a correlation between average velocity, flow and density (Olstam, 2005).

Optimal Velocity Model

One of the more recent stimulus-response models was developed by Bando *et al.* (1995) and is called the Optimal Velocity Model (OVM) since it is based on the premise that vehicles accelerate or decelerate to a particular 'optimal' velocity, which is constructed as a function of the headway and current velocity. Vehicle length is taken into account with headway and all driver behaviour is identical.

The OVM was derived from the following simple dynamical equation:

$$\ddot{x}_i = \kappa V(s_i) - \dot{x}_i \tag{2.20}$$

where x_i is the position of vehicle i, $\ddot{x}_i$ is the resultant acceleration, $\dot{x}_i$ is the current velocity of vehicle i, $V(s_i)$ is the optimal velocity for a headway of s_i, $i = 1, 2, \cdots, N$ where N is the number of vehicles and κ is a sensitivity constant (assumed to be independent of i and identical for all vehicles).

As the headway shrinks, the velocity of the following vehicle decreases to ensure that a collision with the leading vehicle does not occur. Likewise, an expanding headway results in an increasing velocity which does not exceed the optimal velocity. This means that V must have the following properties:

- Is a monotonically increasing function

- $|V(s)|$ has an upper bound when $v_{max} \equiv V(s \to \infty)$

The following steady state flow equation satisfies the above properties:

$$x_n^{(0)} = bn + ct \tag{2.21}$$

A periodic boundary condition is established for the steady state flow where N vehicles travel on a circuit of length L, with the $(N+1)^{th}$ vehicle being in fact the first vehicle. The Fourier series is used with Equation (2.20) and Equation (2.21) to confirm stability of the model in a steady state flow when $V'(b) < \frac{\kappa}{2}$ for a given headway b.

Bando *et al.* (1995) chooses the hyperbolic function tanh for V. The acceleration equation for the OVM written in slightly different notation is thus:

$$\frac{dv_i(t)}{dt} = a_i(t) = \kappa[V(s_i(t)) - v_i(t)] \tag{2.22}$$

where

$$s_i(t) = x_{i+1}(t) - x_i(t) - l_{i+1} \tag{2.23}$$

In Equation (2.23) l_{i+1} is the length of vehicle $i+1$, and this is usually selected to be $5m$ in simulations to average out vehicles that can range from small cars to large trucks. κ is a sensitivity parameter. The resultant optimal velocity V based on tanh of the headway is as follows:

$$V(s) = V_1 + V_2(\tanh(C_1 s_i - C_2)) \tag{2.24}$$

where V_1 and V_2 are velocity constants for controlling the optimal velocity, and C_1 and C_2 are parameter constants.

Overall the OVM is structurally simple and computationally efficient, and has been calibrated using empirical data by Helbing and Tilch (1998). In addition, it can describe properties of real traffic flow, the evolution of traffic congestion and the formation of stop-and-go waves (Jiang *et al.*, 2001).

However, this model displays unreasonably high acceleration in free driving conditions (due to the behaviour of tanh) and unrealistic deceleration when there is a relatively small

headway even if the leading vehicle is travelling much faster than the following vehicle (Helbing and Tilch, 1998). To overcome these deficiencies, Helbing and Tilch (1998) developed a Generalized Force Model (GFM) shown in Equation (2.25), and though this model did show some improvements unreasonable deceleration is still an issue (Jiang *et al.*, 2001; Gaididei *et al.*, 2009).

$$\frac{dv_i(t)}{dt} = \kappa \left[V\left(s_i(t)\right) - v_i(t) \right] + \lambda \Theta(-\Delta v) \Delta v \tag{2.25}$$

where Θ is the Heaviside function and λ is a sensitivity constant.

The OVM was later extended by implementing a delay τ and replacing t with $(t - \tau)$ on the right hand side of Equation (2.22) by Bando *et al.* (1998). In effect, this introduces a driver reaction delay to the OVM. However, to our knowledge, very little follow-up work on this has occurred, and it does not address the fundamental issues with the OVM that subsequent work has highlighted.

Further work with the OVM is continuing, including further investigation of driver reaction time delays (Davis, 2003), incorporating lateral separation and overtaking expectation (Tang *et al.*, 2005; He and Sun, 2013), considering more than just one leading vehicle to improve stability and traffic congestion (Lenz *et al.*, 1999; Xue, 2003; Peng *et al.*, 2008; Ge *et al.*, 2008; Mo *et al.*, 2008; Li and Zang, 2013) and analysis to enhance understanding of the model (Sawada, 2006).

Full Velocity Difference Model

The Full Velocity Difference Model (FVDM) was presented by Jiang *et al.* (2001) to try to mitigate the unreasonably high acceleration and unrealistic deceleration that the OVM displayed (Helbing and Tilch, 1998) and that the GFM could not entirely overcome. This was done by introducing a 'velocity difference' step function. Similar to the OVM, Jiang *et al.* (2001) also showed that the FVDM would be stable when $V'(b) < \frac{\kappa}{2} + \lambda$. This leads to the FVDM equation:

$$\frac{dv_i(t)}{dt} = \kappa \left[V\left(s_i(t)\right) - v_i(t) \right] + \lambda(s_i)\Delta v_i(t) \tag{2.26}$$

$$\Delta v_i(t) = v_{i+1}(t) - v_i(t) \tag{2.27}$$

where κ is a sensitivity parameter, λ is a step function defined by:

$$\lambda(s_i) = \begin{cases} a, & s_i \leq s_c \\ b, & s_i > s_c \end{cases} \tag{2.28}$$

and $\Delta v_i(t)$ is the velocity difference. The parameters are set to $a = 0.5s^{-1}$, $b = 0$, $s_c = 100m$.

Adding $\lambda(s_i)\Delta v_i(t)$ to the OVM equation shifts the tanh function up or down depending on whether the leading or following vehicle has a higher velocity. Since there is no stretching or shrinking of tanh due to these changes, the acceleration or deceleration configuration for the FVDM remains unchanged from the OVM's pattern. The FVDM also uses a step function to determine when the difference in velocity should start to take effect, and this threshold is established as a parameter.

The FVDM takes both the positive and negative velocity difference of the following and leading vehicles into account, thus overcoming the problem in both the OVM and GFM where these two models decelerate when there is a small headway but the leading vehicle's velocity is greater (Jiang *et al.*, 2001).

Full Velocity and Acceleration Difference Model

The Full Velocity and Acceleration Difference Model (FVADM) is an extension of the FVDM presented by (Zhao and Gao, 2005), who introduced an 'acceleration difference' to the FVDM, where the acceleration difference between the leading and following vehicles is appended to the FVDM's velocity difference step function, making the model inherently more complicated. A positive acceleration difference indicates that the leading vehicle is accelerating faster than the following vehicle and a negative acceleration difference implies the reverse.

In this way the FVADM tries to avoid collisions where an acceleration difference becomes important between two vehicles, *ie:* in the case where the following and leading vehicles are travelling at the same velocity, have a relatively small headway and a sudden deceleration

of the leading vehicle occurs. In this situation, the OVM, FVDM and GFM will all fail to recognise the need to decelerate rather quickly, and thus a collision can potentially occur (Zhao and Gao, 2005).

The acceleration difference is also implemented using a step function, similar to that of the FVDM's velocity difference step function, where the difference in acceleration becomes effective once the space distance headway is equal to or less than $100m$. The equation for the FVADM is:

$$\begin{aligned}
\frac{dv_i(t)}{dt} &= \kappa \left[V\left(s_i(t)\right) - v_i(t) \right] + \lambda(s_i)\Delta v_i(t) \\
&\quad + k(s_i)g(\Delta a_i(t-1), a_{i+1}(t))\Delta a_i(t-1) \\
\Delta a_i(t) &= a_{i+1}(t) - a_i(t) = \frac{dv_{i+1}(t)}{dt} - \frac{dv_i(t)}{dt} \\
g(\Delta a_i(t-1), a_{i+1}(t)) &= \begin{cases} -1, & \Delta a_i(t-1) > 0 \quad \text{and } a_{i+1}(t) \leq 0 \\ 1, & else \end{cases}
\end{aligned} \tag{2.29}$$

where $k(s_i)g(\Delta a_i(t-1), a_{i+1}(t))\Delta a_i(t-1)$ is the acceleration difference term and

$$k(s_i) = \begin{cases} c, & s_i \leq s_c \\ d, & s_i > s_c \end{cases}$$

is the velocity difference term.

Hence the FVADM has two step functions — one to invoke the velocity difference and another to invoke the acceleration difference. Again as for the FVDM, the transition for both differences will not be smooth due to the step function.

Intelligent Driver Model

The Intelligent Driver Model (IDM) is another robust stimulus-response car-following model (Treiber *et al.*, 2000b). It is derived from the phenomena of phase transitions that change from free-flowing traffic to stop-start traffic on freeways and uses two ratios to control the acceleration and deceleration of vehicles.

The first ratio acts as an acceleration term and consists of the actual velocity versus the desired velocity. It allows vehicles to freely accelerate as if they are on an open road with

no leading vehicles or obstacles in front of them. This is balanced by the second ratio, which is comprised of the minimum desired headway (or gap between vehicles) versus the actual headway, and varies dynamically with the velocity of the vehicle. This term determines the braking acceleration (*ie:* deceleration) for the vehicles which would occur as a result of the vehicle attaining the desired velocity (defined as a parameter), or if the vehicle has not attained the desired velocity yet, having an obstacle or leading vehicle in front of it to prevent further acceleration.

With these two ratios continually balancing each other depending on the vehicle's interaction with its environment and other vehicles, the model has been shown to be relatively effective at simulating real-world vehicle movement when accelerating and braking under normal driving conditions (Treiber *et al.*, 2000b). Vehicle behaviour also tends to be more realistic in deceleration scenarios where the space distance headway is either a negligible factor or where the space distance headway is the determining factor, *eg:* in emergency braking situations.

The IDM's acceleration of a vehicle with a length l_i is determined by its own velocity $v_i(t)$ at position $x_i(t)$,the space distance headway $s_i(t)$ and the difference in velocity $\Delta v_i(t)$ between vehicle i and $i+1$:

$$\frac{dv_i(t)}{dt} = a\left[1 - \left(\frac{v_i(t)}{v_0}\right)^{\delta} - \left(\frac{s^*(v_i, \Delta v_i)}{s_i(t)}\right)^2\right] \tag{2.30}$$

$$s^*(v_i, \Delta v_i) = s_0 + s_1\sqrt{\frac{v_i}{v_0}} + v_i T + \frac{v_i \Delta v_i}{2\sqrt{ab}} \tag{2.31}$$

where:

$v_i(t)$ = current velocity of the following vehicle
v_0 = desired velocity
s^* = desired minimum headway
s = actual headway
T = desired safety time headway
a = maximum acceleration
b = desired deceleration
δ = acceleration exponent

On a free open road, when $s_i(t) \to \infty$, the vehicle's acceleration tends to:

$$a\left(1 - \left(\frac{v_i(t)}{v_0}\right)^{\delta}\right) \tag{2.32}$$

and consequently, as $v_i(t) \to v_0$, there is a tendency for the vehicle to decelerate:

$$-a\left(\frac{s^*}{s_i(t)}\right)^2 \tag{2.33}$$

The model's parameters are empirically measurable and have a reasonable interpretation. As such, the parameters can be modified to suit different circumstances, for example the maximum acceleration a and desired deceleration b can be varied based on the conditions of the vehicles or road (Treiber *et al.*, 2000a). The acceleration exponent δ controls the rate of a vehicle's acceleration, with small values of δ producing a smoother (and thus more realistic) acceleration than larger values. Other points to note is that the IDM does not incorporate a discontinuity as the FVDM and the FVADM do (*ie:* a step function) with respect to when the velocity and acceleration have an effect in the model, hence any change in acceleration tends to be smoother.

The IDM is relatively simple both conceptually and in its definition. It also encompasses a few desirable properties, including a simple and computationally efficient update equation, realistic responses to most generic traffic situations and has an equivalent macroscopic model that could facilitate alternative analysis methods (Hennecke *et al.*, 2000). Hence the IDM tends to be quite popular in the literature (Davis, 2004; Hoogendoorn and Hoogendoorn, 2010; Treiber and Kesting, 2012). In addition, extensions to the IDM have also been investigated, for example, Chen *et al.* (2009) enhanced the model to incorporate multi-anticipative behaviour, where models scan several vehicles ahead rather than just the one vehicle ahead, and named this version the MIDM. As well, Treiber *et al.* (2006) derived the Human Driver Model (HDM) from the IDM to incorporate reaction time delays and anticipation behaviours that humans exhibit.

Discussion

In stimulus-response models, maintaining a safe distance between vehicles remains a priority to prevent collisions, however a sensitivity element is added that moderates the response of vehicles. The models also incorporate the notion of a desired or optimal velocity in different ways which is designed to get the vehicles to this speed without breaking the safe-distance imperative (Hoogendoorn and Bovy, 2001), a reflection of realistic driving behaviour. Model parameters can usually be altered to suit, and models can not only be applied to vehicles but also pedestrian traffic with some modifications (Helbing and Molnár, 1995), (Cristiani *et al.*, 2012a). Conversely, these models are more complex math-

ematically, do need to be calibrated (Hoogendoorn and Hoogendoorn, 2010) and tend to have a significant number of parameters, which can make it difficult to configure them. Due to this, changing a parameter to improve the model for a specific set of traffic circumstances may have adverse affects in other situations which were depicted relatively accurately before.

2.4.1.3 Action Point Models

The underlying concept of *action point* models (also known as *psycho-physical* models) is the notion of using heuristic rules that check thresholds (action points) which, when exceeded, lead to a change in vehicle behaviour. They were first discussed in the 1960's and have continued to receive some attention (Kumamoto *et al.*, 1995; van Wageningen-Kessels *et al.*, 2014). An example of an action point is where the headway distance drops below a threshold, triggering the need for the following vehicle to react by decelerating. Building a set of these rules then governs the overall behaviour of the following vehicle.

These models improve on other types of models by dealing more realistically with the following situations:

- Vehicles are not affected by the behaviour of other vehicles in the vicinity when a large headway between vehicles exists.
- With small headways, vehicles are only affected if the changes in relative velocity and headway are large enough for these variations to be detected.

Whilst these models can be efficient and the rules are usually easily interpretable, the rule-based nature makes vehicle reactions non-smooth and the rules themselves must attempt to explicitly cover every possible situation, making calibration difficult. For example, the model based on the work by Wiedemann (1974) has been incorporated into the micro-simulation package VISSIM (Gao, 2008). However, thresholds where action points are triggered are applied subjectively, and may change with difference scenarios, thus tend not to be reliable in all situations.

2.4.1.4 Fuzzy Logic Models

Fuzzy logic is a branch of uncertainty modelling which reinterprets classical binary logic and set theory by allowing a variable to have a *degree* of its value, for example a fuzzy binary variable can have a value between 0 and 1. This has been used to modify existing driver models to incorporate the inherent uncertain estimations that real human drivers make about the state of vehicles around them. The idea is that since humans are not as precise in their observations of velocity or relative distance as a computer is, sets that define estimations of observations are created and used in the driver models *eg:* velocity can be defined as very low, low, moderate, high, very high (Olstam, 2005). A fuzzy value is then defined according to the available set that approximates the true (though unknown) state values and the driver model produces reaction based on these approximations. For example, if the vehicle is at moderate velocity, the desired velocity is high, and have a large headway, then the vehicle can increase velocity.

This was initially applied to the GHR model by Kikuchi and Chakroborty (1992), then subsequently to another model called MISSION (Wiedemann and Reiter, 1992) which was followed closely by implementations by Yiaki *et al.* (1993) and others (Chakroborty and Kikuchi, 1999), (Chakroborty and Kikuchi, 2003), (Khodayari *et al.*, 2011). However, calibration of these models is a difficult proposition since the values being dealt with are not absolute and little work has been done in this area, making fuzzy logic models less robust than other models that are based on precise numbers (Brackstone and McDonald, 1999), (Olstam, 2005). Moreover, they are still based on the same underlying driver models and so will inherit the same basic behaviours and issues of these models.

2.4.1.5 Other Model Variations

Car-following models have been extended in other ways, one of which is to consider vehicles and drivers on an individual basis rather than assuming that all vehicles and drivers have identical behaviour. This extension is referred to in the literature as *multi-class* models and means that the model parameters such as sensitivity, reaction time and desired velocity can be varied across vehicles rather than having these as homogeneous values (van Wageningen-Kessels, 2013). Most micro-simulation packages are able to apply this diversity of behaviour.

Another extension to car-following models is termed *multi-anticipation* and relates to having more than one leading vehicle affecting the behaviour of the following vehicle (van Wageningen-Kessels, 2013). This concept has been applied to several well-known models since then, including the GHR model (van Wageningen-Kessels, 2013), the OVM (Lenz *et al.*, 1999) and the IDM (Treiber *et al.*, 2006), with others extending these works. Ossen and Hoogendoorn (2006) combined both multi-class and multi-anticipation in their model to account for drivers that would look further ahead than others.

However, although the variation in parameters increases the 'mix' of vehicle behaviours, the models underlying both the multi-class and multi-anticipation extensions remain essentially the same. Thus the fundamental behaviours and issues of these base driver models are still in effect.

2.4.1.6 Discussion

In the preceding sections it can be seen that most continuous car-following models essentially follow safe-distance rules with additional information factored in to improve the accuracy of driver behaviour. The models are thus classified into different variants on the safe-distance theme. An exception to this are action point models which implement rules when specific actions need to be taken rather than adding in extra functionality to depict more precise driver behaviour. Of course in theory, an infinite list of rules can be used to model continuous car-following traffic flow, however this is infeasible in practice since it requires vast amounts of computing power and does not necessarily guarantee a more accurate representation of driver behaviour.

2.4.2 Discrete Cellular Automata Models

Discrete cellular-automata models, also called *particle-hopping* models (Nagel *et al.*, 1998; Knospe *et al.*, 2000), are traditionally referred to as car-following models but are of a discrete nature rather than a continuous one. Thus in this thesis a distinction is made between these two types of microscopic models, referring to continuous types as 'continuous car-following' models and discrete types as 'discrete cellular-automata' models. Discrete cellular-automata models describe traffic flow as a lattice of cells of equal size where vehicles move from cell to cell with each timestep. They are thus essentially an integer-

based version of continuous car-following approaches in that they model individual vehicles by considering gaps to the vehicle in front when making movement decisions but do so using a discrete cell grid rather than a continuous line. This makes them much more efficient and scalable to simulate than continuous car-following models, particularly if an appropriately parallel high-performance computer is available. Thus these models are often used to simulate traffic on large-scale motorway networks.

2.4.2.1 Rule 184

One of the most basic cellular automata algorithms is the Rule 184 cellular-automata system (Wolfram, 1986), which is a generic one-dimensional binary cellular automaton rule that has, amongst other areas, been adapted to cellular automaton traffic flow. However, Rule 184 can only handle single-lane systems and simple vehicular movement and is thus inappropriate for simulating traffic flow on a road network where more complex structures occur. Another model based on cellular automata is the Biham-Middleton-Levine (BML) cellular-automata model, a two-dimensional analogue of Rule 184 (Biham *et al.*, 1992), which shows phase transitions of vehicle movement but is not conducive to simulating traffic flow on a road network that contains traffic junctions (D'Souza, 2005).

2.4.2.2 Nagel-Schreckenberg Algorithm

A more useful alternative cellular automaton system that is also based on Rule 184 is the Nagel-Schreckenberg (N-S) algorithm (Nagel and Schreckenberg, 1992). It is a discrete microscopic model that is relatively simple to understand, implement and analyse, is computationally inexpensive and can simulate a traffic network containing roads and intersections. Similar guidelines to those used by car-following models (such as calculating acceleration based on vehicle pairing) are employed, but occur at a more granular level of detail due to the discrete cells. Nevertheless, the principal benefits of discrete cellular-automata models over continuous car-following models also stem from this basis in simple discrete cells. Specifically, it facilitates fast computation via integer-only operations since the states are fixed and finite, and massively parallel implementation is also possible due to the short-range interactions between vehicles (Helbing, 2001; Kari, 2005).

The N-S algorithm for single lane traversal consists of four basic steps, where steps 1–3

are applied to each vehicle before all vehicles are allowed to move forward their respective number of cells in step 4:

$v_i(t)$ is the velocity of a vehicle i at timestep t
v_ℓ is the maximum velocity and can be equated to the speed limit
$g_i(t)$ is the number of empty cells to the ahead vehicle at timestep i
$p_i(t)$ is the random probability that the vehicle will brake at timestep t
$x_i(t)$ is the position of the vehicle at timestep t

Step 1: Acceleration component
If $v_{i-1}(t) < v_\ell$ then $v_i(t) = v_{i-1}(t) + 1$

Step 2: Braking component due to other vehicles
If the gap $g_i(t)$ after Step 1 is smaller than $v_{i-1}(t)$ then $v_i(t) = min(v_{i-1}(t), g_i(t))$

Step 3: Randomisation component
Using random probability of $p_i(t)$, the velocity $v_i(t)$ is reduced by one unit after Step 2 for all vehicles to which the probability applies, *ie:* $v_i(t) = v_i(t-1)$

Step 4: Driving component
After Steps 13, the new velocity $v_i(t)$ for each vehicle is determined and each vehicle is moved by $v_i(t)$ cells, where $x_i(t) = x_{i-1}(t) + v_i(t)$

In essence, all vehicles want to be able to travel as fast as possible to a limit of v_ℓ (Step 1) but also need to avoid collisions with vehicles ahead (Step 2). A randomisation element which decreases velocity is factored in to account for external fluctuations such as human driver behaviour, the weather, road conditions, etc and is applied to all vehicles (Step 3). Finally when all calculations for vehicles have been done, each vehicle is moved forward the specified number of cells.

Despite their simplicity, discrete cellular-automata models still provide empirically meaningful results at a microscopic level of detail (Knospe *et al.*, 2004), though with more

erratic acceleration and not as much precision as continuous car-following models. Moreover, it is well known that discrete cellular-automata models are typically far simpler to extend than continuous car-following models for modelling more complex situations such as lane changing behaviour or merging (Laval and C, 2006; Burzyńsky and Kosińksi, 2009). This is due to the fact that discrete cellular-automata models only roughly approximate driver behaviour, hence unlike continuous car-following models they are not significantly affected by introducing rough approximations of lane-changing behaviour. In addition to the performance of discrete cellular-automata models over continuous car-following models, empirical studies have shown that discrete cellular-automata models generate more realistic vehicle spacing, whilst continuous car-following models tend to be better with precision on speed and acceleration predictions (Ranjitkar *et al.*, 2005a).

2.4.2.3 Other Variants

An interesting variant on the cellular-automata approach is the 'continuous cellular-automata' by (Yeldan *et al.*, 2012), where cells are the vehicles themselves, and these cells may be located anywhere along the road. Fuzzy logic is used to relax the discrete nature of cellular-automata driver decisions and introduce continuous variables. This is explicitly aimed at retaining the computational efficiency of cellular-automata approaches whilst also improving their granularity. However, they provide no empirical indication of how much efficiency is retained in comparison to a classic discrete cellular-automata model.

A review of some of the more widely-used cellular-automata models is provided by Knospe *et al.* (2004), and Pandey *et al.* (2014) offer a synopsis of cellular-automata models developed for heterogeneous traffic and potential improvements.

Some recent and interesting developments either combine a discrete cellular-automata model with the OVM continuous car-following model (Helbing and Tilch, 1999) or add three-phase theory to a cellular-automata model (Kerner *et al.*, 2002). Research is continuing on improving cellular-automata models and their applications (Kerner *et al.*, 2011; Kokubo *et al.*, 2011; Meng and Weng, 2011; Yeldan *et al.*, 2012; Habel and Schreckenberg, 2014).

2.5 Synopsis of Continuous and Discrete Models

The main advantage of continuous car-following models over discrete cellular automata models is that their calculations are very fine-grained due to the use of floating point operations, resulting in precise update equations. This gives them the potential to accurately depict realistic driver and vehicle behaviour and be open to detailed analysis of the actions produced by the models in comparison to data collected from real drivers. This is in contrast to discrete cellular-automata models, in which calculations are integer-based and are therefore relatively imprecise and rule-based. This has an impact on the accuracy of analysis and results in relation to measuring real-world data.

As more accuracy comes with more complexity, it follows that continuous car-following models are computationally more expensive, resulting in higher execution times. This tends to make the use of continuous car-following models infeasible for simulating the entirety of large road networks. Moreover, due to the fact that vehicles may be positioned at any point along a road, building reasonable models for lane-changing and merging is difficult due to the need to expand the model to handle the second dimension of other lanes and the vehicles therein. On the other hand, due to integer calculations, discrete cellular-automata models tend to be computationally efficient and are thus more suitable for studying large road networks. Furthermore, multiple lanes are more easily incorporated and manipulated via lane-changing and merging actions due to the simpler nature of the models, making this type of model a better choice for problems that require more than one lane (Nagel *et al.*, 1998). It is also relatively straightforward to utilise parallel programming with discrete cellular-automata models as all vehicle positions are updated simultaneously (Nagel and Schreckenberg, 1992; Hoogendoorn and Bovy, 2001).

Taking into account these relative advantages, it would be ideal to have a mixture of continuous car-following and discrete cellular-automata models in some particular areas of a road network where their respective strengths are most useful and their weaknesses have negligible impact. For example, the continuous model would be most suited for the precision-oriented regions of the network such as junctions, and sections of the network that contain multiple lanes, merge points and straight roads can be driven by the discrete model. Such heterogeneous models exist (see Section 2.7 for further discussion on this topic), but studies have been largely focused on mixing microscopic and macroscopic models and to a lesser extent mesoscopic models.

2.6 Macroscopic Versus Microscopic Models

2.6.1 Summary of Macroscopic Models

Macroscopic models are less computationally intensive than either microscopic or mesoscopic models due to the fact that velocity is calculated using traffic density over each section rather than calculating velocity for individual vehicles at each timestep. This allows for comparatively fast simulation (Bellemans *et al.*, 2002). These models also have fewer parameters to deal with and thus it is less time-consuming to calibrate and requires less calculations than the other types of models. Not only are macroscopic models applicable to traffic, they are also well-suited to other areas of research, such as optimal predictive and adaptive control ().

On the other hand, macroscopic models are based on the assumption that the Law of Conservation used for naturally occurring laws of physics holds for traffic flow. These laws are derived from physical features based on the molecular level and are therefore assumed to be smoothly continuous, whereas traffic flow equates to individual vehicles which is inherently discrete in nature, thus a discrete problem is being modelled with a smooth function. Furthermore, there are additional margins of error since human drivers themselves do not behave in accordance with these laws either (Papageorgiou, 1998). Due to the specification and definition of macroscopic properties, individual vehicle movements are not calculated in macroscopic models, only aggregate traffic flow is, making it impossible to track specific vehicles. As such, only average driver behaviour can be estimated rather than individual driver behaviour. The partial differential equations used in these types of models are also difficult to solve analytically, and more often than not some form of numerical approximation is required.

2.6.2 Summary of Microscopic Models

Since microscopic models are concerned with individual vehicles, they can be applied to specific traffic situations and provide important information that is difficult to extract from a more collective perspective. Not only can individual vehicle movements be tracked very accurately, but different driver behaviour can potentially be applied to different vehicles. Urban traffic environments comprise of detailed and precise movements of vehicles around

intersections, making them particularly suited to be simulated by microscopic models. The equations used are also mathematically simple to understand and compute and work well in networks with a relatively low number of vehicles to track.

In contrast to macroscopic models which are derived from the physical properties of flow movement in the form of partial differential equations (see Section 2.2), microscopic models attempt to replicate human driving behaviour using more of a heuristic approach. Although reasonable assumptions are made as to how a human drives and reacts to external stimuli in a traffic environment, these are still largely reliant on 'rule-of-thumb' or 'if-then-else' conjectures applied to human behaviour (Hoogendoorn and Bovy, 2001), (Papageorgiou, 1998). This is an issue since human behaviour is inherently inconsistent, for instance different drivers will not react the same way when confronted with similar situations, and even the same driver may react in different ways at different times given the same set of circumstances. Thus the models may replicate normal, routine traffic flow accurately, but may falter when boundary conditions are implemented. Note that since discrete cellular-automata models divide the road into identically-sized cells, vehicle movement is simpler and so boundary conditions do not have the same extreme affect as they do on continuous car-following models. For both continuous car-following and discrete cellular-automata models, using heuristics means that the models require a large number of parameters for calibration (Hoogendoorn and Bovy, 2001).

2.7 Heterogeneous Models

As mentioned in previous sections, each type of traffic flow model has its relative strengths and weaknesses and this is taken into account when selecting a model for a particular simulation problem. It would be optimal, however, to be able to choose different models to simulate specific parts of a network where their positive features can be taken and their negative aspects can be minimised.

Such heterogeneous (or hybrid) systems have been proposed for the purposes of mixing macroscopic with microscopic elements. The objective is to utilise the fine detail of individual vehicles in microscopic models at critical sections, such as traffic junctions, and, conversely, work with the more computationally efficient aggregate approach of macroscopic models elsewhere where detail is not so crucial, such as freeway on-ramps. These

heterogeneous approaches are referred to as multi-scale systems (Helbing *et al.*, 2002; Burghout *et al.*, 2005; Newell, 2011), reflecting their use of models with differing resolution of detail.

The main obstacle facing multi-scale systems is the transition from one model to another. Due to their different resolutions, the different models will parameterise traffic differently, and so the handover between models when transitioning from one modelling regime to another requires some method to relate the properties of one model to the other without losing information or affecting traffic flow at the boundary. This can be cast as a well-posed problem by imposing constraints on the macroscopic and microscopic parameters at the boundary (Herty and Moutari, 2009; Lattanzio and Piccoli, 2010).

Subsequent mathematical analyses of the heterogeneous approaches demonstrate their usefulness over a purely macroscopic approach. However, such 'instantaneous' transitions can also lead to unrealistic constraints on, or reactions from, the behaviour of the models due to their different level of resolution (Bourrel and Lesort, 2003). To overcome this, Bourrel and Lesort (2003) introduce a transition zone in which both models are run. The incoming model continues to be used as the traffic simulation in this zone, but critically the outgoing model is given time to reach a valid state before taking over the simulation role. Cristiani *et al.* (2012b) propose an alternative in which a microscopic and corresponding macroscopic model are coupled and run simultaneously, using a bias term to control which model is dominant at any location. This overcomes the transition-boundary problem as both models are active everywhere, but at the computational cost of having to maintain both models.

In contrast, very little attention has been paid to mixing different microscopic models within the same network since such a heterogeneous network would not provide any multi-scale information. However, mixing different *types* of microscopic models can still be beneficial for modelling and performance reasons, as previously discussed in Section 2.5. In this area, Yeldan *et al.* (2012) has attempted to mix the continuous aspects of car-following into a cellular-automata model via fuzzy logic, but does not investigate the effect on traffic flow of having separate car-following and cellular-automata models operating heterogeneously in the one road network. As with multi-scale approaches, the main issue with such a model is likely to be the transition point from one model to another and whether this switch-over causes any instabilities in the system. Hence this thesis examines precisely this issue in Chapter (5).

2.8 Micro-Simulation Packages

The concept of a multi-scale approach has been applied to commercial traffic simulation packages, where systems are built based on an assortment of existing macroscopic, mesoscopic and microscopic models or concepts and are commonly used as analysis tools for traffic flow to show benefits and limitations, and make critical design decisions in particular scenarios or even for specific municipalities (Papageorgiou, 2007; Stevanovic *et al.*, 2008; Mathew and Radhakrishnan, 2010). The exact approaches chosen to govern boundary transitions between modelling regimes in these systems is not available due to their proprietary nature, and with very limited implementation details available, there are documented reservations about their accuracy (Bloomberg and Dale, 2000). Moreover, these packages provide for mixing different model resolutions (macroscopic versus microscopic) but not multiple models of the same resolution (such as two or more microscopic models).

It is interesting to note that these micro simulations often follow similar precepts to the different types of microscopic models examined in this chapter. For example, AIMSUN is based on the same principles as safe-distance models, MITSIM is derived from the GHR model, and PARAMICS and VISSIM are based on action point models (Olstam, 2004). Two macroscopic systems are METANET, a simulation developed by Messmer and Papageorgiou (1990) which provides a balanced trade-off between accuracy and computational complexity, and RENAISSANCE (Wang *et al.*, 2006). TRANSIMS is a N-S cellular automata tool developed by Nagel *et al.* (1997). A survey of 57 of the most prominent microsimulations is presented by Algers *et al.* (1997), with research continuing to this day (Rakha, 2003; Zhang, 2004; Panwai and Dia, 2005; Laagland, 2005; Hawas, 2009; Soria *et al.*, 2014). A few of the above tools are briefly touched on below.

Documentation provided by Transport Simulation Systems (TSS) suggests that its AIMSUN system comprises macroscopic, mesoscopic and microscopic levels of detail, where vehicular flow is shown at the macroscopic level of detail but simulated using a microscopicmesoscopic hybrid (Barceló *et al.*, 1998). The system uses an extended Gipps' model (Gipps, 1981) for the microscopic part of the simulation, and a mesoscopic model developed by Burghout (2004) and Burghout *et al.* (2005) to make a hybrid of the two (Barceló *et al.*, 2005).

CORSIM is an urban traffic modelling system and is comprised of two other distinct sub-

simulation packages: FREESIM for simulating freeway flow and NETSIM for representing non-freeway urban traffic (Gao, 2008), and they are implemented by using macroscopic and microscopic principles, respectively (Bloomberg and Dale, 2000; Prevedouros and Wang, 1999).

INTEGRATION is another multi-scale system, where traffic flow is simulated only at a microscopic level of detail and then macroscopic features and behaviours are captured for ease of analysis (van Aerde *et al.*, 1996; Prevedouros and Wang, 1999). There are also agent-based simulations, such as the Multi-Agent Traffic Simulation Toolkit (MATSim-T), which directs agent-based traffic and uses phase modelling and a signal-timing algorithm to control the intersections (Horni *et al.*, 2009).

2.9 Empirical Analysis of Driver Models

Within the literature there has only been limited empirical analysis of 'driver model' behaviour in urban traffic flow, *ie:* how the models react in typical vehicle interactions in an urban setting. In particular, exploring situations with the models involving intersections and their inherent behaviours has been largely overlooked in favour of examining behaviour on freeways (free-flowing traffic) or theoretical mathematical analysis.

For example, Esser and Schreckenberg (1997) build a simulation tool to evaluate traffic management strategies when traffic density is close to the carrying capacity of roads. In this case, the cellular automata N-S algorithm is used, however, only overall traffic behaviour such as throughput and correlations between intersections is analysed rather than detailed interactions between vehicles.

Others either emphasise traffic flow stability (Treiber *et al.*, 2007; Pueboobpaphan and van Arem, 2010), examine additional improvements for stability in traffic flow (van Arem *et al.*, 2006; Schakel *et al.*, 2010), or investigate the phenomena called hysteresis which is a characteristic of congested traffic flow where the flow does not always go back to normal immediately after a disturbance, and is especially found in stop-and-go flow (Treiber *et al.*, 2000a; Papageorgiou *et al.*, 2008; Ahn and Vadlamani, 2010).

Furthermore, most simulations used for traffic flow analysis only concentrate on one model

type (Esser and Schreckenberg, 1997; Treiber *et al.*, 2000a; Kesting and Treiber, 2008; Daganzo *et al.*, 2011). Yet others have shown that heterogeneous models are valuable tools, but have mostly examined a multi-scale microscopic/macroscopic mixture (Helbing *et al.*, 2002; Bourrel and Lesort, 2003; Cristiani *et al.*, 2012b).

In contrast, the focus of this thesis is on modelling driver behaviour in urban settings, where the emphasis is on how the vehicles interact with each other in common traffic situations. This is important since if the detailed behaviour of a driver model is unrealistic, it calls into question the validity of any results or conclusions drawn about the aggregate traffic flow behaviour of a simulation based on that model. Since the microscopic stimulus-response continuous models are currently an active section of research, this thesis examines the behaviour of a variety of these car-following models in several typical urban scenarios relating to intersections.

2.10 Summary

The major traffic flow models, together with their advantes and disadvantages, are summarised in the tables below.

Table 2.1: Summary of macroscopic models.

Model	Advantages	Disadvantages
LWR	• 1st order model • Handles congested conditions with modifications	• Unique soln not guaranteed • Changes in traffic state produce infinite accel
Payne	• More accurate than LWR • Addresses infinite accel behaviour from LWR • Addition of merging term • Discretisation of PDEs into ODEs to derive numerical soln and reduce computation time	• More complicated than LWR • Unique soln not always guaranteed
Aw & Rascle	• Ability to handle multiple lanes • Macro/micro hybrid model developed • Addresses some shortcomings of LWR	• More complex than Payne model

Table 2.2: Summary of microscopic continuous models.

Model	Advantages	Disadvantages
Pipes' Model	• Simple	• Unpredictable behaviour not considered
Newell's Model	• Simple • Applies an effective time delay	• Inadequate stop-and-go flow handling
Gipps' Model	• Relatively accurate and realistic	• Relatively complicated, large number of parameters
GHR Model	• Simple • Has macro version	• Small changes in relative velocities may cause large reactions • Vehicles still react with large headways
OVM	• Simple and computationally efficient • Depicts properties of real traffic flow	• Unreasonably high accel in free driving conditions • Unrealistic decel for relatively small headway
GFM	• Overcomes OVM's unreasonable high accel	• Issue with unrealistic deceleration
FVDM	• Overcomes OVM's and GFM's unrealistic decel issues	• Unreasonably high accel • Non-smooth transition due to step function
FVADM	• Avoids collisions where accel diff vital	• Non-smooth transition due to step functions
IDM	• Conceptually, computationally simple • Realistic in emergency decel scenarios • Equivalent macro model	• Cautious with accel and decel for large headway
Action Point Models	• Large headway has no impact on close vehicles • Small headway only affects vehicles if large change in relative velocity and headway	• Difficult to calibrate

Table 2.3: Summary of microscopic discrete models.

Model	Advantages	Disadvantages
Rule 184	• Simple, basic model	• Only handles single-lane systems • Able to deal with only very simple vehicular movement
BML	• Can show phase transitions of vehicular movement	• Unable to simulate traffic intersections
N-S	• Simple to understand, implement and analyse • Computationally inexpensive • Can simulate roads and intersections	• Single lane only, but can be extended

Chapter 3

Simulation Infrastructure

The goals of this thesis require the implementation of a flexible framework to allow for different mathematical driver models to be efficiently compared and tested in varying traffic situations, in particular urban traffic conditions. The underlying elements in this structure are the mathematical driver models, which are essentially complex formulas that endeavour to encapsulate driver behaviour given the traffic context as accurately as possible. A model on its own, however, is a theoretical concept, and thus needs a mechanism that will allow it to repeat its calculation over a specified number of steps using a feedback loop *ie:* a 'simulation'. A simulation controls the model calculations by the use of a 'timestep'. This is an arbitrary timeframe in which the model's computations are applied to all vehicles before the simulation continues with the next timestep.

To test models so that comparisons are interpretable, have context, and can be replicated as necessary, requires a specific set of conditions. These traffic 'scenarios' (or situations) are generally centred around areas of high interest (*eg:* where traffic flow changes) and can effectively test the model's reaction to those changes.

Given that different models will need to be tested with various traffic scenarios in the simulations, the development of a flexible system where components can be swapped seamlessly and the structure can be modified as required to run the simulation is essential. This means that the system's basic building blocks such as links (roads) and nodes (intersections) must be adaptable to suit both the model being tested and the traffic situation being assessed.

A system, mainly been written in C# with some C++ helper classes, was hence developed to support these requirements, including the ability to construct road networks of different configurations, with Matlab being used for analysis purposes. This chapter describes the details of the system's infrastructure and its simulation execution.

3.1 Scope

Flexibility and responsiveness to changes in configuration and simulating different models is essential to support the objectives of this thesis as outlined in Chapter 1. In terms of model types, macroscopic and mesoscopic models have not been considered for this investigation, since a mixture of macroscopic / microscopic models has been quite thoroughly examined in other research (van Aerde *et al.*, 1996; Helbing *et al.*, 2002; Bourrel and Lesort, 2003; Olstam, 2004; Wang *et al.*, 2006; Lattanzio and Piccoli, 2010; Bevrani and Chung, 2011; Newell, 2011). Rather the focus here is on testing different microscopic models combined, including both continuous car-following and discrete cellular automata variants, either on their own as a homogeneous structure or an amalgamation of the two to produce a heterogeneous network. The latter option has had very little exploration in the literature and is thus of interest.

Models that are considered for examination in this thesis have been reviewed at some length in Chapter 2. The simplest of these models is the Optimal Velocity Model (OVM) (Bando *et al.*, 1995), which was modified to produce the Full Velocity Difference Model (FVDM) (Jiang *et al.*, 2001) and the Full Velocity and Acceleration Difference Model (FVADM) (Zhao and Gao, 2005). Lastly, the Intelligent Driver Model (IDM) (Treiber *et al.*, 2000b) is examined, a model that is based on different premises to the above-mentioned models.

The road network structure itself must be adaptable to different traffic structures such as various types of urban intersections *eg:* t-junctions, and be able to handle different starting positions and numbers of vehicles per road section. The models themselves do not inherently incorporate multi-lane actions (such as lane-changing and merging), and so separate algorithms need to be constructed to support these operations. Hence only simple single-lane roads are included in the system so that results can be directly attributed to the models rather than potentially being associated with the implementation of the auxiliary algorithms.

Urban settings with the characteristic stop-and-go traffic flow and acute right-angle turns have a more complicated structure than freeways. This forces vehicles to respond more acutely since the traffic flow changes more dynamically and gives rise to more variety in vehicle reactions to changing situations. Urban traffic also provides a broader choice of

traffic scenarios for model testing. Since testing the models under more extreme conditions is a primary aim, an urban configuration was chosen for the system.

A set of distinct types of nodes (intersections) have been selected to connect the links (road sectors) together in the system and to provide the means to test specific traffic scenarios. These include a *t-junction* where vehicles can either turn left or right, a *four-junction* which allows traffic to turn left, right or to go straightforward, and a *throughway* that does not modify traffic flow but directs vehicles straight through to another link. Links are either of a microscopic continuous or microscopic discrete nature, depending on the model being tested.

Links are responsible for carrying vehicles, and as all vehicles have equivalence in the system, different driver behaviour (*ie:* passive versus aggressive driving) and different types of vehicles (*eg:* trucks versus motorcycles) which would have different lengths and accelerations, are not considered. This means that every vehicle is interchangeable, but the decision-making of each vehicle is still independent and unique, which allows for unbiased model testing.

3.2 Network Modelling

3.2.1 System Outline

To make the system as adaptable as possible with respect to testing models, it is essential that as many components of the system can be seamlessly interchangeable with comparable items without affecting the simulation. This means that the system will have the ability to create a variety of network configurations with different types of nodes and links (continuous and discrete) quickly and smoothly, depending on which model and scenario are being tested.

Vehicle routing and decision making around the network is done by the use of conditional probability matrices that are assigned to each intersection in the initialisation phase of the simulation, called the *transition probability* of the intersection. Each outgoing link has a specific probability of being selected as a destination conditional upon the incoming link that a vehicle is approaching the intersection on (see Section 3.3 for more details). The

vehicles themselves are responsible for deciding which direction to take according to this transition probability. Intersection nodes consist of a mini-network of 'internal' nodes that route vehicles safely (*ie:* without collisions) through the intersection. Thus once a vehicle has decided on a direction, it navigates a route through the intersection node in order to make it through to the chosen outgoing link. It is the intersection node's task to guide the vehicle correctly through its internal nodes and links rather than having the vehicle direct itself, since model performance is under consideration rather than driver behaviour.

Nodes are joined by one-way directional links. A link represents a single lane of traffic, hence a dual-carriage road would require two links, one in each direction. The direction that a link is connected to a node determines whether that link is *incoming* to the node or *outgoing* from the node. Typically, a link represents a section of road between two intersections, though it may be broken into subsections if necessary with simply 'throughway' nodes joining the subsections. Different types of links exist, specifically a continuous link versus a discrete link. These support different driver models — car-following or cellular automata respectively. Hence a heterogeneous network can be built by placing the different link types in different sections of road within the same network. One type of link would then connect as an incoming link to a given node and that node's corresponding outgoing link could then be a different type of link. The node is then the switch-over point between the two driver models operating on each link.

Whilst the system has been implemented in such a way that collisions are avoided within intersections due to the focus being on testing models in stop-start situations, it is still possible for collisions to occur if a vehicle overruns the vehicle ahead of it along a straight link. If this occurs during a simulation, it would be a failure of the model, and hence collisions are detected throughout the system.

Timesteps essentially control the pace of the simulation, with the next timestep not being invoked until all calculations for each vehicle have been executed for the current timestep. The length of each timestep is an arbitrary decision, and due to the fact that one of the models being tested is of a discrete nature (*ie:* only produces integers rather than floating point numbers) all simulations have a one second timestep interval.

The system generates data for individual vehicles at each timestep (*eg:* position, headway, velocity, etc). These disparate pieces of information are extracted from the system and amalgamated together for collective analysis purposes where specific questions can be

answered, *ie:* is the headway consistently within the safety distance or are vehicles either too close or too far apart; is there extreme acceleration or deceleration in situations where there should be neither, etc. Careful selection of scenarios for testing purposes enables the exploration of the models' capabilities and limits. The feedback gathered from the data is helpful in determining which model performs better in which circumstances, and conclusions can be drawn on the strengths and weaknesses of the models.

3.2.2 Simulation Design

As mentioned previously, the simulation's task is to propagate vehicles along the links and nodes that form the network's topology according to the link's active driver model calculations. Each link potentially has a different driver model executing on it, allowing for the building of heterogeneous networks. Thus the network links must be able to support the different types of driver models, with the main issue being continuous versus discrete models since different continuous models can all operate on a continuous-type link, but are not suitable for use on discrete links and vice-versa. Therefore two types of links are implemented to support these two categories of models. Links can be seamlessly swapped from one link type to another with no further consequences on the rest of the network's operation since nodes act to isolate the workings of different links.

3.2.2.1 Simulation Progression

Prior to running, the simulation sets some initial conditions, including parameters for the driver models (often referred to as 'calibration') and probability distributions for transitioning vehicles from one link to another via nodes. A timestep counter is implemented to control the movement of each vehicle for every action that they take. This timestep defines the discrete time interval that the simulation progresses time forwards (typically an interval of one second is used but finer or coarser granularity can be employed).

Time progression occurs in rounds, where at each discrete timestep the next (predicted) position of each vehicle is calculated using the model's formula and the current state of other vehicles on the network. Only when the new position for every vehicle has been determined will the simulation update every vehicle to the new position. This *predict-update cycle* ensures that model update decisions are always made using the previous

timestep state of all other vehicles rather than intermixing new state data with old.

Finally, any problems or decisions the vehicle may encounter after this update that are outside the scope of the driver models must be handled by the simulation in a realistic manner. These include:

- Intersections — These act like traffic marshal obstacles to vehicles and oblige a vehicle to decelerate on approach. When the intersection is clear of oncoming traffic, the vehicle is allowed to accelerate again, though the rate of acceleration is determined by the driver model.
- Collisions — Accidents between vehicles may occur due to driver model error and this is detected and handled by the system.
- Route decision-making — Deciding which direction to proceed at an intersection is determined by the transition probability that is associated with the intersection. The driver model is given back control after a route has been mapped out through the intersection using the probabilities and the basic node structure that comprises the intersection.

It is assumed that the model itself will handle all other issues related to acceleration and deceleration.

3.2.2.2 Routing and Route Planning

Nodes connect incoming links to outgoing links and arbitrate the decisions for choosing which outgoing link an incoming vehicle will be moved on to (simulating the process of a driver making a routing decision). Underpinning this decision making, each node is assigned a transition probability matrix by the simulation at the initialisation stage before any vehicles commence movement.

For the purposes of this thesis, these probabilities are randomly generated and remain associated with the node for the life of the simulation (the only restriction is that u-turns have probability of zero). The decision of which way to travel when getting to an intersection is of course restricted by the structure of the intersection itself *eg:* a t-junction

would allow for only two choices, either turning left or right, with the probabilities attached to the particular t-junction determining which direction the vehicle is most likely to turn. Note that a throughway does not give a vehicle any other option except for going straight so there are no probabilities attached to this intersection type.

A route plan is implemented for all vehicles a distance of $50m$ ahead of its current position, simplifying the predict phase of each timestep by looking far enough ahead so that the vehicle knows where it is going (the plan). It is then up to the model to execute this plan. This is essential for upcoming intersections, where the vehicle needs to know which direction to proceed for the given choices available and the probability of taking each direction that the intersection provides.

3.2.2.3 Vehicle State

A simulation is composed of the network topology chosen, the driver models active on each link and the information of all vehicles in the system. Only the latter (the vehicles) changes during the running of the simulation timesteps, hence the *state* of the simulation is considered to be the *combined state* of all vehicles within it. Thus the simulation tracks all relevant vehicle state details at every timestep including:

- Link — link that the vehicle is travelling on.
- Position — location of the vehicle in metres (m) along the link. A position of zero implies the vehicle is at the beginning of the link.
- Velocity — the velocity that the vehicle is travelling at on the link in metres per second (m/s).
- Headway — the distance between the current vehicle and the vehicle ahead of it in metres (m).

Other pieces of state information about a vehicle also exist, but are identical for all vehicles to avoid vehicle properties from affecting experimental results. These include:

- Vehicle length — the amount of space a vehicle takes up on the link length-wise in metres (m).

- Level of driver aggressiveness — all vehicles act and react in the same manner, mediated by the driver model controlling their behaviour, as individual driver behaviour is ignored.

These are constant values within the system and so it is not necessary to track them as part of the vehicle state.

Finally, note that certain properties of a real vehicle are instead completely described by the mathematical driver model rather than an attribute of the vehicle. In particular, the performance capabilities (acceleration and deceleration) of a vehicle are an outcome of the model calculations – part of the aims of this thesis is to analyse how realistically models react, hence it is important not to impose limits on these reactions. The maximum acceleration is set as a constant for all models.

3.2.2.4 Predict-Update Cycle

The simulation runs a predict-and-update cycle at each timestep for each vehicle. In general, the system predicts (calculates) each vehicle's next move according to the relevant driver model and (if applicable) node decision link routing and then updates (executes) the move after all predictions have been performed for all vehicles. During prediction, the relevant vehicle state information is provided to the model so that the acceleration can be calculated. The acceleration is then applied to the vehicle's current state (adjusting velocity, and in turn position) to calculate how far the vehicle will move in this timestep. This is used to determine where the vehicle will be positioned for the update step (taking into account node routing decisions).

Predict Predict forecasts the positions, velocities and accelerations of vehicles in the next timestep based on the current data of these parameters. This is done so that the system determines where vehicles will end up given prevailing conditions, including whether a vehicle will transit a node or move to another link in the next timestep. Other external issues such as potential collisions, however, are ignored at this point. The vehicle's route plan is updated to include the estimated new data.

Update This stage is split into two phases. Phase one performs an update of every vehicle's position according to the results of the prediction for that vehicle. This may involve transferring a vehicle from one link to another. This ensures that all vehicles have been updated to their new state. Phase two of the update then determines the (new) headways between all vehicles and passes this to the appropriate driver model to calculate each vehicle's new acceleration, ready for the next timestep's predict step.

3.2.3 Links

The basic task of a link is to join two nodes of any type together. For example, a link can connect one end of a link to a t-junction node and the other end to a throughway node, acting as a means of transporting vehicles between two nodes.

Links have the following attributes:

- Length — the length of the link in metres (m). Note that a link may have zero length, which is useful when constructing sets of nodes that define traffic flow within an intersection (see Section 3.2.4.2).
- Type — the category of link, either continuous or discrete.
- Speed limit — the maximum velocity at which a vehicle travels in metres per second (m/s).
- From node — the node that the link is outgoing from.
- To node — the node that the link is incoming to.
- Collision flag — a flag to indicate whether vehicles have collided on the link during the last-processed timestep.

Links keep track of the vehicles that are travelling on them and are able to add and delete vehicles whenever necessary, for example, when vehicles leave links or enter links, or when collisions occur and vehicles need to be cleaned up. Only single lane links are implemented since multiple lanes would add complexity to the network by allowing for lane-changing and merging, which is behaviour that is beyond the scope of this thesis.

Depending on which type of driver model is being simulated, links can be of either a continuous or discrete nature. This is due to the different way calculations are done by the respective models, which changes where and how vehicles are placed on the links for each timestep.

3.2.3.1 Continuous Links

In continuous car-following models the road is viewed as a continuous space containing vehicles that can be located at any particular point. Each vehicle is represented by its position on a link, with the position being a floating point value. Thus the lengths of the links and the maximum speed can be any value in continuous distance and time space.

Due to this, computations done by the driver models retain high precision during simulations, and the vehicle is moved to the new position by the exact calculated amount of distance for each timestep. This leads to a more fine grained and accurate representation of real world vehicle motion at each timestep, not only allowing for more realistic vehicle behaviour but also avoiding the accumulation of rounding errors. However, this comes at the cost of increased computation since the models tend to be more complex in attempting to produce more realistic vehicle motion.

3.2.3.2 Discrete Links

For discrete cellular automata models each link is divided into equal-sized units called 'cells'. Each cell can be either empty or occupied by a vehicle. The length of the link is defined by the set of cells that it is comprised of, and so $\textit{length} = \textit{number of cells} \times \textit{cell length}$ since all cells are the same size. As a consequence the number of cells per link is known, and the number of cells divide evenly into the link length, ensuring that no partial cells are created. This results in vehicle velocities and speed limits being rounded to the nearest whole cell.

Unlike the continuous car-following models, cellular automata driver models are based on integer values for position, velocity and acceleration. Thus vehicles may only move a discrete number of cells each timestep. This limits the accuracy of vehicle positioning and motion and so reduces the accuracy of the model approximation of real-world traffic.

However, the simplicity of these models increases computational speed.

In this thesis, the assumption is that a vehicle fully occupies a single cell and does not occupy any other cells. This simplifies the driver model's calculations. Some models allow partial occupation of cells by vehicles at the cost of increased computational complexity.

3.2.4 Nodes

Nodes are connected to each other via links and their purpose is to correctly transfer vehicles from one link to another. Each node is connected to one or more incoming links and one or more outgoing links. All nodes have a conditional probability matrix defining the likelihood of a vehicle transitioning from a given incoming link to an outgoing link that is used to control the expected traffic flow choices that vehicles make.

Nodes can contain other nodes within them. This specifically facilitates the ability to define a single intersection node whose complex internal structure is defined by a set of contained (internal) nodes and links. External road links then 'attach' to the composite parent (intersection) node, and the parent node (knowing its own internal structure) re-attaches these external links to the correct internal node so that traffic flows correctly for that intersection according to the internal structure. See Figures 3.2 and 3.3 for examples. This facilitates both ease of reuse of intersection nodes and to hide the complexity of an intersection from external links.

Nodes have the following attributes:

- Name — a description to uniquely identify a node
- Type — type of node *ie:* basic, throughway, t-junction or fourway-junction
- List of incoming links
- List of outgoing links
- Transition probability matrix

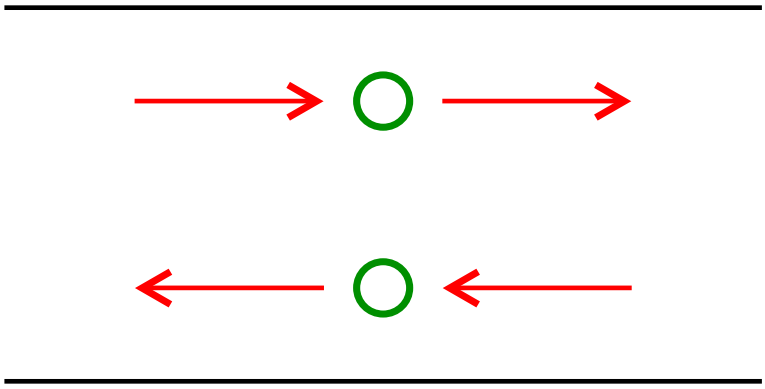

Figure 3.1: Basic node. Solid red arrows are incoming or outgoing links to / from the basic node indicating traffic flow, green circles represent the basic nodes.

3.2.4.1 Basic Nodes

Basic nodes only represent a single point in space. This implies that all incoming links to a basic node will converge to the same location. Figure 3.1 shows the traffic flow directions (red arrows) and the basic nodes (green circles). On its own, this is of limited use since it would result in vehicle collisions. Instead, basic nodes are used as 'building blocks' to construct the internal details of guiding traffic within the more complex composite nodes from incoming links through to the correct outgoing link without producing collisions.

For defining transition probabilities, basic nodes define a conditional probability matrix:

$$P(\mathcal{O}|\mathcal{I}) \tag{3.1}$$

where $\mathcal{O}$ is an outgoing link and $\mathcal{I}$ is an incoming link. This defines the probability of a vehicle that is approaching an intersection on link $\mathcal{I}$ choosing to transit to link $\mathcal{O}$ upon exiting the intersection. A matrix of size $\mathcal{O} \times \mathcal{I}$ is used to represent this probability. A vehicle randomly samples from the matrix in order to select its outgoing link according to the probability distribution implied by the matrix.

3.2.4.2 Composite Nodes

Composite nodes represent intersections in the system. Each intersection contains a mini-network of basic nodes connected by links that have zero length. The purpose of these

zero length links is to act as a hinge between two basic nodes to facilitate a change in direction within the composite node, thereby channelling traffic along internal pathways to the appropriate outgoing link.

The shape and complexity of this internal structure depends on the structure of the intersection, with each junction type requiring a distinct configuration to correctly move traffic from incoming links to outgoing links. As such, all intersections follow the set of road rules applicable to the particular junction type so that vehicles transit through safely and effectively.

Each composite node will have a different number of incoming and outgoing links depending on what type of intersection it is representing. For example, a t-junction has two side-road links (one incoming and one outgoing) and four main road links (two incoming and two outgoing in opposite directions). Note that all roads in this thesis are two-way thus each intersection has the same number of incoming links as outgoing links.

Similar to basic nodes, a composite node defines a matrix for $P(\mathcal{O}|\mathcal{I})$ to specify the transition probabilities from incoming to outgoing links. However, unlike basic nodes a composite node is merely a container for a network of internal (basic) nodes that the vehicle *actually* transfers through. Thus the composite node's transition probabilities must be mapped (copied) to the transition probabilities of the internal nodes it is comprised of, and in such a way that maintains the transition configuration of the overall composite node as seen from outside the intersection. For example, if there is a 70% chance of travelling straight and 30% chance of turning left at an intersection, the internal node probabilities must be set such that 70% of vehicles travel straight and 30% of vehicles turn left.

This thesis utilises three types of intersection: throughways, T-junctions and fourway-junctions. Each type has a different structure and hence must map its transition probabilities onto its internal nodes differently.

Throughway Figure 3.2 shows the internal structure of a throughway intersection. This type of intersection consists of two incoming links and two corresponding outgoing links, therefore there is no deviation in traffic flow in this structure. Throughway nodes are useful for breaking a single section of road into subsections so that each subsection may execute a different driver model.

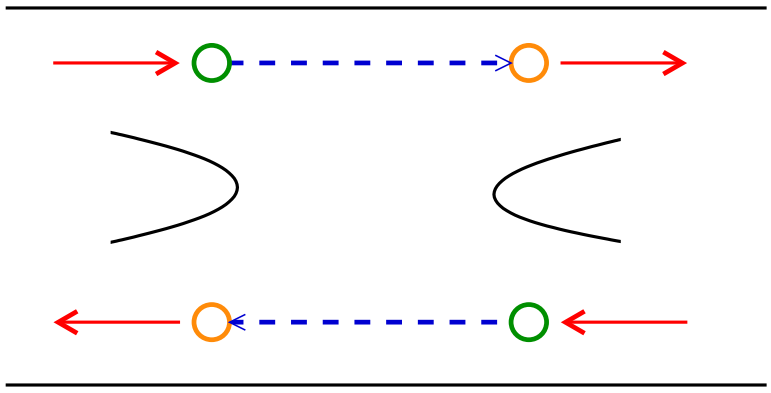

Figure 3.2: Throughway intersection in simulation. Solid red arrows are incoming or outgoing links to / from the junction, dotted arrows represent internal transitions within a junction, green circles represent entry nodes and yellow circles represent exit nodes. There is no potential for collisions in this intersection.

Since the throughway structure is quite simple, its transition probability is also simple: each incoming link has only one possible outgoing link (probability = 1.0), and hence the probability matrix $P(\mathcal{O}|\mathcal{I})$ is an identity matrix. Mapping this to the internal nodes is also straightforward — each incoming/outgoing pair is connected to a basic node that is disconnected from all other nodes inside the throughway, therefore each internal node has a 1×1 matrix $P(\mathcal{O}|\mathcal{I}) = 1.0$.

T-Junction T-junctions incorporate three incoming and three outgoing links in a 'T' configuration (see Figure 3.3). The link that terminates at the intersection of all the links is termed the 'feeder' link in this thesis and this link must give-way to vehicles travelling on the main links. The feeder link has a choice to turn either left or right while the main links can either travel straight or turn into the feeder link. The probability matrix $P(\mathcal{O}|\mathcal{I})$ is a $3x3$ matrix to specify the three different directions a vehicle can turn at in a t-junction, note that the probabilities for the u-turn entries are all zero so that the system does not allow u-turns.

The t-junction has a more complicated transition probability mapping than the throughway. Since this intersection type allows vehicles to change direction, the basic nodes within the intersection will have different tasks. There are 'entry' nodes which are the first basic nodes that a vehicle encounters when entering the t-junction, and they are the critical point around which the route mapped through the intersection transpires. The

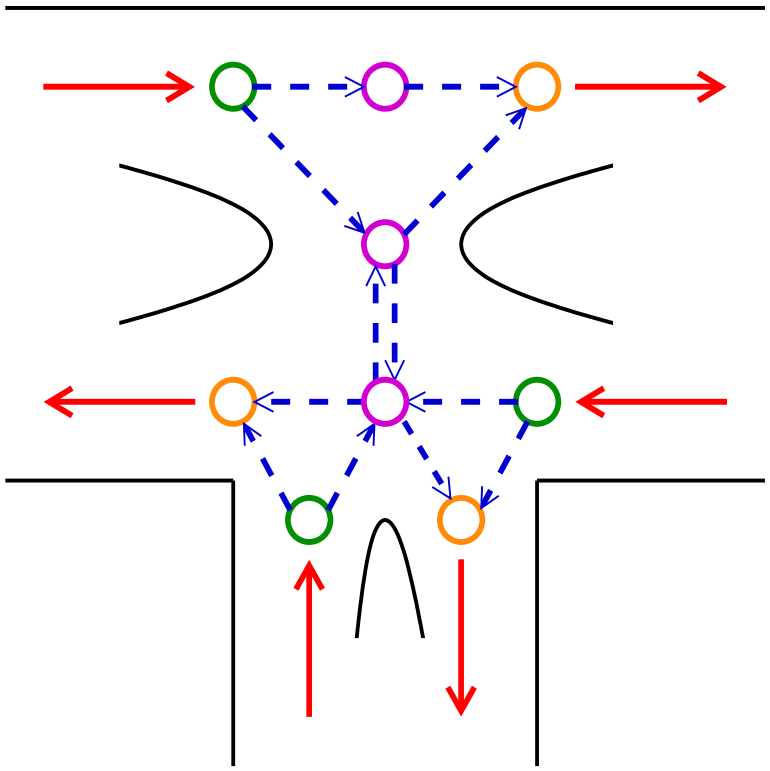

Figure 3.3: T-junction intersection in simulation. Solid red arrows are incoming or outgoing links to / from the junction, dotted blue arrows represent internal transitions within a junction, green circles represent entry nodes, yellow circles represent exit nodes and magenta circles represent staging nodes where a potential collision may occur.

'exit' nodes are the last basic nodes that vehicles must traverse through to leave the t-junction. In between these two basic nodes are 'staging' nodes, and their job is to safely move vehicles from the entry node to the correct exit node as designated by the vehicle's route plan. This is done by transferring the transiting vehicle from their current direction to the new direction via a 'path' that is comprised of basic nodes and internal zero length links. Staging nodes can also be used for collision detection by recognising when vehicles cross the same path.

A single basic node can be used in multiple pathways by vehicles, where it is the incoming link that differentiates the path being travelled by each vehicle. See Figures 3.4 and 3.5 for an example where two vehicles taking different routes have a potential for colliding on the staging nodes since they have an overlap on some parts of their paths. As can be seen, the same staging node is traversed by both vehicles, and this would be a potential collision

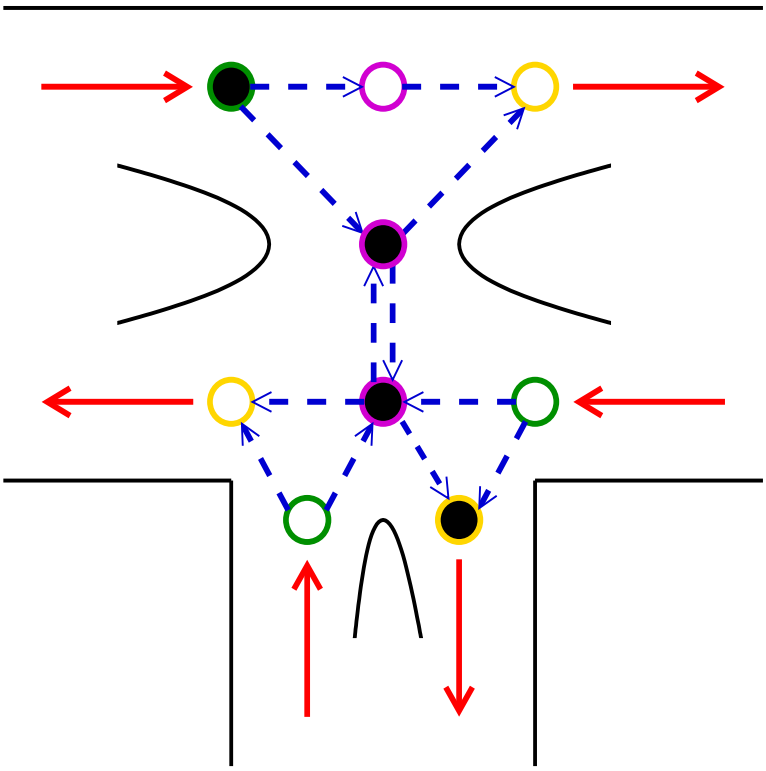

Figure 3.4: One possible path a vehicle can take through a T-junction. Path is indicated by black-coloured in circles.

point since at the moment when a vehicle enters the intersection it also technically exits the intersection at the same time due to the links being of zero length (and of course nodes have no length inherently). In essence this means that vehicles cannot 'sit' inside an intersection, which is unrealistic but does remove this circumstance as yet another problem the simulation has to handle.

Fourway-Junction In a four-way junction (Figure 3.6), two roads cross over and traffic on either road can either move straight forward or turn left or right, thus it has four incoming links and four outgoing links. In this thesis, all fourway-junctions define one main road that has right of way, with the second road being a feeder road that is required to give way to traffic on the main road. This avoids the possibility of deadlock situations that could occur in give-way-to-the-right scenarios if four vehicles arrive at the intersection simultaneously.

For a four-way junction the probability matrix $P(\mathcal{O}|\mathcal{I})$ is a $4x4$ matrix to specify the

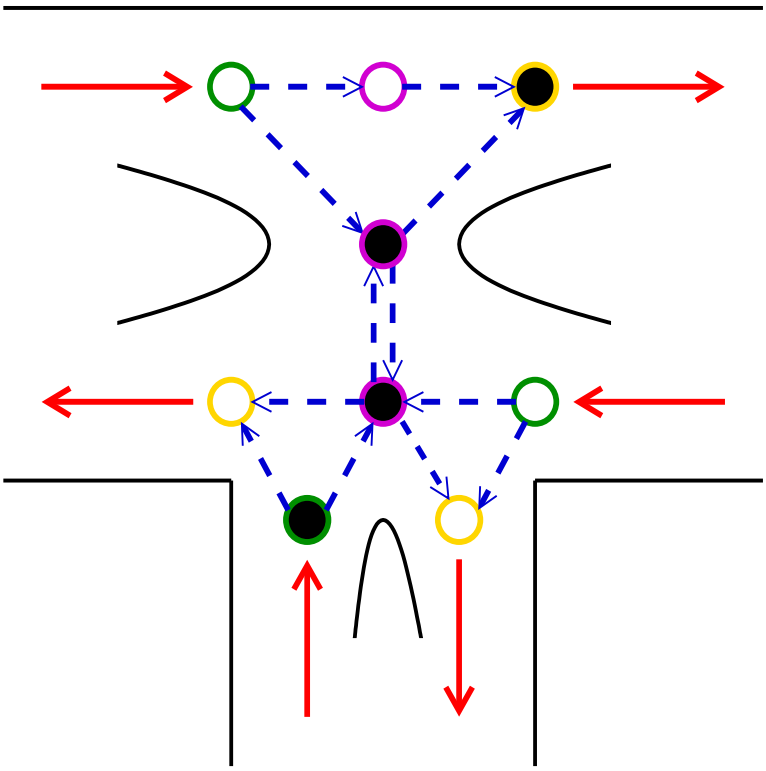

Figure 3.5: One possible path a vehicle can take through a T-junction. The path is indicated by black-coloured in circles.

four different directions of the intersection, and again excludes a u-turn by setting the probability for this option to zeroes. Entry, exit and staging nodes also facilitate vehicle movement through the intersections as discussed for t-junctions, but the organisation of these nodes is different since a fourway-junction is more complicated. See Figure 3.6 for a comprehensive view of this arrangement.

Note that a roundabout is a variant on a fourway-junction and is widely used in real-world traffic situations. However, it has not been implemented here since it is also possible to produce a deadlock situation due to the give-way-to-the-right requirement of roundabouts if four vehicles arrive simultaneously from each direction. The likelihood of this occurring is heightened by the wide safety margins the system employs to avoid collisions (see Section 3.2.5.2). This is necessary since the focus of investigation in this thesis is on the driver models in stop-start traffic, and not the effect of different types of intersection on traffic flow.

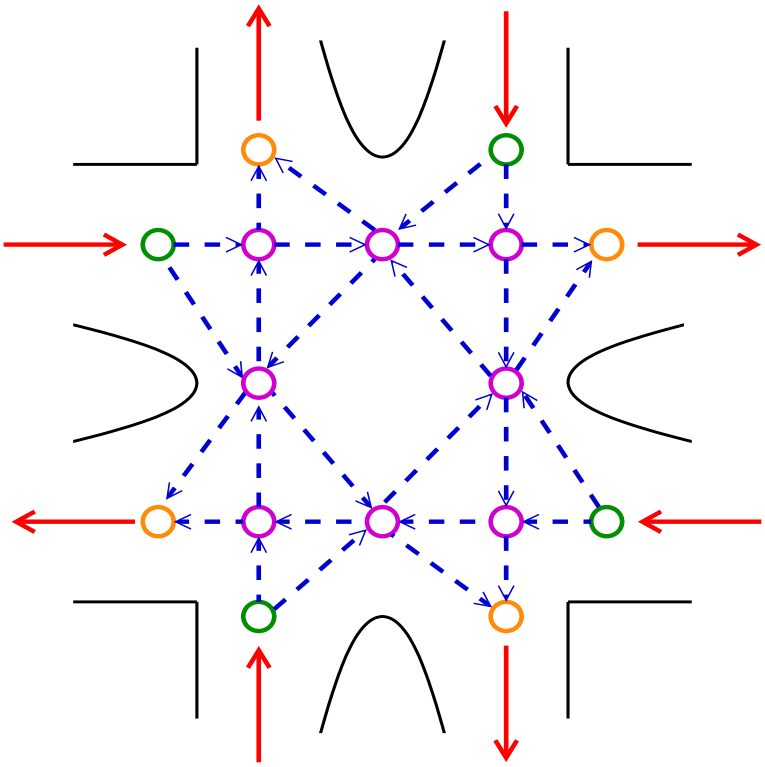

Figure 3.6: Fourway-junction intersection in simulation. Solid red arrows are incoming or outgoing links to / from the junction, dotted blue arrows represent internal transitions within a junction, green circles represent entry nodes, yellow circles represent exit nodes and magenta circles represent staging nodes where a potential collision may occur.

3.2.5 Intersection Traffic Management

3.2.5.1 Controlled and Uncontrolled Intersections

Driver models are only concerned with the movement and interaction of vehicles, and are independent of other structures that may exist in a simulation system such as intersections. However, traffic flow in an urban environment must be managed effectively to support the driver model process and design traffic scenarios for analysis. This is the main task of intersections. A controlled intersection is one where devices (such as traffic lights) dictate which vehicles can cross the intersection, and when. This is usually done by using a time delay between different directions of travel in a round-robin pattern so that each direction gets fair a turn while the other directions have to wait.

When a vehicle approaches an intersection node, the vehicle's route plan that directs it through the node activates, allowing the vehicle to know which road link it will transition to when exiting the intersection. This is because the links in the composite node are each of zero length, and the internal nodes follow in close succession to each other with no apparent spacing between them. This means that a vehicle transitioning through the external node will never actually be on the link but rather will be hopping from node to node. The time to transition through the external node is only one timestep as vehicles do not spend any time on the internal links or nodes. It is therefore vital for the vehicle to plan a route through the external node's mini-network before entering the external node.

In this thesis, all intersections in this system are uncontrolled. This is because some scenarios for testing the models require interplay between vehicles which are only possible under uncontrolled conditions. For example, after giving way, a vehicle can slot in very quickly behind a passing vehicle when the way is clear and thus test how the model reacts in this circumstance. This is not possible to do in a controlled environment such as a traffic light since the intersection waits a pre-determined amount of time before allowing vehicles from another direction to enter the intersection. As such the node types adopted by the system are throughways (no change of direction, just channel traffic through), t-junctions (possibility of turning left or right) and fourway-junctions (can turn left or right, or go straight ahead).

3.2.5.2 Give-Way Processing

Intersections that are uncontrolled rely on conventional road rules to transfer vehicles through. The direction of traffic movement is therefore dynamic and is dependant on which vehicles have the right of way with respect to oncoming traffic. If a vehicle has right of way, the intersection is effectively acting as an open road for that vehicle. On the other hand, a vehicle that must give way essentially views the intersection as an obstacle on its path. The latter situation in fact operates identically to having a leading vehicle parked at the intersection — to the following vehicle, the leading vehicle blocks the path and the follower must decelerate to a stop behind it. In other words, if the intersection in a give way situation is interpreted by an oncoming vehicle as a zero-velocity leading vehicle at the intersection boundary, the driver model itself will use this as its headway and will (or should) take appropriate action to decelerate smoothly to a halt. No additional special processing is necessary — the onus of reasonable behaviour is on the driver model.

This has the benefit that an intersection needs to only 'switch' between an open or blocked state for any given incoming link and the simulation then provides the appropriate headway (either to the next vehicle or intersection respectively) to the driver model of any oncoming vehicle to react accordingly. To do this, the intersection queries all of its incoming links and decides which vehicles will need to give way, if any, based on distances to oncoming traffic and the links they are travelling on (*eg:* main road or feeder road).

However, a driver model will almost certainly produce poor results if the intersection flips erratically between an open and blocked state. To avoid this, the intersection is conservative in its safety margins. Specifically, it will assume a vehicle that has *potential* to be in a give way situation (*eg:* on a feeder road) is blocked *unless* it is certain that there is no vehicle which will arrive at the intersection in time to cause the give way situation to occur (*eg:* no nearby vehicles on the main road). Note that since all vehicles plan their routes ahead (see Section 3.3), the intersection will have all necessary information available to determine whether a vehicle may or may not cause a give way situation.

The margins used to define whether a give-way situation exists are deliberately chosen to be high (at least twice the distance required for the 'turning' vehicle to accelerate to the speed limit) to ensure that right-of-way vehicles are not impeded. Though this margin is conservatively high, it removes poor intersection choices as a source of collision in the simulation. However, collisions may still occur since the driver models themselves may not react appropriately to prevent them from happening (either at an intersection or within a road section), hence the system must detect collisions.

A collision occurs between two vehicles when the following vehicle overtakes the leading vehicle within one timestep, *ie:* they switch positions so that the following vehicle becomes the leading vehicle and vice versa. After a collision has been identified, the system halts the vehicles involved and they are removed from the network by the link three timesteps after the collision has occurred (simulating an accident and pull over to the side of the road).

Note that the speed at which a turn can safely be navigated by a real vehicle is not part of the system. This is because there is no definition as to how sharp any turn in the system is. Although desirable, such processing would introduce another layer of vehicle flow control, making it more difficult to clearly analyse the behaviour of different *driver models* (the goal of this thesis) as opposed to the necessary *simulation infrastructure implementation*

to support the analysis. Note that in Chapter 4, there *is* some processing specially added to model this more realistic slowing for a left hand turn from a main road to a side road (*ie:* not a give-way situation). However, this was done specifically for the purposes of that chapter and is not generally used elsewhere.

3.3 Routing Decision-Making

Routing vehicles through a network requires some type of planning. Simulations typically either plan out the full route of a vehicle given their source and destination or direct the vehicles to select a direction at each decision point (intersections), or a combination of both Esser and Schreckenberg (1997).

The former approach outlines the entire route for the vehicle, taking an initial starting position and detailing every link and node that the vehicle will pass through to a destination point (fully-planned routing). This mirrors drivers in the real-world, who tend to pre-plan their journeys from start to finish and do not drive around aimlessly. In order for such a fully-planned scenario to be effective, a shortest path finding algorithm (like Dijkstra's algorithm (Zhan, 1997)) must be implemented, which means extra computation and complexity for the simulation. The second approach could be termed 'just-in-time' routing, since the vehicles randomly choose their next decision only when they reach an intersection point.

However, neither of these approaches is appropriate for the simulations in this thesis. Fully-planned routing is computationally expensive and unnecessary for evaluating the detailed behaviour of individual vehicles. Specifically, this thesis is interested in the performance of the driver models rather than route selection. The simulation will also run in a closed system where no vehicles leave the network, and therefore destination points do not exist since the vehicles drive until the simulation terminates. On the other hand just-in-time routing means that other vehicles on the network will not be able to anticipate whether they are in a give-way situation or not. For example, a vehicle that is on a main road and indicates to turn left is informing other vehicles looking to enter the main road that they are not in a give-way situation.

Instead, this thesis takes a hybrid strategy, referred to as 'short-term route planning',

where all vehicles plan ahead by making a series of just-in-time decisions to generate a route plan that will cover the immediate future. Planning ahead is still implemented but is restricted to a short distance, and in this thesis the distance is twice the stopping distance of the vehicle at its current velocity, or $50m$ if the stopping distance is below that. The advantage of this approach is that a route plan is still created but it is simple and computationally inexpensive, and allows for tracking individual vehicle decisions so that these can be aggregated for analysis. Also, with no destination points, vehicles can travel through the network freely until the simulation terminates.

3.3.1 Short-Term Route Planning

Short-term route planning for a vehicle routing strategy allows for limited forward planning, so that journeys are smooth and not disrupted by unforeseen circumstances whilst keeping the computational component low. Projecting ahead is most crucial when vehicles approach an intersection, since it is in this circumstance that the vehicle must choose which direction to take, and the intersection itself must determine whether an incoming vehicle will need to give way or not (see Section 3.2.5.2).

Whilst intersections determine whether a vehicle must give way or not, the vehicle itself decides which direction it should take given the configuration of the intersection *ie:* a t-junction allows for a left or right turn whilst a fourway-junction allows for a left, right or straight ahead direction. Depending on the direction the vehicle chooses, it has to be determined which internal links and nodes within the intersection that the vehicle must travel on to transit through the intersection.

To facilitate consistent decision making regardless of which vehicle is approaching an intersection, vehicles sample from the fixed transition probability $P(\mathcal{O}|\mathcal{I})$ defined by the intersection. Sampling occurs by generating a random number from the uniform distribution $U(0..1)$ and using this lookup the index at which the cumulative probability of $P(\mathcal{O}|\mathcal{I} = i)$ meets or exceeds that number for incoming link i. The selected index is the index of the outgoing link.

Note that $P(\mathcal{O}|\mathcal{I})$ is not a uniform distribution. This is to emulate real-world conditions where traffic is heavier on some roads than on others. To emulate this, $P(\mathcal{O}|\mathcal{I})$ is generated randomly, with only u-turns explicitly set to zero.

The unique probability matrices generated for each intersection in the network are unchanged for the duration of the simulation. This is important since route planning occurs in advance of the vehicle actually entering the intersection(s) it is planning for. Moreover, the internal links within an intersection are of zero length and so it takes the vehicle one timestep to traverse the relevant internal nodes and links in the intersection. Therefore short-term route planning must be performed to select a route through the intersection before the vehicle actually enters the junction.

3.4 Summary

In this chapter we discuss a system that facilitates the simulation of traffic used to investigate driver model behaviour in an urban environment. To allow for flexibility and to achieve the aims of this thesis (see Chapter 1), the system was constructed using both continuous and discrete links for microscopic models, and various types of nodes were used to configure different types of intersections. The intersection arrangements include throughways, t-junctions and fourway junctions, and they are not only used to direct the traffic along the correct links, but also act as obstacles for the driver models to ensure that vehicles behave properly at intersections since this knowledge is not incorporated into the driver models themselves. A probability matrix was assigned to each intersection to control the throughput of each direction connected to that intersection.

To manage traffic flow effectively, short-term route planning was incorporated to facilitate movement through intersections by providing feedback to vehicles of other traffic also potentially transitioning through the same intersection. This simulation will be utilised for the investigations presented in the following chapters.

Chapter 4

Car-Following Model Behaviour Comparison in Urban Scenarios

The previous chapter introduced the simulation infrastructure developed to support the research goals of this thesis. However, due to the proliferation of markedly different car-following (continuous) microscopic driver models proposed in the literature ((Gipps, 1981; Gazis *et al.*, 1961; Bando *et al.*, 1995; Treiber *et al.*, 2000b; Kumamoto *et al.*, 1995; Kikuchi and Chakroborty, 1992; Wiedemann and Reiter, 1992; Nagel and Schreckenberg, 1992) etc), it is unclear which car-following model would be most suitable to employ. Whilst reviews listing the general strengths and weaknesses of each model exist (Hoogendoorn and Bovy, 2001; van Wageningen-Kessels *et al.*, 2014), to this author's knowledge no detailed *empirical* comparison of a range of car-following models has been conducted. Moreover, very little work exists on examining driver models in *urban* stop-start scenarios, with most analyses conducted on the free-flowing traffic found in freeways. Whilst it has been shown that some models such as the OVM, GHR and IDM have flaws that subsequent models attempt to overcome (Jiang *et al.*, 2001; Olstam, 2005; Treiber *et al.*, 2000b), no systematic empirical study has been undertaken to analyse the performance of a range of contemporary models, nor placed issues in the context of realistic everyday driving situations that are found in urban environments.

As a consequence, a selection of stimulus-response models was chosen for empirical investigation. As discussed in Chapter 2 these models are an evolution over the earlier safe-distance models such as Newell's model (Newell, 2002) and Gipps' model (Gipps, 1981) and there has been a resurgence of focus on stimulus-response type models in the last decade or so (van Wageningen-Kessels *et al.*, 2014). Action point models were not considered since although they also use safe-distance and stimulus-response concepts, their basis in rules and thresholds would require significant fine-tuning and urban settings do not follow the same rules as freeway traffic. Finally, fuzzy logic models, multi-class and multi-anticipation models are all extension of an underlying stimulus-response model rather than

an innovation hence analysing their behaviour would not provide any valuable insights into the fundamental model's behaviour.

Thus this chapter's purpose is to empirically investigate the effectiveness of several well-known and widely-used stimulus-response microscopic driver models in the context of urban traffic flow: the Optimal Velocity Model (OVM), the Full Velocity Difference Model (FVDM), the Full Velocity and Acceleration Difference Model (FVADM) and the Intelligent Driver Model (IDM). These experiments do not utilise the entire simulation infrastructure described in Chapter 3, but rather focus on examining the behaviour of the driver models in a variety of common urban scenarios involving stop-and-go manoeuvres around intersections. These scenarios are by nature short-lived (*eg:* braking for a yellow light, entering a road behind another vehicle, etc) and so occur within a small section of road and typically involve only pairs of vehicles. Once the scenarios have played out the vehicles would then enter into a free-flowing traffic situation, which is well-studied in the literature and is thus of limited interest here.

4.1 Traffic Flow

The nature of traffic flow in the physical world lends itself to being classified into two broad categories: 'freeway' flow and 'stop-and-go' flow. Freeway flow is typically comprised of progressive acceleration and deceleration phases, for example in merging actions, whilst the stop-and-go flow pattern forces vehicles to accelerate and decelerate relatively quickly and abruptly due to traffic devices such as intersections.

A simple yet effective method which traffic models use to moderate and control vehicle behaviour is the concept of *leading* and *following* vehicle interactions. The leading vehicle is the vehicle in front of the following vehicle, and the following vehicle's behaviour is dictated by the actions of the leading vehicle. If there is no leading vehicle most models will calibrate their parameters to ensure reasonable behaviour in this case *ie:* realistic acceleration and velocity bounded by the speed limit on the part of the leading vehicle.

4.1.1 Freeway Flow

In freeway flow the propagation of vehicles occurs smoothly with accelerations and decelerations being dictated by traffic diverging or converging in a relatively fluid motion due to lanes splitting or joining together. Since road interruptions such as intersections are absent from this setup, no stop-and-go actions occur. This means that freeway flow lends itself well to being modelled as aggregate vehicle flow rather than individual vehicle movements, a situation that suits macroscopic models well (Hoogendoorn and Bovy, 2001) since they approach traffic flow from a collective perspective. Microscopic models have also been applied to freeway flow (Helbing *et al.*, 2002), though due to their higher computational cost versus macroscopic models it has been recommended to utilise these only when detailed information of vehicle movements is needed such as found in the micro-simulation packages PARAMICS (Wilson, 2001) and AIMSUN (Bevrani and Chung, 2011).

In terms of flow analysis, a considerable amount of research has been devoted to studying the overall flow of freeway traffic, regardless of whether the driver model is macroscopic or microscopic. In particular, there is significant interest in studying areas of congestion (bottlenecks) associated with on-ramps, closing of lanes, uphill gradients, etc, and their associated shockwave propagation effects through the upstream traffic (Treiber *et al.*, 2000a). Little effort has been made to analyse vehicle-to-vehicle interactions in detail to ascertain whether their low-level behaviour is realistic (although this could only apply to microscopic models).

4.1.2 Stop-And-Go Flow

Stop-and-go flow requires driver models to appropriately handle sharp accelerations and decelerations of vehicles as well as other common interactions between vehicles, such as a following vehicle suddenly also becoming a leading vehicle to another vehicle after passing a junction. The intersections in urban environments create the stop-and-go nature of traffic flow, and it is difficult to model collective flow here since the intersection itself controls the flow rate, and this rate changes depending on the traffic context around the intersection (*eg:* give-way occurs only when oncoming right-of-way traffic is present). Hence it is more appropriate to model individual vehicle behaviour rather than collective flow here. This leads to relatively more complex models that are computationally heavy. However, this is

offset by the increased accuracy in simulating realistic vehicle performance.

Thus microscopic models are used extensively for modelling stop-and-go flow since these models monitor the movement of individual vehicles very precisely and can easily take into account the effect of intersections on vehicle flow.

4.1.3 Leading and Following Vehicles

Microscopic car-following models are based on the premise that vehicles that are behind ('following vehicles') another vehicle ('leading vehicle') will react appropriately when the leading vehicle decelerates or accelerates, such as keeping a minimum safe distance so that collisions will not occur. This means that the following vehicle by definition will always have another vehicle in front of it to influence its actions. However, if the leading vehicle does not have a vehicle in front of it and is therefore not a following vehicle itself, how should this leading vehicle operate?

Most models assume leading vehicles will accelerate to the speed limit before travelling at constant velocity unless they encounter an obstacle in front of them (*ie:* another vehicle or an intersection) and then these leading vehicles become following vehicles, reacting to the actions of the obstacle in front of them. Thus one simple way of simulating traffic flow for the purposes of analysis is to implement a circuit-style road where all vehicles will have a vehicle in front of them while they travel around, essentially creating a closed system.

Another method employed uses a straight road which is 'open' at both ends, where vehicles are 'generated' from one end and 'dropped' off at the other, thus having an open system where vehicles appear and disappear. Here, the first vehicle will not have another vehicle in front of it, whereas all other vehicles will form a chain following this lead vehicle (until that vehicle 'drops' off at the end of the road).

In both schemes, the driver model of the following vehicle utilises information about its state relative to the leading vehicle to make acceleration decisions (headway, relative velocity, etc — the precise information used depends on the driver model). If no vehicle is ahead (*ie:* it is the first vehicle), then the system will represent this by defining the headway as being infinite to the first vehicle's driver model, allowing it to accelerate unhindered to the speed limit.

As discussed in Section 3.2.5, this thesis also portrays intersections as if they are a (potential) stationary leading vehicle. This virtual 'vehicle' will have zero velocity and zero acceleration in a give-way situation, and will become the leading 'vehicle' for any vehicle approaching the intersection.

One issue with intersections is that they compel a vehicle to make a choice of which direction to take, affecting the determination of which vehicle should be considered the leading vehicle ahead of it. If the intersection is in a give-way state, then it becomes the leading 'vehicle'. However, if the intersection determines that the approaching vehicle has right-of-way, it becomes important to know what direction that vehicle will take in order to find the distance to the closest leading vehicle *along that direction after the intersection.* It is therefore vital that a route plan, especially through an intersection, is implemented for each vehicle so that the system is aware of which vehicle becomes a leading vehicle to another vehicle when the latter vehicle has made its move. Note that if no leading vehicle exists for a particular vehicle that is transiting the intersection (*ie:* there is no other traffic in the vicinity) then the 'leading' vehicle in this case is deemed to be infinity.

Taking advantage of the way leading and following vehicles interact, more sophisticated road structures can be inserted in urban environments without having to alter the models to handle them. In the case of an intersection, this can be viewed as a stationary vehicle or 'obstacle', and thus will become the leading vehicle for the model when a travelling vehicle approaches the intersection. This vehicle will then be able to act accordingly via the model's rules, becoming a following vehicle as soon as the intersection is detected and decelerating. The intersections can also act as open roads for vehicles when the way is clear from oncoming traffic.

Models discussed in this chapter calculate a vehicle's acceleration for each step in a simulation, and for the leading vehicle this would be zero, unless an obstacle (*ie:* intersection or another vehicle) is detected close enough for this vehicle to have to react by decelerating so that no collision occurs. The following vehicle's acceleration is calculated according to the leading vehicle's acceleration and by maintaining a safe space distance (headway) between the two vehicles. This means that if the leading vehicle decelerates, then the following vehicle has to adjust its acceleration accordingly so that no collision occurs and a safe headway is preserved.

For all of the models considered here, if no leading vehicle exists (*ie:* it is the first vehicle)

it is deemed that the headway is of infinite length, which will allow for constant acceleration. Another assumption made is that the acceleration is constant for each timestep in the simulation until the vehicle reaches the speed limit, at which point the acceleration becomes zero.

To determine how robust some of these models are to acute decelerations and sudden additions of following vehicles, four common space-continuous car-following microscopic models are analysed using traffic flow simulations, with the emphasis on how the following vehicles react to the leading vehicle's actions in an urban road setting.

Comparisons are performed between the OVM, FVDM, FVADM and the IDM. Note that all of these models can be classified as stimulus-response models which not only incorporate properties of safe-distance models, but are enhanced by the addition of reactions to external stimuli (see Chapter 2).

As these are microscopic models, the low-level behaviour of vehicles is examined rather than the aggregate behaviour as found in macroscopic models (see Chapter 2), and the goal is to find the conditions where each model performs poorly in terms of mimicking real driver behaviour in stop-and-go traffic scenarios.

The models' respective behaviours in different traffic situations are compared so that their effectiveness in simulating relatively realistic traffic flow can be ascertained and can be benchmarked against real-world GPS data. For the comparison, real-world microscopic measurements via GPS tracks are used to verify the credibility of each set of these results.

It is found that only the IDM approximates real-world driver behaviour to a reasonable level in all situations analysed. However, the IDM only represents the 'average' behaviour of drivers, rather than embodying a distribution of all types of drivers, as would be exemplified by real data collected via GPS.

4.2 Continuous Car-Following Models

As discussed in Chapter 2, car-following stimulus-response microscopic models are derived using the interaction dynamics between a leading vehicle and a following vehicle. In

specific terms, it is the measurement of the difference of the space distance between the leading and following vehicles, known as the *headway*, and is denoted as a function s_i. More complex models also incorporate information on velocity or acceleration differences between the leading and following vehicles.

In general, the models calculate the change in velocity for each timestep for each vehicle, in other words, the acceleration is determined. There is also a term used in the literature called *desired velocity* which is the velocity that the model wishes to achieve, but is vaguely defined. It may be assumed that the desired velocity would equate to the speed limit, however, speed limits in the real world change from one road to another. This means that some scaling of the models may have to be performed to ensure that vehicles can reach and maintain specified speed limits when experiments are run.

One of the earliest of these types of models is the OVM (Bando *et al.*, 1995), which takes the hyperbolic tangent (tanh) of the headway to determine an optimal velocity $V(s)$ for the following vehicle. A plethora of subsequent models have extended the OVM, including the FVDM (Jiang *et al.*, 2001), which adds a linear velocity difference between the leading and following vehicles, and the FVADM (Zhao and Gao, 2005), which augments the FVDM by appending a linear difference in acceleration between the leading and following vehicles. An alternative car-following model not based on the OVM is the IDM (Treiber *et al.*, 2000b), which uses ratios for velocity and headway to determine the appropriate acceleration of the following vehicle.

4.2.1 Optimal Velocity Model

The Optimal Velocity Model (OVM) calculates the acceleration that would be required to achieve an optimal velocity, $V(s)$, which is based on the space distance headway with the leading vehicle (if the leading vehicle exists). If a leading vehicle does not exist, then the vehicle will accelerate according to the acceleration parameter until it reaches the optimal velocity.

An interesting feature of the OVM is that the acceleration behaviour of vehicles is controlled by applying the function tanh to the headway of the current vehicle (*ie:* the distance between the vehicle ahead and the current vehicle). The shape of tanh not only compels vehicles to attain the optimal velocity as quickly as possible by accelerating rapidly, it also

keeps vehicles from exceeding the optimal velocity once they reach this speed.

Note that the headway measurement for the following vehicle is taken at the front of the leading vehicle, thus the calculation must take this into account. The OVM does this by subtracting the length of the ahead vehicle as well as the position of the following vehicle to get the headway of the following vehicle (see Equation (4.2)). For the reader's convenience the equation below shows the OVM acceleration calculation, reproduced from Section 2.4.1:

$$\frac{dv_i(t)}{dt} = \kappa \left[V\left(s_i(t)\right) - v_i(t) \right] \tag{4.1}$$

where

$$s_i(t) = x_{i+1}(t) - x_i(t) - l_{i+1} \tag{4.2}$$

and

$$V(s) = V_1 + V_2 \tanh(C_1 s_i - C_2) \tag{4.3}$$

For the purpose of this thesis, the OVM has been calibrated with empirical data from Helbing and Tilch (1998) where $\kappa = 0.85 s^{-1}$, $V_1 = 6.75 m/s$, $V_2 = 7.91 m/s$, $C_1 = 0.13 m^{-1}$, $C_2 = 1.57$.

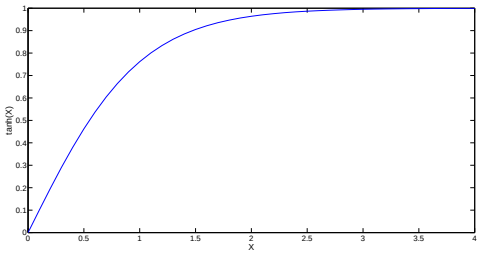

Figure 4.1: Graph of tanh().

When examining a graph of tanh (see Figure 4.1), it can be seen that when this function is positive in the X-axis direction, it rises sharply until it almost reaches the upper bound and then tapers off, closing to but never reaching the upper bound. As $X \to +\infty$, the function goes to the upper bound. Both these properties of tanh have been used in the OVM, where $\tan X$ is the *optimal or desired velocity* to be achieved and X is a function

of headway and current velocity (*ie:* $C_1 s_i - C_2$ from Equation (4.3)). In the case of an infinite headway the curve becomes effectively a vehicle's velocity over time, so that any acceleration of vehicles is initially acute until the vehicle approaches the speed limit (*ie:* upper boundary) and then remains at that velocity until such time that the vehicle encounters another vehicle or an obstacle (at which point the headway term will affect the calculation of X).

Note that this is how the vehicle would behave in theory, yet in practical terms when the vehicle reaches the upper bound of tanh() there is some form of moderation happening, that is for each timestep in a simulation, the vehicle alternates between small accelerations and decelerations since the upper bound prevents the vehicle from ever reaching it, plus there are rounding factors to take into account. On the other hand, the shape of tanh does imply the existence of various anomalies, for example, too high an acceleration occurs in certain situations and unrealistic deceleration arises in others (Zhao and Gao, 2005), both of which can cause abnormal traffic behaviour.

The optimal velocity for the OVM has been calibrated at $(V_1 + V_2) = 14.66m/s = 52km/h$, which effectively represents the speed limit v_0. This thesis scales the OVM to match a different speed limit by using $\omega = \frac{v_0}{V_1+V_2}$ as a scaling factor. This means that Equation (4.4) becomes:

$$V(s) = \omega V_1 + \omega V_2 \tanh(C_1 s_i - C_2) \tag{4.4}$$

The OVM uses two basic components to decide whether to accelerate or decelerate — $V(s_i(t))$ represents the velocity it wants to achieve and $v_i(t)$ corresponds to the velocity it actually has, with both elements being with respect to the following vehicle. Since tanh of the headway is used to reach an optimal velocity, the closer the headway is to zero, the lower the velocity of the following vehicle will be. As a consequence, for higher velocities the model will force increasingly larger headways, regardless of the behaviour of the leading vehicle. Having the optimal velocity V generated by tanh of the headway means that the OVM is initially 'in a hurry' to get to this optimal velocity (see the graph of tanh).

Applying the κ multiplier (calibrated to 0.85) means that the optimal velocity is held back slightly at every timestep to simulate the fact that a real-world vehicle cannot instanta-

neously accelerate to any given velocity, and that a real-world driver will moderate their acceleration as they reach their desired velocity. So if an initial acceleration of $5m/s^2$ is required to get to optimal velocity in the current timestep, this is then translated into a $4m/s^2$ approximate acceleration due to κ. In the subsequent timestep the change in the vehicle's position will only be $4m/s$ and thus an extra $1m/s^2$ is needed to get to the original $5m/s^2$ requirement. κ is again applied in the next timestep but this time against a required acceleration of $1m/s^2$, producing a gradual tapering off of acceleration rather than abrupt and unrealistic 'on-off' behaviour. However, the initial acceleration is still very high, suggesting that whilst the OVM performs relatively realistically in flowing freeway traffic with its characteristic gradual changes in flow velocity, it may perform oddly in urban traffic with its stop-and-go traffic flow due to intersections.

It is known that the OVM has cases of unreasonable behaviour when the leading vehicle is moving significantly faster than the following vehicle (Jiang *et al.*, 2001). If the headway is small, the following vehicle will decelerate rapidly despite the leading vehicle's higher velocity making this an inappropriate response. This is due to the OVM's lack of consideration of the relative velocity of the two vehicles. However, the OVM remains included in this study to provide a baseline of performance from which to measure other models.

4.2.2 Full Velocity Difference Model

The Full Velocity Difference Model (FVDM) is based on the OVM and strives to minimise some of the problematic effects of the OVM's reliance on space distance headway to determine an optimal velocity. It does this by introducing a velocity difference term (*ie:* velocity headway) with respect to the leading and following vehicle.

If the velocity difference is positive then the leading vehicle is travelling faster than the following vehicle and vice versa for a negative velocity difference. This will then determine how the following vehicle behaves with respect to the leading vehicle. The FVDM equations are re-listed below for the reader's reference:

$$\frac{dv_i(t)}{dt} = \kappa \left[V\left(s_i(t)\right) - v_i(t) \right] + \lambda(s_i)\Delta v_i(t) \tag{4.5}$$

$$\Delta v_i(t) = v_{i+1}(t) - v_i(t) \tag{4.6}$$

where λ is a step function defined by:

$$\lambda(s_i) = \begin{cases} a, & s_i \leq s_c \\ b, & s_i > s_c \end{cases} \tag{4.7}$$

and $\Delta v_i(t)$ is the velocity difference. The parameters are set to $a = 0.5s^{-1}$, $b = 0$, $s_c = 100m$, and with an adjustment to the OVM parameter $\kappa = 0.41$ (Jiang *et al.*, 2001).

The direct addition of $\lambda(s_i)\Delta v_i(t)$ to the OVM equation will shift the tanh function up or down depending on which vehicle, leading or following, is travelling faster. Thus the acceleration or deceleration patterns remain unchanged in the FVDM from the OVM since there is no stretching or shrinkage of *tanh* due to these changes. The FVDM also uses a step function to heuristically determine when the difference in velocity should start to take effect; this is set to $100m$ (Jiang *et al.*, 2001), and so if $s_i(t) > 100$, the velocity difference will have no effect and the model functions like the OVM. When $s_i(t) \leqslant 100$, the effect of the velocity difference is taken in account (as $0.5 \times \Delta v$). In this way the FVDM can be considered a hybrid of a stimulus-response and an action point model.

In essence the model relies on the space distance headway as the main determining factor for optimal velocity, but uses the velocity difference to apply a mitigating effect on the OVM's weaknesses. One issue with this approach is that the step function does not allow for smooth transitioning between the case when the space distance headway solely determines acceleration and when the difference in velocity starts to have an effect. Another problem affecting the FVDM includes unrealistic behaviour of vehicles under emergency conditions (Zhao and Gao, 2005). However, as this thesis is concerned with common (non-emergency) urban situations, this issue will not be directly examined.

4.2.3 Full Velocity and Acceleration Difference Model

The Full Velocity and Acceleration Difference Model (FVADM) is a further evolution of the FVDM, where the acceleration difference between the leading and following vehicles is added to the FVDM's velocity difference step function. The difference in acceleration takes effect once the space distance headway is equal to or less than $100m$. In the case where the acceleration difference is activated, it will be given a value of $0.5\Delta dv/dt$, otherwise it is zero and thus has no effect on the acceleration calculation of the following vehicle.

As with the FVDM's velocity difference step function, the acceleration difference step function is not smooth thus some results are unrealistic around this discontinuity. The equation for the FVADM is reproduced below from Section 2.4.1.2:

$$\begin{aligned}
\frac{dv_i(t)}{dt} &= \kappa\left[V\left(s_i(t)\right) - v_i(t)\right] + \lambda(s_i)\Delta v_i(t) \\
&\quad + k(s_i)g(\Delta a_i(t-1), a_{i+1}(t))\Delta a_i(t-1) \\
\Delta a_i(t) &= a_{i+1}(t) - a_i(t) = \frac{dv_{i+1}(t)}{dt} - \frac{dv_i(t)}{dt} \\
g(\Delta a_i(t-1), a_{i+1}(t)) &= \begin{cases} -1, & \Delta a_i(t-1) > 0 \quad \text{and } a_{i+1}(t) \leq 0 \\ 1, & else \end{cases}
\end{aligned} \tag{4.8}$$

where $k(s_i)g(\Delta a_i(t-1), a_{i+1}(t))\Delta a_i(t-1)$ is the acceleration difference term and

$$k(s_i) = \begin{cases} c, & s_i \leq s_c \\ d, & s_i > s_c \end{cases}$$

is the velocity difference term.

Parameters were set as follows according to Zhao and Gao (2005): $c = 0.5s^{-1}$, $d = 0$, $s_c = 100m$. Like the FVDM, the velocity difference is the difference in velocity between the leading and following vehicles and furthermore, the acceleration difference is the difference in acceleration between the leading and following vehicles, where a positive acceleration difference indicates that the leading vehicle is accelerating faster than the following vehicle and a negative acceleration difference implies the reverse. The FVADM uses this difference in acceleration to adjust its response over the FVDM in a similar manner to how the FVDM uses velocity difference to affect the base OVM's decision making.

4.2.4 Intelligent Driver Model

The basic premise of the Intelligent Driver Model (IDM) calculation involves balancing the ratio of desired velocity versus actual velocity (the acceleration component) against the ratio of desired headway versus actual headway of a vehicle (the deceleration component). These are used to calculate the acceleration of the vehicle (Treiber *et al.*, 2000b), and the equation is shown below for the reader's reference:

$$\frac{dv_i(t)}{dt} = a\left[1 - \left(\frac{v_i(t)}{v_0}\right)^{\delta} - \left(\frac{s^*(v_i, \Delta v_i)}{s_i(t)}\right)^2\right] \tag{4.9}$$

$$s^*(v_i, \Delta v_i) = s_0 + s_1\sqrt{\frac{v_i}{v_0}} + v_i T + \frac{v_i \Delta v_i}{2\sqrt{ab}} \tag{4.10}$$

where:

$v_i(t)$ = current velocity of following vehicle	T = desired safety time headway
v_0 = desired velocity	a = maximum acceleration
s^* = desired minimum headway	b = desired deceleration
s = actual headway	δ = acceleration exponent

The following parameters are the suggested values for simulation (Treiber *et al.*, 2000b), and are used in this Thesis:

v_0 = speed limit in m/s	$a = 0.73 m/s^2$
$s_0 = 2m$	$b = 1.67 m/s^2$
$s_1 = 0m$	$\delta = 4$
$T = 1.6s$	

On a free open road, when $s_i(t) \to \infty$, the vehicle's acceleration tends to:

$$a\left(1 - \left(\frac{v_i(t)}{v_0}\right)^{\delta}\right) \tag{4.11}$$

and consequently, as $v_i(t) \to v_0$, there is a tendency for the vehicle to decelerate:

$$-\,a\left(\frac{s^*}{s_i(t)}\right)^2 \tag{4.12}$$

The exponent for the acceleration component has been calibrated to 4 and the exponent for the deceleration component is a constant at 2. Both of these ratios are then subtracted from 1 and multiplied by the maximum acceleration a. Using the IDM's equation, the following set of conditions and results can occur with the IDM:

- (desired velocity < actual velocity) and (desired headway < actual headway) = close to the maximum acceleration

- (desired velocity > actual velocity) and (desired headway < actual headway) = fairly acute deceleration at a rate greater than the maximum acceleration
- (desired velocity < actual velocity) and (desired headway > actual headway) = less acute deceleration at a rate that is still greater than maximum acceleration
- (desired velocity > actual velocity) and (desired headway > actual headway) = extreme deceleration at a rate that is greater than max accel

The above synopses show that the IDM accelerates when the vehicle has yet to reach its desired velocity and its desired headway, a circumstance that occurs where traffic flows freely without congestion or stop-and-go flow. In the other situations, the IDM is more cautious and decelerates at a rate depending on the difference between the desired and actual elements. This means that in urban traffic situations the IDM will react conservatively and tend to decelerate when it can safely maintain velocity or even accelerate slightly. The model, however, is relatively simple and computationally efficient, having been shown to react reasonably to common free-flow traffic flow (Hoogendoorn and Bovy, 2001).

4.3 Empirical Driver Model Comparison

The objective of this chapter is to investigate the empirical behaviour of the various chosen driver models under typical urban scenarios where vehicles are interacting with each other as well as road intersections. The goal is to identify scenarios that, whilst completely ordinary in day-to-day traffic, produce unreasonable reactions from the driver models in question. Scenarios are deliberately limited to common and relatively simple traffic scenarios so that it is clear what a reasonable reaction to the situation would be and thus it is unmistakable when and how the driver models react improperly. Moreover, the lack of complicating factors should also facilitate ascertaining the cause of any unreasonable reactions. In contrast, in unusual or emergency situations the correct course of action for a vehicle is not necessarily obvious — there may be many acceptable choices, or even no reasonable choice at all (in the case of a serious emergency).

Experiments are split into two analyses: *pairwise interaction analysis* and *real-world driver benchmark analysis*.

4.3.1 Pairwise Interaction

The first analysis consists of scenarios which isolate a pair of vehicles and explores the reactions of the following vehicle to specific short-term actions of either the following or leading vehicle (the precise nature of which varies between scenarios). This tests each driver model independently on a set of common traffic events in isolation from any other vehicle activity. The following types of scenarios are tested:

- Normal free-flowing traffic where vehicles travel at a constant moderate velocity and keep a safe headway. Variations include the leading vehicle having slightly higher or lower constant velocity than the following vehicle.
- An accelerating vehicle moving safely in front of a another vehicle that is travelling at a moderate steady velocity. An overtaking maneouvre is used to effectively demonstrate this event, even though this thesis does not investigate lane changing actions.
- Vehicles approaching an intersection. Variations include a vehicle turning safely from a side road onto a main road behind vehicles; a vehicle turning safely from a side road onto a main road in front of vehicles; a vehicle turning safely from a main road into a side road; and a vehicle aborting an entry from a side road onto a main road due to safety issues.

4.3.2 Real Driver Benchmarking

The second analysis concentrates on comparing the driver models' behaviours against real-world driver behaviour and analysing how well each model represents actual driver responses to accelerating and braking scenarios. This tests model reactions over time. In this case the models are applied to a simple road network where vehicles travel at widely-spaced intervals (*ie:* avoiding detailed pairwise interactions) and interact with intersections.

All models are run in turn on the same network and the behaviour of the vehicles is analysed against real-world GPS data collected from vehicles driven by real drivers on urban roads. Comparison is limited to two scenarios: (1) accelerating from standstill with

no traffic ahead and (2) braking from the speed limit to a halt for a give-way intersection with no traffic ahead.

The comparison set is necessarily limited to these two scenarios since they are the only two scenarios where all other confounding factors can be made constants. In particular, a different possible scenario is to approach a give-way intersection and proceed without coming to a halt (*ie:* no right-of-way traffic exists). This will involve not only braking but also a large variability in the minimum velocity, depending on the intersection and visibility. Moreover, this minimum velocity in the infrastructure from Chapter 3 is defined by the intersection rather than the driver model. Similarly, a scenario involving accelerating to turn-in to a main road from a side road requires some definition of the maximum turning velocity, a variable that the driver models simply do not represent.

In contrast, acceleration from standstill and braking to a halt require only knowledge of the speed limit and initial (or final) velocities of zero. No turns, other vehicles or any other factors are involved, thereby providing a test based solely on the driver models' behaviour.

4.4 Experiments

4.4.1 Pairwise Interaction Analysis

The goal of these experiments is to use everyday traffic scenarios to encapsulate each set of circumstances where a driver model's resultant acceleration (*ie:* reaction) is unreasonable, particularly in comparison to the other models being evaluated. In these experiments the driver models are provided with parameters representing a single traffic scenario at a single moment in time, run in isolation from an ongoing simulation to provide an understanding of how models perform in these situations.

Scenarios are derived by taking every possible combination of parameters and inferring valid real-world situation that these parameters could represent, or discarding the parameter combination if the parameters do not represent a common urban driving situation. The valid scenarios are split into two groups: ordinary traffic conditions to free-flowing driving conditions which most models should respond reasonably to; and intersection-based traffic conditions. The latter represents many common urban scenarios that are unusual

in freeway traffic flow and may involve significant reaction on the part of a driver, such as reacting to a leading vehicle that brakes to turn off onto a side road.

The speed limit in all experiments is set at $70km/h$ as this velocity is large enough to highlight problem areas, as it allows for enough difference between the high and low values used in these experiments to show distinct reactions in the two diverse cases. Additionally, this speed limit is typically found in urban areas so will give a good indication of how the models would operate in this type of environment. The headway in the initial experiments is set at the two-second-rule that allows for a safe margin between vehicles at any velocity.

This empirical evaluation only assesses one particular time instant to give an insight into how the models react to a particular situation, rather than considering the response to an ongoing simulation — an evaluation of the models' response over time is discussed in Section 4.4.2.

4.4.1.1 Free-Flowing Conditions

As a first test of the models, simple baseline traffic scenarios of vehicles are initially selected. These include vehicles travelling at constant velocity at the speed limit in free-flowing conditions, vehicles stopping for a give-way intersection, and vehicles slowing down at a traffic junction to turn either onto a main road or a side road. Parameters are chosen so that vehicles travel under 'normal' conditions, that is, all vehicles travel at the same velocity within the speed limit, with clear safe distance headways for that speed limit. The response to this event by each of the models is examined. Since the scenarios themselves are routine traffic occurrences, the goal is to uncover the situations where the models respond inappropriately even under very ordinary conditions.

Note that the list of scenarios only includes instances where at least one model produced unreasonable results — other scenarios were investigated but produced no anomalies and so to avoid burdening the reader they are not discussed.

4.4.1.2 Intersection Conditions

To identify other scenarios, all combinations of parameters were generated to produce the set of all situations that a driver model can theoretically encounter. The focus was on identifying parameter combinations that are representative of normal vehicle interactions in and around *intersections*. Many of these combinations would be considered unusual in the free-flowing traffic conditions that the driver models have largely been evaluated on, but are in fact quite reasonable in the context of an intersection. For example, a driver will often pull out from a side road and accelerate directly behind another vehicle when entering into traffic flow on a main road, and this will result in a small headway for a few moments even though such a headway is typically an undesirable trait.

Thus intersection-based scenarios that commonly occur and are distinct from free-flowing traffic conditions were identified — if no such scenario could be identified, the particular combination was disregarded. Combinations that are internally inconsistent were also disregarded — for example, if both vehicles have a high velocity then it is not possible for the difference in velocity to be high. Finally, combinations where all models produced reasonable reactions were not of interest since they implied the scenario did not provide a significant test of the driver models.

4.4.1.3 Scenario Parameter Selection

From a total of 64 possible scenarios, 32 scenarios are internally inconsistent and the remaining 32 scenarios were further considered. Of these, the majority (25 scenarios) either returned reasonable responses from every model (typical for almost all scenarios with large headway), were similar to another chosen scenario (*eg:* where relative acceleration has no real importance so only a single acceleration scenario was chosen) or represented unrealistic situations. For an example for the latter, a scenario containing low headway and with the following vehicle travelling significantly faster than the lead vehicle implies that a collision is imminent — such a scenario does not naturally arise in the course of daily driving except in cases of driver failure.

The remaining seven scenarios were run against the models and each model's acceleration response was evaluated against the expected reaction for that scenario — descriptions of

the circumstances that each of the remaining seven scenarios represent and their corresponding parameter values can be found in Section 4.4.1.4.

In terms of the definition of parameters, the following paragraphs describe the low and high values chosen as part of the experiments.

Headway s_i — the low value is set at either $10m$ or $20m$ depending upon the scenario in question, corresponding to $2-4$ car lengths. This gives a case where the following vehicle is relatively (but not excessively) close to the leading vehicle and should be affected by any actions that the leading vehicle takes. Conversely, the high value is $100m$, which is large enough so that there should be no real impact on the following vehicle since the leading vehicle is very far ahead.

Velocity v_i — the low velocity value for the following vehicle is typically set to 10% of the speed limit; with a speed limit $v_0 = 70km/h$ used in all scenarios, the low velocity is $7km/h$. The high value in this case is set at 90% of the speed limit (*ie:* $63km/h$) rather than the speed limit in order to allow the driver models flexibility to choose their own response.

Velocity difference Δv_i — for the low value, this is set to either 0 or $7km/h$, depending upon the needs of the scenario. For the high value Δv_i is set to $63km/h$. Note that the value may be either positive (where the leading vehicle travels faster than the following vehicle) or negative (the inverse).

Acceleration difference Δa_i — for the low value this is set to either 0 or $0.5m/s^2$ (*ie:* $2km/h$ per second). For the high value the acceleration difference between the two vehicles is $2m/s^2$ (*ie:* $7km/h$ per second), a constant that applies to both acceleration and deceleration. Note that choosing a conservative value for Δa_i here avoids inadvertently transforming a common scenario into an unusual one. Finally, the value may be either positive or negative, indicating whether the leading or following vehicle is accelerating faster.

Table 4.1 summarises these definitions of low and high. Note that not all driver models

Parameter	Low	High	Applicable To
s_i	$10m$ or $20m$	$100m$	All
v_i	$\pm 7km/h$	$\pm 63km/h$	All
Δv_i	0 or $\pm 7km/h$	$\pm 63km/h$	All but OVM
Δa_i	0 or $\pm 0.5m/s^2$ $(2km/h/s)$	$\pm 2m/s^2$ $(7km/h/s)$	FVADM only

Table 4.1: Parameters used in pairwise interaction experiments. Speed limit $v_0 = 70km/h$.

use all parameters (*eg:* the OVM does not utilise velocity or acceleration difference) — only those parameters that are relevant are passed to the respective driver models.

4.4.1.4 Scenarios

The seven analysed scenarios and their contextual descriptions are as follows — see Table 4.2 for a definition of the precise parameter values used. The first four scenarios relate to typical main road driving between intersections and all models should perform reasonably since the situations are similar to freeway traffic flow. In contrast, the latter three scenarios represent situations in and around intersections and this is where some or all models may produce poor or unwarranted responses. In the figures depicting each scenario, vehicles are represented by squares with the leading vehicles coloured yellow and the following vehicles shown in green. Blue is used to indicate velocity, with solid blue arrows representing the velocity of the vehicle it is overlaid on — arrow length depicts velocity magnitude, and zero velocity is represented with a blue circle. Similarly, red indicates acceleration, with arrow length showing magnitude, the direction (up or down) showing acceleration or deceleration respectively and a red circle depicts zero acceleration.

Scenario 1 — Normal Traffic Flow A Figure 4.2 depicts this scenario, where two vehicles are travelling at a *constant* velocity near the speed limit, and with a reasonable headway margin of $20m$. Whilst this is a closer headway than preferred since $20m$ is just over a one second gap at $70km/h$, it is not cause for alarm. There are many possible circumstances where this case would arise, such as a bunching up of traffic due to a speed limit reduction or one vehicle changing lanes to slot in front of another vehicle. Note that this thesis does not specifically implement or investigate lane-changing behaviour; the *concept* of this scenario arising as a consequence of a lane change is presented to give the

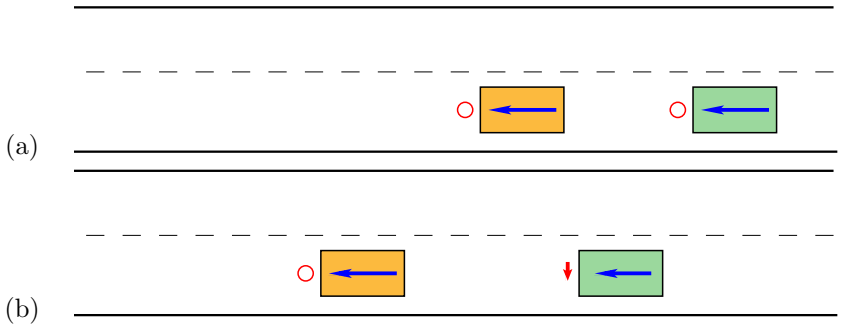

Figure 4.2: Scenario 1 — Normal Traffic Flow A: Vehicles travelling along a road near the speed limit and at a constant velocity with a $20m$ headway. Boxes represent vehicles, with yellow indicating a leading vehicle and green indicating a following vehicle. Red arrows represent acceleration / deceleration and blue arrows represent the velocity of vehicles. Circles indicate that acceleration (red) or velocity (blue) is zero.

reader an intuitive context from which to interpret the parameters used for this scenario. The expected reaction should thus be for the following vehicle to decelerate somewhat (*ie:* lift off the accelerator pedal) in order to increase the gap towards a more comfortable distance of two seconds.

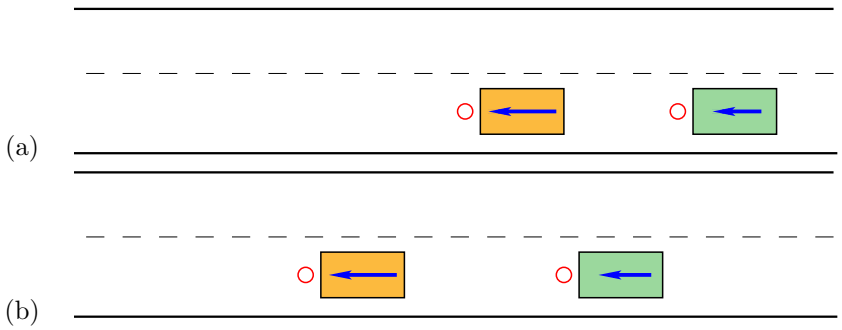

Figure 4.3: Scenario 2 — Normal Traffic Flow B: Vehicles travelling along a road near the speed limit and with a $20m$ headway, where the leading vehicle is moving slightly faster than the following vehicle.

Scenario 2 — Normal Traffic Flow B This scenario is similar to Scenario 1 except that the leading vehicle is moving slightly *faster* than the following vehicle, with both vehicles maintaining a steady velocity and a safe headway. Figure 4.3 illustrates the evolution of this scenario, with the leading vehicle pulling away from the following vehicle. Compared to Scenario 1, the expected reaction would be for the following vehicle to

maintain its velocity or decelerate only slightly since the headway will naturally grow.

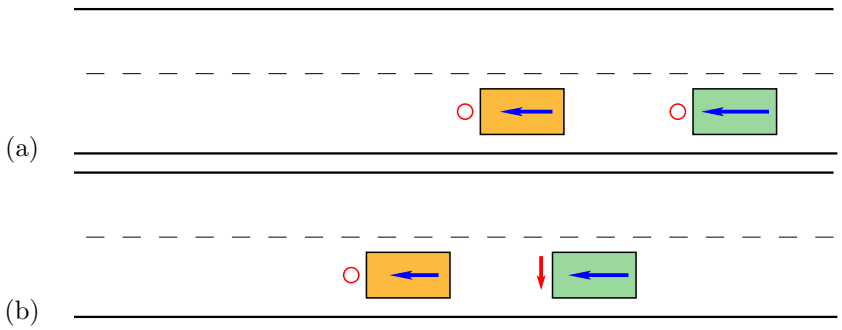

Figure 4.4: Scenario 3 — Normal Traffic Flow C: Vehicles travelling along a road near the speed limit at $20m$ headway, where the leading vehicle is moving slightly *slower* than the following vehicle.

Scenario 3 — Normal Traffic Flow C This scenario is again similar to Scenarios 1 and 2 except that the leading vehicle is moving slightly *slower* than the following vehicle, with both vehicles maintaining a steady velocity and comfortable distance between each other. Figure 4.4 shows this scenario, with the following vehicle catching up slightly to the leading vehicle. Due to this, it would be expected that the following vehicle must decelerate moderately (more than Scenario 1) in order to avoid reducing the headway.

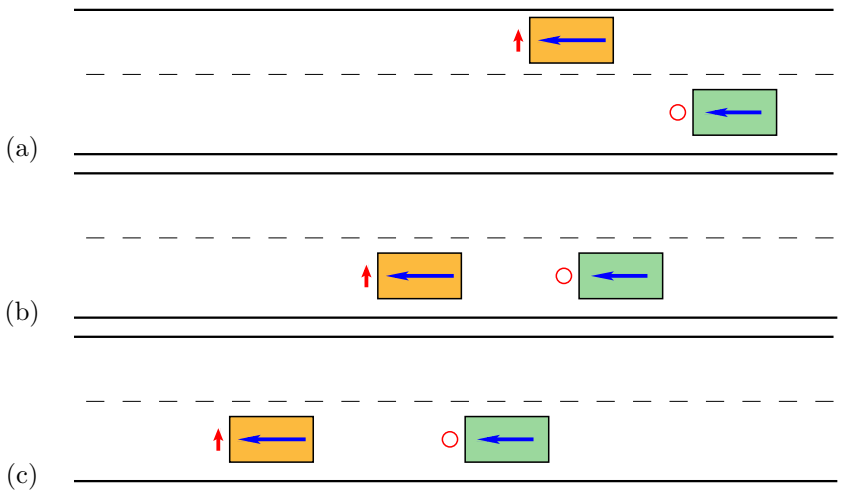

Figure 4.5: Scenario 4 — Overtaking Manoeuvre: The lead vehicle is travelling near the speed limit in the second lane, (a) overtakes then (b) lane changes $20m$ ahead of the following vehicle, and (c) continues to accelerate up to the speed limit. The following vehicle maintains their sub-speed-limit velocity.

Scenario 4 — Overtaking Manoeuvre This scenario shares similarities to Scenario 2 in that the leading vehicle is moving faster than the following vehicle whilst maintaining a safe distance. However, in this scenario the leading vehicle is also accelerating slightly in comparison to the following vehicle, as is shown in Figure 4.5. Although this is a minor variant of Scenario 2, the most representative circumstance where this scenario can arise is when the leading vehicle has just changed lanes to complete an overtaking manoeuvre, maintaining acceleration for a few moments to ensure they do not affect the following (overtaken) vehicle. Again, this is to provide an applicable context to the parameter values for the reader and is not the literal implementation.

At the time of the lane change (Figure 4.5b), the overtaken driver typically would not react noticeably to the leading vehicle, particularly with a reasonable headway of $20m$ (four car lengths). Hence the driver models should produce no acceleration or deceleration response. However, the driver models have no built-in consideration for lane changing occurrences — to the driver models, the lead vehicle simply 'appears' suddenly in front of the following vehicle. The subsequent response to this should vary amongst driver models, and may produce unreasonable reactions.

Scenario 5 — Turn onto Main Road Behind Traffic In this scenario a vehicle on a side road gives way to traffic on the main road before turning left to join traffic on the main road. The vehicle on the side road thus arrives at the intersection at a relatively low velocity and minimal braking since the vehicle has to give-way to oncoming traffic but does not necessarily have to come to a complete halt. In the scenario illustrated in Figure 4.6a, the vehicle on the side road comes to a complete halt to wait for the last vehicle on the main road to safely pass.

When the following vehicle on the main road has gone by the intersection whilst travelling at a constant velocity, the vehicle on the side ride pulls out onto the main road behind this vehicle (Figure 4.6b).

Once the leading vehicle on the side road has safely turned left onto the main road, it then becomes a following vehicle to the vehicle on the main road, which also then changes from a following vehicle to a leading vehicle as shown in Figure 4.6c. The new leading vehicle maintains a constant velocity while the new following vehicle accelerates relatively quickly to the speed limit.

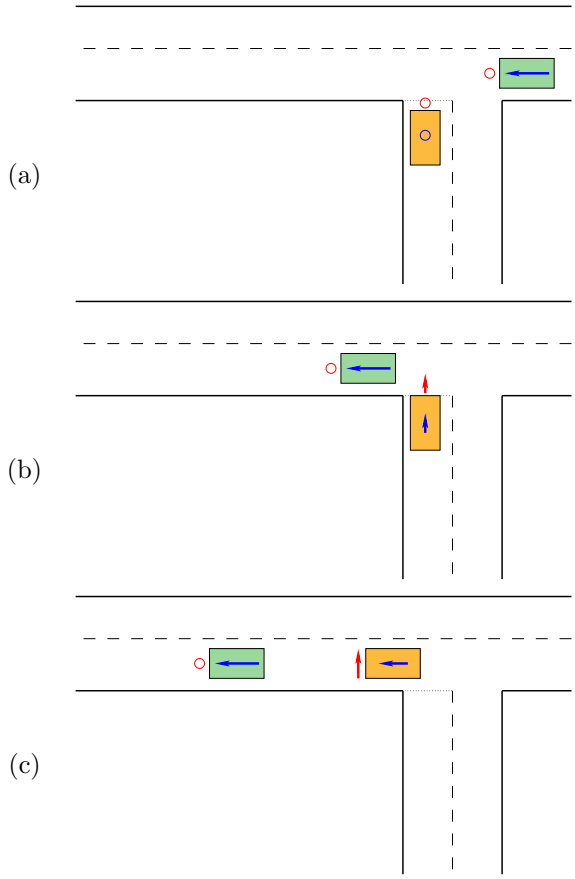

Figure 4.6: Scenario 5 — Turning onto Main Road Behind Traffic. (a) Vehicle awaits main road's traffic to pass the intersection, (b) moving from standstill to enter main road, (c) slotting in directly behind leading vehicle.

As with Scenario 4, the entrance onto the main road of the following vehicle means that a leading vehicle abruptly 'appears' close ($10m$) in front of the former. Since this leading vehicle is going much faster, there is in fact no issue. However, the driver models may consider the situation to be more radical and react inappropriately due to this.

Scenario 6 — Turning into Side Road In this scenario (Figure 4.7), two vehicles are travelling on a main road with significant headway between them ($100m$). The lead vehicle is approaching an intersection and intends to turn left into the side road. The vehicle thus slows down relatively quickly, as depicted in Figure 4.7a — since the following vehicle is relatively far behind it has no need to brake yet. Subsequently (Figure 4.7b), the leading vehicle begins to turn into the side road, still decelerating slightly, whereas

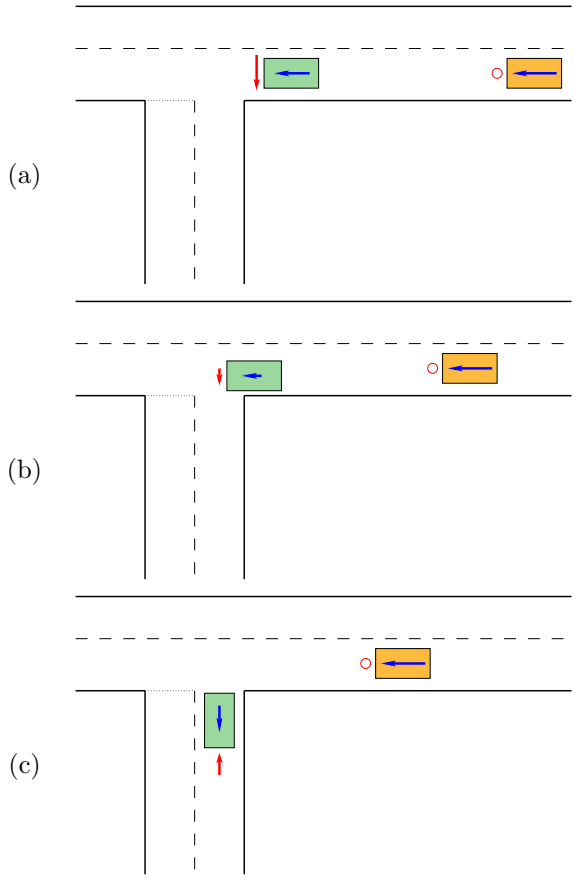

Figure 4.7: Scenario 6 — Turning into Side Road. (a) Lead vehicle approaches intersection, decelerating in preparation for the turn, with a large headway ($100m$) to the following vehicle. (b) Lead vehicle begins to turn into the side road with the following vehicle closing, (c) the lead vehicle enters the side road and the following vehicle continues on the main road.

the following vehicle begins closing the headway gap but not not so much as to warrant a braking reaction since the driver will anticipate the lead vehicle's change into the side road. Figure 4.7c then shows the leading vehicle having turned left into the side road and accelerating, opening the main road for the following vehicle to continue travelling.

At no point should the following vehicle need to decelerate significantly, since the driver anticipates that the leading vehicle will be leaving the main road and the headway is quite large. However, whilst this is a very common occurrence, such anticipation is not part of any of the driver models, and so their response is difficult to predict.

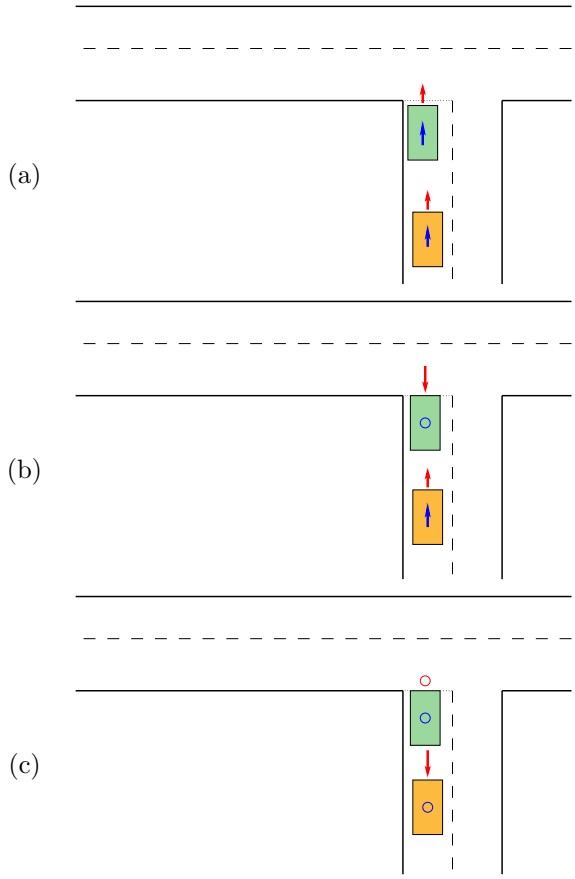

Figure 4.8: Scenario 7 — Aborted Entry onto Main Road. (a) Two vehicles begin entering a main road. (b) Lead vehicle notices a hazard (*eg:* oncoming traffic) and brakes to halt, (c) which should cause the following vehicle to also brake to a halt.

Scenario 7 — Aborted Entry onto Main Road Here two vehicles approach an intersection from a side road (Figure 4.8), with the leading vehicle about to turn left onto the main road, accelerating slightly to start entering the intersection, but aborting this action due to oncoming traffic and coming to a halt before actually having entered into the intersection. Having kept a safe distance and velocity for the approach to the intersection, the following vehicle should also be able to come to a stop behind the leading vehicle, only needing to decelerate slightly before coming to a standstill.

This scenario can almost be considered an emergency situation, thus including it in this investigation can be debatable. However, it does demonstrate what may happen in a circumstance where there is a controlled deceleration, then slight acceleration before having to come to a sudden standstill from a relatively low velocity. Some of the models may

overreact to the leading vehicle coming to an abrupt halt from a slight acceleration, where the expectation is that the vehicle would continue to accelerate, and this response will depend on how quickly the particular model is designed to get to the speed limit (*ie:* the OVM wants to get to the optimal velocity as soon as possible).

Scenario	Headway	Velocity	Δv_i	Δa_i	Expected Response (m/s^2)
1	$20m$	$63km/h$	$0km/h$	$0m/s^2$	-low...0
2	$20m$	$63km/h$	$7km/h$	$0m/s^2$	-low...0
3	$20m$	$63km/h$	$-7km/h$	$0m/s^2$	-low...0
4	$20m$	$63km/h$	$7km/h$	$0.5m/s^2$	-low...0
5	$10m$	$7km/h$	$63km/h$	$-2m/s^2$	+high
6	$100m$	$63km/h$	$-56km/h$	$-2m/s^2$	0...+low
7	$10m$	$7km/h$	$-7km/h$	$-2m/s^2$	-low

Table 4.2: Parameters used for each scenario. The Expected Response is the acceleration that a reasonable human driver would take for the following vehicle in this scenario. Positive values for Δv_i and Δa_i indicate the leading vehicle is travelling faster than the following vehicle, whereas negative values indicate the opposite.

4.4.2 Real Driver Benchmark Analysis

A simple road network was constructed to evaluate the models in more real-world conditions, where vehicles face everyday traffic devices, such as intersections, and must obey traffic rules and interact with other vehicles in the system. Each model uses the same network and parameters to simulate traffic movement.

Since the purpose is to study traffic flow behaviour as vehicles accelerating from a standstill and braking to a halt at a give-way intersection under simulation conditions, sections of the simulation where these situations occur were induced and extracted from the network. The results produced by the models over these segments was compared against real-world GPS data, collected whilst driving on urban roads that replicate the simulation conditions.

It is a relatively simple task to set up in the simulation a situation where a vehicle stops at an intersection (*eg:* a vehicle on a side road approaches a main road with heavy traffic). However, for real-world GPS measurements, conditions need to be carefully selected so that they are compatible with the simulations. For example, in the stopping situation, the

only data that can be considered is where the vehicle is not impeded by other vehicles as it approaches a give-way intersection that will require halting, or else the leading vehicle can affect the following vehicle's behaviour. Thus GPS data was collected exclusively from the following situations:

- Accelerate from a standstill — GPS data was recorded only for times when the vehicle is at the head of queue at a traffic light, the light is initially red and the vehicle is stopped at the light. The driver then accelerates normally to the speed limit when the light turns green.
- Brake to a halt — GPS data was recorded only for times when a vehicle approaches from a distance to a red light with no other vehicle ahead, and the driver is able to choose the rate of deceleration without external influencing factors. The light also had to remain red until the vehicle came to a complete stop.

4.5 Results and Analysis

4.5.1 Pairwise Interaction Results

4.5.1.1 Results and Analysis

Scenario 1 — Normal Traffic Flow A In this scenario the expected response is for no change in velocity or just a small deceleration, and as such the OVM's response to brake excessively is an overreaction to the given situation, decelerating at just over $4m/s^2$, which would equate to a vehicle travelling at $100km/h$ and then coming to a halt in about 7 seconds. The FVDM and FVADM both brake at about half the deceleration rate of the OVM at just under $2m/s^2$, which can be associated with a vehicle braking from $100km/h$ in just over 14 seconds, which is still an unreasonable response. The IDM also brakes but does so in a much more moderate manner at $1.4m/s^2$ (analogous to braking from $100km/h$ to $0km/h$ in 20 seconds), although the fact that the model still decelerates in this circumstance is somewhat concerning.

The braking that is occurring in this scenario for all models suggests that the models are not completely comfortable with what could be considered reasonable headways with

typical urban velocities whilst maintaining a steady velocity between the two vehicles. If the scenario would have been allowed to continue running, the vehicles would have eventually slowed their acceleration when the headways eventually became large enough for each model.

Scenario 2 — Normal Traffic Flow B This scenario is similar to Scenario 1 with the difference being that the leading vehicle has a slightly *higher* relative velocity to the following vehicle, and it is expected that the vehicles respond with either maintaining a steady velocity or a decelerating slightly. In this case, the OVM has the same response, braking as hard as in Scenario 1, an unwarranted action in this circumstance. The FVDM and FVADM both react less severely than in Scenario 1, by decelerating at about half the rate, which is also quite a bit less than the OVM in this instance (just under $1m/s^2$ which equates to coming to a halt from $100km/h$ in about 28 seconds). Only the IDM has a reasonable reaction, producing only a relatively slight deceleration of $0.14m/s^2$, which can be attributed to other factors such as different driver behaviour and / or weather, road conditions.

Given that the leading vehicle is travelling at a slightly faster velocity than the following vehicle and both vehicles are not accelerating or decelerating whilst keeping a reasonable headway for the given velocity, the unwarranted braking actions of all models with the exception of the IDM suggests that these models have difficulties with sensible headways for a standard speed limit of about $63km/h$ around urban areas. This seems to indicate that these models assume that relatively moderate velocities require excessive headways for safety when this is not only unrealistic but also unnecessary.

Scenario 3 — Normal Traffic Flow C This scenario is similar to Scenario 1 with the slight variation being that the leading vehicle has a slightly *lower* relative velocity to the following vehicle, but the expected response is the same. Here the OVM brakes just as heavily as in Scenarios 1 and 2, and once again this is an acute overreaction to a normal and safe situation. The IDM's response is not much better, decelerating at a rate of $3.5m/s^2$, which corresponds to a vehicle travelling at $100km/h$ and coming to a halt in 8 seconds, an excessive reaction to the circumstances. Both the FVDM and FVADM respond by braking less than the OVM and the IDM, but still behave inappropriately by decelerating at just under $3m/s^2$, which is equivalent to coming to a halt from $100km/h$

in about 9.5 seconds.

All models respond with excessive braking. This is not surprising given that this also happened in Scenario 2, where the leading vehicle moved at a slightly faster velocity. However, what is unexpected is that the IDM is outperformed by both the FVDM and the FVADM in this situation. Although all three of these models take velocity difference into account, they do so in different ways.

The FVDM and the FVADM have a headway threshold where this velocity difference is active, set at $100m$ in this thesis (see Section 2.4.1.2). This means that at a headway of $20m$ this would be in effect, and thus the deceleration is not as acute as in previous scenarios, though the rate of deceleration is still unwarranted given the circumstances.

On the other hand, the IDM attempts to balance acceleration with deceleration using ratios of desired versus actual velocity and headway respectively at all headway distances (see 4.2.4). With the leading vehicle having a slightly slower velocity, the IDM's response to decelerate at a relatively rapid rate is due to its cautious approach to deal with velocity and headway changes, although the extent of its reaction is still disproportionate.

Scenario 4 — Overtaking Manoeuvre The expected response in this scenario is the same as above, and in this case the OVM brakes very hard at the same rate as the previous scenarios, even though the leading vehicle is accelerating whilst the following vehicle is travelling at a constant velocity, and again this is a very disproportionate response to the situation. The FVDM and FVADM both decelerate as well, but at more acceptable rates of almost $1m/s^2$ and just under $0.8m/s^2$ respectively, equivalent to braking from $100km/h$ to zero in 28 seconds and 38 seconds respectively. The IDM also decelerates but this is negligible at $0.14m/s^2$.

The severe braking exhibited by the OVM once again highlights the inadequacy of this model to respond realistically to normal traffic situations where there is adequate spacing and moderate velocities. Deceleration is still present in all other models but the rates of deceleration are all within acceptable bounds and can be explained away by small variations in driving styles and / or road, weather conditions, etc.

Scenario 5 — Turn onto Main Road Behind Traffic In this scenario the expected response is acceleration of vehicles since real drivers would accelerate strongly since they anticipate that the leading vehicle on the main road is travelling much faster and the driver must bring their vehicle up to speed to enter into the flow of traffic. Both the FVDM and FVADM follow this pattern, accelerating at $27m/s^2$ and $23m/s^2$ since both take into account the large positive difference in velocity to suggest acceleration is justified. However, whilst in the correct range this is actually an impossible acceleration since it would achieve $100km/h$ in just over 1 second. This occurs because the FVDM and FVADM use velocity difference additively on the basic OVM, thus a large velocity difference causes a corresponding over-acceleration. For the FVADM the negative acceleration difference means the FVADM will moderates this response as compared to the FVDM, but not by much.

On the other hand, the OVM actually *decelerates* at $1.85m/s^2$. Clearly this is inappropriate and is caused by the reasonably close headway. Similarly, the IDM responds by accelerating rather slowly at $0.7m/s^2$ — whilst not as inappropriate as the OVM's braking, the IDM's response is odd since its equations take into account velocity difference. Upon further analysis, the IDM's low acceleration rate can be attributed to the model's tendency to be cautious about accelerating — with larger headways the IDM will increase its rate of acceleration markedly.

Scenario 6 — Turning into Side Road The expectation in this scenario is for the following vehicle to maintain its velocity of about $63km/h$ whilst the leading vehicle turns into a side road well ahead of the following vehicle. Interestingly, none of the models react in this manner, with the FVDM and the FVADM overreacting the most by braking extremely hard at rates of around $7m/s^2$ and $8m/s^2$ respectively, corresponding to a vehicle coming to a standstill from $100km/h$ in under 4 seconds. This is clearly excessive for the situation. The IDM also decelerates, but at a more moderate rate of $1.5m/s^2$, equal to a vehicle braking from $100km/h$ to $0km/h$ in 19 seconds, roughly the same as a real-world driver lifting off the accelerator pedal. Whilst this is not unreasonable it is not strictly necessary in the given circumstances since the headway is large. The OVM is the only model that does not brake, instead it accelerates at a rate of $1.64m/s^2$ to bring the vehicle up to the speed limit.

The FVDM and FVADM both consider the velocity difference between a leading and

following vehicle, with the FVADM also taking into account the acceleration difference, hence these two models will react to a marked difference in the two vehicles' velocity. However, the amount of braking they exhibit in this scenario equates to an emergency situation, when this is in reality quite a normal everyday occurrence, especially since the headway is large. The IDM's deceleration is similarly due to the velocity difference but the size of the reaction is far more realistic and indicates a more conservative nature where the model prefers to decelerate, even slightly, in a given situation unless there is an open road ahead. In contrast the OVM actually accelerates towards the speed limit quite aggressively due to the OVM's propensity to accelerate to its optimal velocity as quickly as possible with a large or non-existent headway.

Scenario 7 — Aborted Entry onto Main Road This situation involves an unexpected (though not emergency) element, but due to the low velocities involved it is expected that the models should react by decelerating slightly to come to a halt. Along these lines the OVM decelerates at a slow rate of just over $0.5m/s^2$ which corresponds to a vehicle coming to a standstill from $10km/h$ in 5 seconds, a reasonable reaction in the circumstances. The FVDM and FVADM decelerate much quicker, at rates of just over $1m/s^2$ and just over $2m/s^2$, equating to a vehicle travelling from $10km/h$ to $0km/h$ in roughly 2 seconds. These rates are relatively hard braking but could be justifiable for the circumstances.

On the other hand, the IDM actually *accelerates* slightly at just under $0.4m/s^2$. This is an unexpected and surprising response to the scenario — further analysis shows that the IDM considers $10m$ to be a large gap and so causes the vehicle to accelerate to close the gap. With smaller gaps ($< 5m$) the IDM will ultimately brake and in a safe manner. The *Red* scenario GPS comparison results from Section 4.5.2.4 highlight that the IDM is somewhat of a late-braking driver model. This is an interesting behaviour since in other scenarios (*eg:* Scenario 6) the IDM tends to be conservative and prefers to decelerate or accelerate only moderately.

Several of the everyday traffic scenarios from the above preliminary experiments were found to cause unreasonable results in one or more of the models tested. Listed below are the traffic conditions in these cases. Note that the leading vehicle dictates the conditions for the following vehicle to handle, and it is the reactions of the following vehicle to these conditions that are of interest. If a leading vehicle has an obstacle in front of it, it then

Scenario	Expected Response	Model	Model (m/s^2)	Response ($km/h/s$)	Scenario	Expected Response	Model	Model (m/s^2)	Response ($km/h/s$)
1	-low...0	OVM	**-4.03**	-14.5	5	+high	OVM	**-1.86**	-6.7
		FVDM	-1.94	-7.0			FVDM	**27.10**	97.6
		FVADM	-1.94	-7.0			FVADM	**23.60**	85.0
		IDM	-1.39	-5.0			IDM	**0.69**	2.5
2	-low...0	OVM	**-4.03**	-14.5	6	0...+low	OVM	1.64	5.9
		FVDM	-0.97	-3.5			FVDM	**-6.97**	-25.1
		FVADM	-0.97	-3.5			FVADM	**-7.97**	-28.7
		IDM	-0.14	-0.5			IDM	-1.47	-5.3
3	-low...0	OVM	**-4.03**	-14.5	7	-low	OVM	-0.53	-1.9
		FVDM	-2.92	-10.5			FVDM	-1.22	-4.4
		FVADM	-2.92	-10.5			FVADM	-2.22	-8.0
		IDM	-3.50	-12.6			IDM	**0.39**	1.4
4	-low...0	OVM	**-4.03**	-14.5					
		FVDM	-0.97	-3.5					
		FVADM	-0.72	-2.6					
		IDM	-0.14	-0.5					

Table 4.3: Scenario results. Model Response is the acceleration that the model suggests for the following vehicle.

becomes a following vehicle to this object and is thus subject to the object's actions.

- *Normal high velocity traffic flow* means that all vehicles are travelling fairly close together with regular spacing between vehicles but within safety margins.
- *Turn into main road* means that a vehicle that has been travelling on a side road turns left into a main road after giving way to the oncoming traffic. This vehicle then becomes the following vehicle of the vehicle that has just passed the intersection, and this new leading vehicle is travelling significantly faster than the new following vehicle.
- *Turn into side road* means that the leading vehicle is turning from a main road into a side road whilst there is a following vehicle behind it.

4.5.1.2 Discussion

It can be seen from Table 4.2 that the OVM tends to be the overall poorest performer, producing a very different response to what is expected in the common free-flowing situa-

tions of Scenarios 1–4. Each of these scenarios only differ in the velocity and acceleration of each of the vehicles, and the headway-focused OVM reacts identically to all of them. However, the OVM does respond best in Scenarios 6 (the lead vehicle turns into a side road) and 7 (the lead vehicle aborts entry onto a main road). This is because in these scenarios the decisive factor is headway — in Scenario 6 there is a large headway and so no action is necessary since the lead vehicle is about to turn off the road, and Scenario 7 has low velocities so problems can be reacted to in a timely manner based on headway. The other models take into account velocity difference and this causes them to overreact in Scenario 6 by braking. Scenario 7 is less clear-cut since it is a low velocity interaction and no model performs poorly, but the OVM produces arguably the most reasonable response.

The FVDM and FVADM improve upon the OVM in Scenarios 1–4 since they *do* take velocity difference into account and this moderates their responses to what is essentially normal free flowing traffic. Unlike the OVM which brakes strongly whenever headway is not comfortably large, the FVDM and FVADM recognise that the headway will naturally grow in most of these scenarios due to their knowledge of the velocity difference between the vehicles. The FVADM responds identically to the FVDM in Scenarios 1–3 since there is no acceleration difference component, but in Scenario 4 (overtaking manoeuvre) the accelerating lead vehicle means that it is even less concerned than the FVDM with slowing to maintain a comfortable headway. It is in Scenario 5 (turning onto main road behind traffic) that the FVDM and FVADM produce erratic responses. Here it would be expected that the driver model will accelerate normally as if there is no lead vehicle ahead, simply because the lead vehicle is moving so much faster that there is no danger of a collision. In fact, the FVDM and FVADM actually accelerate *more strongly* with a fast lead vehicle that is just ahead than they would if the lead vehicle were kilometres away. This is because over $100m$ they act identically to the OVM, and would accelerate normally. Within $100m$ the FVDM and FVADM add in velocity difference, and because this is a large positive value (the lead vehicle is travelling significantly faster) the models greatly increase their rate of acceleration to unrealistic levels (accelerating to $85 - 100km/h$ in one second, a feat that is not possible in any road vehicle). They also perform poorly in Scenario 6, where the low velocity of the lead vehicle that is about to turn overwhelms the large headway and causes the models to produce a disproportionate braking response. In fact, a similar situation occurs with Scenario 7 but since both vehicles are at low velocity the scale of the problem is not as significant.

As for the IDM, in general it behaves quite reasonably in Scenarios 1–4, although it does

decelerate perhaps too strongly in Scenario 3 (normal traffic flow with following vehicle moving slightly faster) due to the IDM's cautious nature at higher velocities. The only scenario of concern for the IDM is Scenario 7 where the IDM actually accelerates when the lead vehicle aborts its entry onto the main road and halts. This is actually the opposite response to what was expected. Closer inspection reveals that the IDM is less cautious at low velocities since the velocity term is based on a ratio of the current velocity versus the speed limit velocity. At low velocities this term becomes small and thus has less effect on determining the action to take. Headway then becomes dominant and $10m$ is certainly a comfortable headway at low velocities. With an even lower headway (*eg:* $5m$) the IDM would ultimately decelerate, and since velocities are low this could be achieved in a timely manner. In the remaining two scenarios the IDM is quite well-behaved, accelerating moderately in Scenario 5 and slowing slightly in Scenario 6 for the lead vehicle turning off. In both these cases the IDM is relatively cautious in its responses but not unreasonably so.

4.5.2 Real World Benchmark Results

4.5.2.1 Data

For benchmark comparison, GPS data for several runs of accelerating from a green light (*Green* scenario) and braking to a red light (*Red* scenario) were captured from three different drivers in three different vehicles.[1] Only data that match the requirements (accelerating at the head of traffic from green, or stopping to a red light with no intervening vehicles, and all in $70km/h$ speed limit zones) could be taken — other runs which were recorded but failed in these criteria (*eg:* light changed from red to green before coming to a complete halt) had to be ignored. Thus in total, there were 20 examples of *Green* and 18 examples of *Red* captured. Data was captured at 1 second intervals, the resolution of the GPS receiver used. This formed the *benchmark set* of data.

[1] Ethics clearance was obtained for this data capture under Curtin Ethics Application SMEC-52-10. All data was de-identified before storage.

4.5.2.2 Error Measurements

Each driver model was run within the simulation to produce one example for each scenario (*Green* and *Red*) — further examples would be identical since the models have fixed parameters and do not use fuzzy logic to vary driver behaviour between examples. Each example was captured at 0.1 second intervals to provide a detailed acceleration/deceleration curve.

The squared error between each example and every sample in the real-world benchmark set was then calculated. However, since benchmark samples varied in their duration and the driver models also varied in their duration between models and in comparison to the benchmarks, it was necessary to linearly stretch or shrink the benchmark samples to match the duration of the driver model being compared against. This ensures the *shape* of the curves are compared rather than the *aggressiveness* of the models versus the benchmarks, which could be corrected with an appropriate scaling of the models' accelerations.

One hundred points are then sampled along the time dimension of the two curves with linear interpolation used to compare the two curves at the same point in time. For a given driver model, the root-mean-square-error (RMSE) is calculated by taking average of the squared error between the driver model curve and a given benchmark curve, and then taking the square root of this average. This gives an indication of the point-by-point error in km/h of the driver model compared to that benchmark.

An additional complication is that it is necessary to define start and end points on both curves for linear stretching to match against. For example, in the *Green* scenario the vehicle accelerates from zero towards the speed limit. Thus the start point is relatively simple to define (when acceleration begins) but defining the end point is less clear-cut. Too early or too late and the stretched curve will differ from the benchmark simply due to a poor choice in end point. A similar situation occurs for the *Red* scenario but in reverse — the beginning of deceleration is difficult to pinpoint since it is gradual whereas the end point is when velocity approaches zero. Poor choices of start/end point would introduce bias against a model and induce an unfairly higher error.

Although dynamic time warping is an algorithm that compares two curves without known start/end points it performs a non-linear stretching to do so (Senin, 2008), whereas a linear stretching is required here. Instead, the RMSE was calculated for *every possible*

end point (for *Green*) or start point (for *Red*) and the start/end point that produced the lowest error across all benchmark samples was utilised. In effect, this finds the best-fitting match between the driver model and all benchmark curves.

4.5.2.3 Green Scenario Results

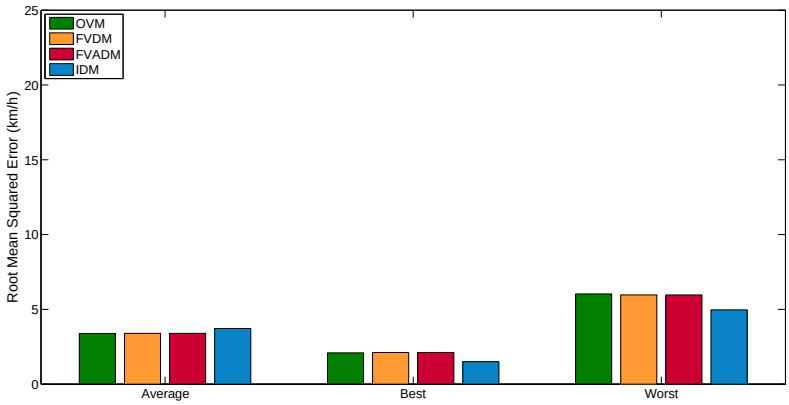

Figure 4.9: Root mean squared error of driver models against real-world driver benchmark dataset for the *Green* (accelerating) scenario.

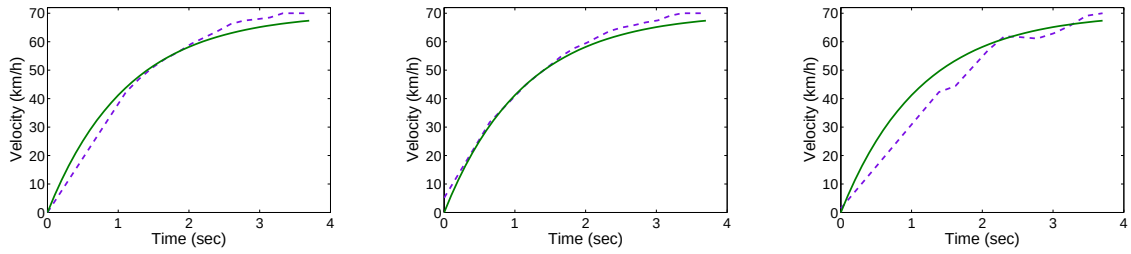

(a) (b) (c)

Figure 4.10: Example OVM model results vs GPS data for the *Green* (accelerating) scenario: (a) Near-average example (b) Best-fitting (c) Worst-fitting. The solid green curve represents the OVM model data and the dashed purple curve represents the GPS data.

Figure 4.9 shows the results of the *Green* scenario. The graph shows the average error, best (minimum) error and worst (maximum) error achieved against the benchmark data for each driver model. Shorter bars indicate that there is a closer fit between the two curves (model vs GPS), and conversely the longer the bars are the worse the fit is. Examples of

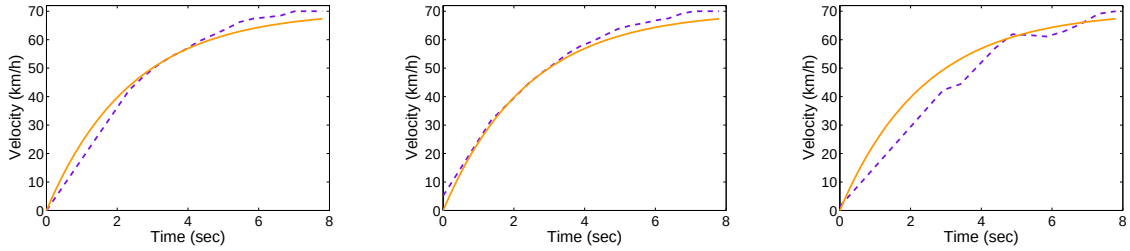

(a) (b) (c)

Figure 4.11: Example FVDM model results vs GPS data for the *Green* (accelerating) scenario: (a) Near-average example (b) Best-fitting (c) Worst-fitting. The solid yellow curve represents the FVDM model data and the dashed purple curve represents the GPS data.

comparing the curves for each model against selected benchmark samples are also provided in Figures 4.10–4.13. Note that the FVDM and FVADM have identical results since no acceleration difference component exists in the *Green* scenario.

All models perform well in this scenario since there is no leading vehicle to affect the calculation Surprisingly, the IDM performs slightly worse on average than the other models, though its worst case is actually slightly better too. However, in both cases the difference is marginal compared to the range of error between the best and the worst cases. Referring to the example curves in Figures 4.10–4.13, it can be seen that all driver models are very similar in their curve shapes, and all fit the real-world benchmarks very closely. In fact, most of the errors in the worst cases occur due to irregularities in the real-world driver's acceleration rather than the driver models.

Although the models are essentially identical in their scaled acceleration curves and error values, it is instructive to examine the raw curves they generate. Figure 4.14 shows the raw (unstretched) curve for all driver models against each other and against the benchmark. Even though the basic shapes are all similar to the OVM is significantly more aggressive than real drivers — so much so as to be unrealistic. In particular, a real driver accelerates to $70km/h$ in roughly 20 seconds whereas the OVM accelerates to $70km/h$ in *less than four seconds*. This is physically impossible for all but high performance vehicles, let alone a reasonable acceleration in urban traffic for the average driver. The FVDM and FVADM are more moderate in their acceleration at 8 seconds, but this is still over twice as aggressive as a normal driver. In contrast, the IDM is very conservative, taking over 40 seconds to

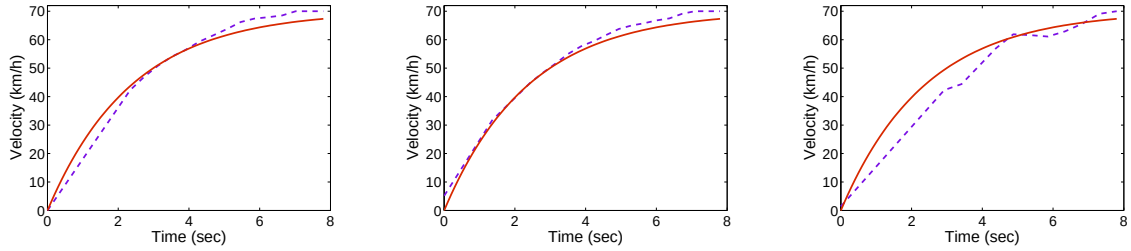

(a) (b) (c)

Figure 4.12: Example FVADM model results vs GPS data for the *Green* (accelerating) scenario: (a) Near-average example (b) Best-fitting (c) Worst-fitting. The solid dark red curve represents the FVADM model data and the dashed purple curve represents the GPS data.

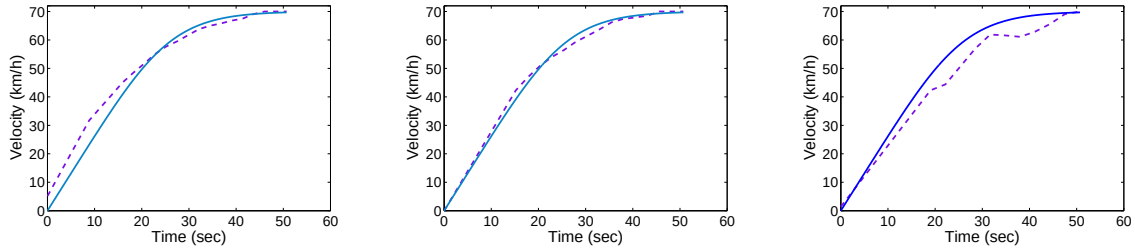

(a) (b) (c)

Figure 4.13: Example IDM model results vs GPS data for the *Green* (accelerating) scenario: (a) Near-average example (b) Best-fitting (c) Worst-fitting. The solid blue curve represents the IDM model data and the dashed purple curve represents the GPS data.

approach $70km/h$.

In this raw sense, none of the driver models provides a good fit for the acceleration from a halt despite all driver models having been calibrated against real-world drivers in freeway traffic flow. This indicates that calibration for one driving situation (free-flowing traffic) does not necessarily transfer well to other situations (urban stop-start traffic). Since the switch between free-flowing and stop-start traffic is indistinct — a highway is a mix of free-flowing sections and traffic lights that become stop-start only if red lights are encountered — it may be difficult to maintain a single calibration to cover all situations satisfactorily. Extensions to the models that vary the driver aggressiveness through additional model parameters may be useful in overcoming this by smoothly altering the aggressiveness of

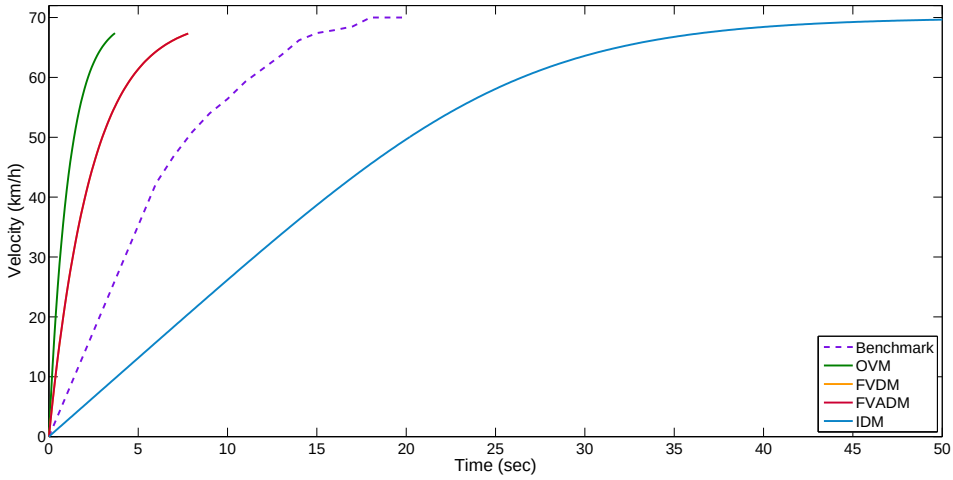

Figure 4.14: Comparison of the raw (unstretched) curves for each driver model and a benchmark sample for the *Green* (accelerating) scenario. FVDM and FVADM are identical curves here, hence the FVDM is not visible. Note how the OVM and FVDM/FVADM accelerate more aggressively than the real driver, and the IDM much less aggressively even though the curve shapes are all similar if stretched/shrunk.

a given vehicle depending on the nature of the traffic (free-flowing or stop-start), but is outside of the scope of this thesis to explore.

4.5.2.4 Red Scenario Results

The error results of the *Red* scenario compared to the benchmark dataset are shown in Figure 4.15, and examples of the curves for each model versus benchmark samples are provided in Figures 4.16–4.19. Note that unlike the *Green* scenario, the FVDM and FVADM both differ in their results since the *Red* scenario involves coming to a halt at an intersection, where the intersection is a 'virtual' vehicle whose presence causes the models to come to a complete stop.

The error results in Figure 4.15 show that the IDM is significantly more accurate than the other models. In fact, its *worst* performance is only slightly more inaccurate than the

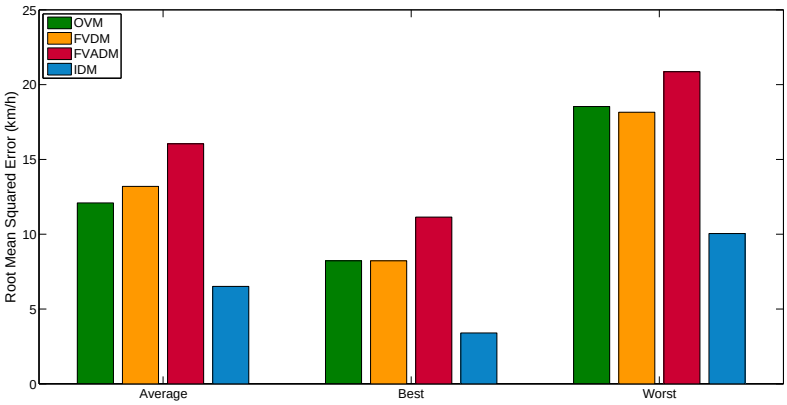

Figure 4.15: Root mean squared error of driver models against real-world driver benchmark dataset for the *Red* (stopping) scenario.

best performance of the OVM and FVDM, and *better* than the best performance of the FVADM. In contrast, the FVADM performs most poorly. This seems counter-intuitive given that the FVADM is considering more information (difference in acceleration). The issue is the FVADM's $g()$ sign function (see Equation (4.8)), which returns -1 if the following vehicle's acceleration is less than the ahead 'vehicle' (the intersection) *and* the ahead vehicle is decelerating or holding steady. Otherwise $g()$ returns $+1$. The idea of $g()$ is to ensure that the follower should decelerate more strongly if both vehicles are braking but the ahead vehicle is not braking as strongly. The problem occurs when the following vehicle is already decelerating strongly due to the disparity in *velocity*. In this case the FVADM's acceleration check increases the the aggressiveness of braking *despite the following vehicle already decelerating strongly*. This gives the FVADM highly aggressive braking behaviour, much more so than a real driver.

Moreover, by examining the examples of Figures 4.16–4.19 it becomes clear that the FVDM and FVADM also produce curves with a highly unusual 'kink' — an initial hard deceleration following by a plateau before a final round of deceleration. These two distinct phases of deceleration occur due to the balancing of the base OVM model term against the velocity difference term. Specifically, the velocity difference induces the FVDM to begin braking earlier than the base OVM. However, at some point the velocity becomes so low that the OVM term's desire to accelerate back up to the speed limit precisely balances the velocity difference term's desire to continue braking. Then when the vehicle's headway to the intersection becomes low enough, the OVM term itself causes a second phase of

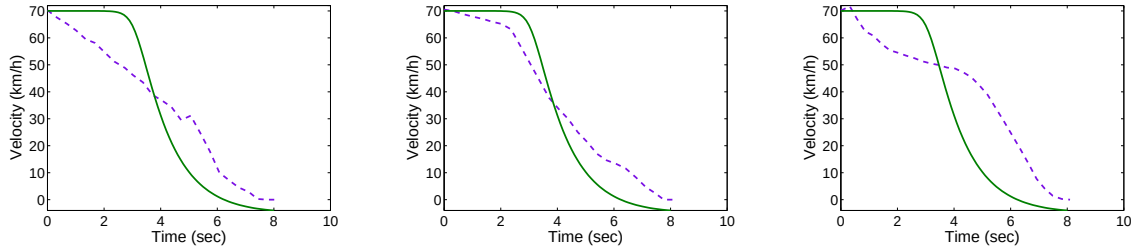

(a) (b) (c)

Figure 4.16: Example OVM model results vs GPS data for the *Red* (stopping) scenario: (a) Near-average example (b) Best-fitting (c) Worst-fitting. The solid green curve represents the OVM model data and the dashed purple curve represents the GPS data.

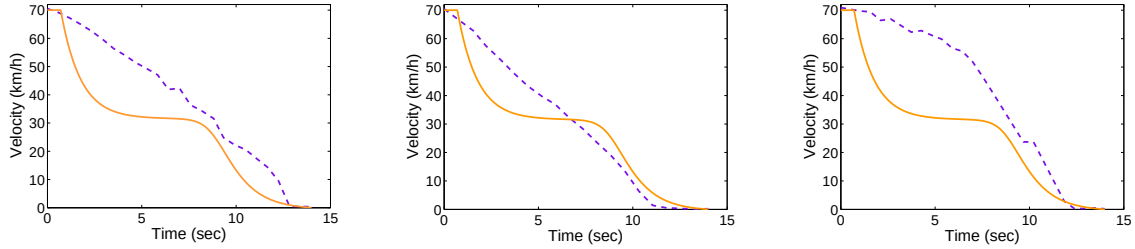

(a) (b) (c)

Figure 4.17: Example FVDM model results vs GPS data for the *Red* (stopping) scenario: (a) Near-average example (b) Best-fitting (c) Worst-fitting. The solid yellow curve represents the FVDM model data and the dashed purple curve represents the GPS data.

deceleration. The FVADM follows a similar pattern except that its first deceleration phase is even more pronounced than that of the FVDM due to the effect of $g()$ described earlier.

The OVM on its own in fact produces a more realistic deceleration curve than either the FVDM or FVADM due to the lack of the 'kink'. However, the OVM curve is not particularly close to the benchmarks, with deceleration being much more aggressive during initial braking.

In contrast the IDM produces quite reasonable matches to the benchmark data set. Its curvature and aggressiveness quite closely follow a real-world driver's behaviour. One incongruity is that the IDM induces a slight deceleration well before a real driver even begins to slow, hence the curves in 4.19 show that the IDM has already slowed down to

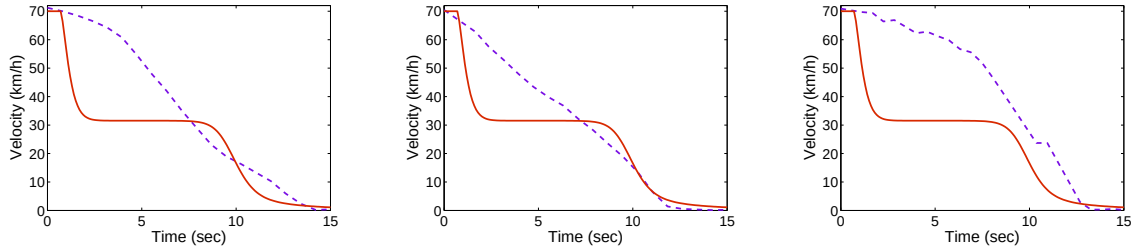

(a) (b) (c)

Figure 4.18: Example FVADM model results vs GPS data for the *Red* (stopping) scenario: (a) Near-average example (b) Best-fitting (c) Worst-fitting. The solid dark red curve represents the FVADM model data and the dashed purple curve represents the GPS data.

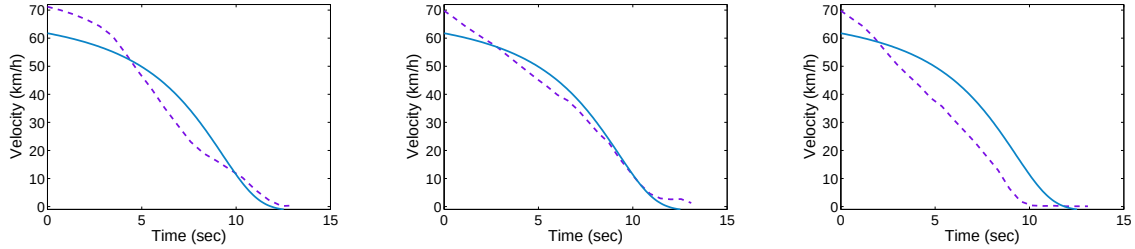

(a) (b) (c)

Figure 4.19: Example IDM model results vs GPS data for the *Red* (stopping) scenario: (a) Near-average example (b) Best-fitting (c) Worst-fitting. The solid blue curve represents the IDM model data and the dashed purple curve represents the GPS data.

$60km/h$ before the real driver begins braking (this occurs due to the 'best fit' matching for error described in Section 4.5.2.2). Again, this shows the conservatism of the IDM; a real driver is anticipating that the light may well turn green as they approach it, and only commits to braking when it is clear this will not occur in time. The IDM has no such anticipation and instead begins to decelerate slowly well in advance of the stopping point.

Note that all driver models actually go slightly negative in their velocity towards the end of each curve. This is caused by their 'overshooting' of the minimum safe distance headway due to the rapid deceleration when coming to a halt. In essence, the driver model attempts to reverse the vehicle a metre or so to return to their accepted safe distance since the 0.1 second interval is not fine-grained enough to allow the models to react quickly enough to eliminate this overshoot entirely.

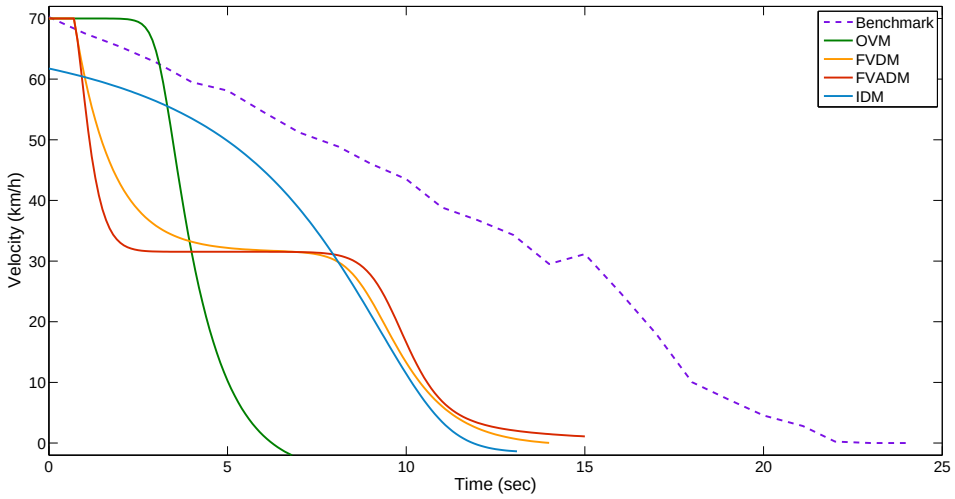

Figure 4.20: Comparison of the raw (unstretched) curves for each driver model and a benchmark sample for the *Red* (braking) scenario.

Figure 4.20 shows the raw (unstretched) curves for each driver model against the benchmark sample, providing an insight into the actual duration each model takes to brake to a halt. As with the *Green* scenario, the OVM is most aggressive in its braking approach, coming to a halt within 7 seconds — over four times faster than a real driver's more gradual braking at 25 seconds. In contrast the FVDM, FVADM and IDM all finish in 12–15 seconds. Note also that the benchmark curve is mostly linear with a slight 'convex' curvature until the final few seconds, indicating that a real driver tends to maintain a steady deceleration until relaxing to coast to a halt. However, the curves of the OVM, FVDM and FVADM are strongly 'concave', advocating an extreme braking force initially and gradually reducing the braking towards the end. On the other hand, the IDM essentially does the reverse by gradually increasing the braking force until the end where the vehicle coasts to a halt. In this way the IDM is far more realistic in its behaviour although it differs from a real driver in that it begins gradual braking very early and builds towards strong braking.

4.6 Summary

This chapter has explored the empirical behaviour of four widely-used stimulus-response microscopic models — the OVM, FVDM, FVADM and IDM. Experiments focused on situations that occur in urban traffic since most research effort has been concentrated on modelling freeway flow. Specific scenarios common in urban roads were designed and the responses of each driver model were analysed. Furthermore, the reactions of each model were quantitatively compared to a set of benchmark GPS-captured data from real drivers for two scenarios: accelerating from a green traffic light and braking for a red traffic light.

The results show that the IDM typically outperforms the other models in emulating real-world driver behaviour, though not in all cases. In the common urban traffic scenarios the IDM produced reasonable reactions to all but one scenario. Its main weaknesses arise from its conservative acceleration, a deceleration curve which involves a gradual onset towards late strong braking and a tendency to be insensitive to headway at low velocities.

The OVM clearly performs most poorly among the models. This is not surprising as the OVM is hampered by neglecting to take the leading vehicle's velocity into consideration, and only relies instead on headway and the following vehicle's velocity to calculate the resultant acceleration. Only where headway is the decisive factor will the OVM perform reasonably.

Of the similar FVDM and FVADM, it is interesting to note that the simpler FVDM typically achieves equivalent or better results, at times by an appreciable margin. The addition of velocity difference between the leading and following vehicles mitigates many of the OVM's issues, but the further addition of acceleration difference in the FVADM tends to both help and hinder that model depending on the situation. Moreover it only serves to moderate poor responses by the base FVDM rather than significantly improve them. This is best illustrated by the deceleration curve of the FVADM which is even more pronounced than the FVDM in their odd 'two-phase' braking profile (see Figure 4.20).

Chapter 5

Stability in Traffic Flow with Heterogeneous Networks

5.1 Stability

Stability of traffic flow is an underlying issue and needs to be addressed in all traffic models. Having stable traffic flow indicates that no inexplicable variances of flow exist in the system and that even normal fluctuations do not propagate and increase downstream in an unreasonable manner to reflect real-world driving conditions. Stability is more commonly a problem in microscopic models since they track individual vehicles and are formulated using heuristics rather than a system of equations as found in macroscopic and mesoscopic models.

The stability of microscopic is typically evaluated in isolation, and is commonly applied to all vehicles and road sections in the traffic network using a single model to ensure stability exists under normal driving conditions. Yet, as different models have varying strengths and weaknesses and thus will be more effective in different situations, it would be desirable to mix multiple models within the traffic network. Heterogeneous approaches that mix microscopic and macroscopic models exist, with some variations on the theme, but mixing different types of microscopic driver models has been largely overlooked and no analysis of the consequences on stability has been made.

A major goal of traffic models is the ability to react realistically to traffic-flow fluctuations, and the central factor in such reactions in a microscopic simulation is the implementation of the 'driver model': the system that models the reactions of a vehicle's driver. Although there is a lack of empirical evidence to show that a driver model always produces a stable and realistic response (Ranjitkar *et al.*, 2005b), it is still a desirable goal of such a driver model to have stability: reacting sensibly to changes in traffic density in the same way

that real drivers react and thereby damping down traffic-flow fluctuations. More formally, stability is the ability of a driver model to maintain a steady-state density among vehicles, and react to a perturbation in density by converging smoothly and monotonically towards a new steady-state density (Pueboobpaphan and van Arem, 2010). This ensures that there are no anomalies in flow caused by the model itself, which would give rise to inaccurate traffic-flow readings from the simulation. This is particularly an issue for microscopic models in which individual car behaviour is modelled, since stability (or otherwise) arises from the interaction of independently updated vehicles rather than an overall governing system of equations, such as is the case in macroscopic or mesoscopic models.

Microscopic driver models can be further divided into two major types: car-following or CF (continuous space) systems and cellular automata or CA (discrete space) systems, where continuous models update the vehicle state via a real-valued system of equations and discrete models update the vehicle state based on integer-valued equations. Although models exist for both approaches that achieve a level of stability, neither approach (continuous nor discrete) can be considered 'superior' to the other: both approaches have their advantages and disadvantages, which can become significant in different areas of an urban road network (for example computational efficiency, single-lane roads versus multi-lane roads, merge points versus intersections) (Hoogendoorn and Bovy, 2001; Yeldan *et al.*, 2012).

Thus it would be beneficial to create a heterogeneous road network composed of microscopic continuous and microscopic discrete road sections where each model type can be utilised in the areas of the network to which they are most suited. Although such a heterogeneous approach has been taken before as a means of mixing microscopic and macroscopic models in the one road network (referred to as multi-scale modelling (Helbing *et al.*, 2002; Newell, 2011)), to our knowledge no work has examined the effect of mixing different microscopic models. In particular, the discontinuities produced at the junction points where the two models meet and associated switching over from one model to another may trigger instability in the network, even in situations where the individual models themselves would show stable traffic flow.

The effects and characteristics of stability are examined by constructing a heterogeneous network that is comprised of two widely used microscopic models: a continuous-space car-following (CF) model, the Intelligent Driver Model (IDM), (Treiber *et al.*, 2000b) and the discrete-space Nagel-Schreckenberg (N-S) cellular automata (CA) model (Nagel and

Schreckenberg, 1992). The network will facilitate in identifying the means for detecting and isolating any instabilities caused by the model switch-over.

5.1.1 Difficulties in Measuring Stability

Ideally, one would measure traffic-flow stability directly. However, due to the nature of traffic networks (signals, intersections, etc) and the response of vehicles to that structure, changes in vehicle headway and density occur as part of normal traffic flow, in essence causing instabilities. For example, intersections may require vehicles to slow down or stop for oncoming traffic or for turning, and, as a consequence, headways between vehicles as they approach an intersection diminish at the same time as density of traffic flow increases at this juncture. Hence instabilities are a normal part of traffic. The problem to be avoided is an unstable model, which will either generate perturbances itself or magnify existing perturbances caused by normal traffic flow. This makes it difficult to measure model stability directly, since one does not know if the instability is coming from a normal traffic-flow source or not. To resolve this difficulty, we eliminate all potential sources of instability generated by the network and define a simple cyclical road network (Figure 5.1) whose parameters are designed to avoid causing any variation in traffic flow. Specifically:

1. Incoming velocities to the model transition node are always constant, that is, at the speed limit.
2. The spacing between successive vehicles is constant, with vehicles travelling at the speed limit.
3. Headway between platoons is large so that platoons will not interfere with each other.
4. The model transition node has no influence on traffic flow and control, and therefore no effect on the velocity or headway of vehicles, *ie:* it does not behave like a traffic light, for instance.

Without traffic instability due to network sources, any effects on density or headway must then be due to the instability caused either by the models' vehicular behaviour or their interaction with the network. Thus model stability will correlate directly with density

quantities that can be measured at every point on the network: vehicle density (number of vehicles at each location per timestep) and vehicle headway (distance to vehicle ahead at each point). Variations in these quantities will imply model instability, and the spatial extent of these quantities will indicate where and for how long the instabilities occur.

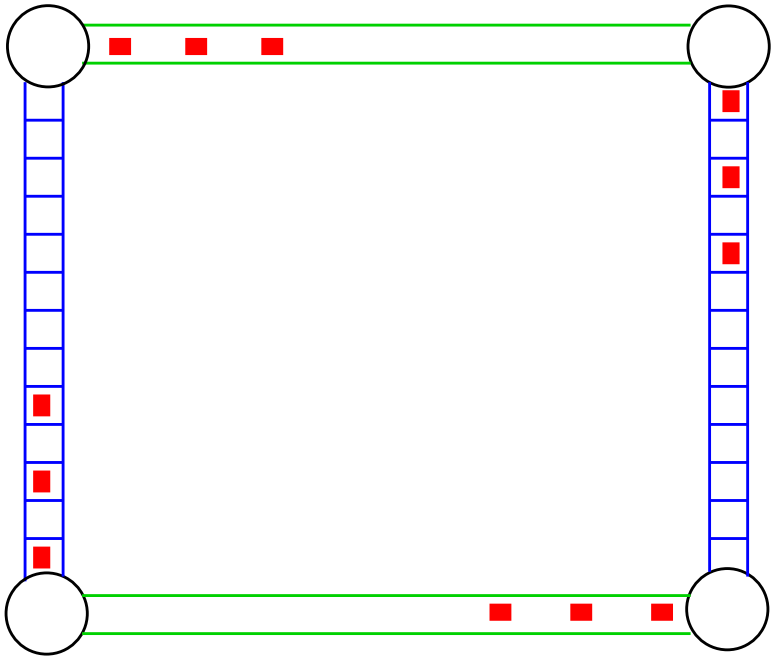

Figure 5.1: Control Network: Heterogeneous simulation with three vehicles per link.

5.2 Microscopic Models Used

The most desirable attributes that all traffic models endeavour to incorporate are accuracy, fast computation times, an ability to handle high volumes of traffic and multi-lane capabilities. As discussed earlier, neither the CF nor the CA models can individually deliver on all of these attributes. Hence we follow the same logic as multi-scale heterogeneous models (Newell, 2011) and seek to examine the behaviour of a mixture of the two types of models in a single network. Specifically, we choose to employ the car-following IDM of Treiber *et al.* (2000b) and the cellular automata N-S model of Nagel and Schreckenberg (1992) due to their widespread and ongoing usage (Treiber and Kesting, 2012; Hoogendoorn and Hoogendoorn, 2010; Gao *et al.*, 2007; Jia and Ma, 2009).

5.2.1 Review of Intelligent Driver Model

For the reader's convenience, a brief description of the formulation of the IDM (Treiber *et al.*, 2000b) is presented here. The basic premise of the IDM calculation involves balancing the ratio of desired velocity versus actual velocity against the ratio of desired headway versus actual headway. These are used to calculate the acceleration of the vehicle. This has been shown to be relatively effective at simulating real-world vehicle movement when accelerating and braking under normal driving conditions (Treiber *et al.*, 2000b). Formally, the IDM's acceleration of a vehicle with a length ℓ_i is determined by its own velocity $v_i(t)$, headway $s_i(t)$ and $\Delta v_i(t)$ the difference in velocity between vehicle i and $(i+1)$:

$$\frac{dv_i(t)}{dt} = a\left[1 - \left(\frac{v_i(t)}{v_0}\right)^{\delta} - \left(\frac{s^*(v_i, \Delta v_i)}{s_i(t)}\right)^2\right] \tag{5.1}$$

$$s^*(v_i, \Delta v_i) = s_0 + s_1\sqrt{\frac{v_i}{v_0}} + v_i T + \frac{v_i \Delta v_i}{2\sqrt{ab}}$$

The model's parameters are empirically measurable and have a reasonable interpretation. As such, the parameters can be modified to suit different circumstances; for example, the maximum acceleration a and desired deceleration b can be varied based on the conditions of the vehicles or road (Hoogendoorn and Bovy, 2001). The acceleration exponent δ controls the rate of a vehicle's acceleration (the driver's aggressiveness), with small values of δ producing a smoother acceleration than larger values.

5.2.2 Review of Nagel-Schreckenberg Algorithm

As with the IDM, this section presents a brief review of the formulation of the N-S algorithm (Nagel and Schreckenberg, 1992). The N-S algorithm for single lane traversal consists of four basic steps, where Steps 1–3 are applied to each vehicle before all vehicles are allowed to move forward their respective number of cells:

$v_i(t)$ is the velocity of a vehicle i at timestep t
v_ℓ is the maximum velocity and can be equated to the speed limit
$g_i(t)$ is the number of empty cells to the ahead vehicle at timestep i

$p_i(t)$ is the random probability that the vehicle will brake at timestep t
$x_i(t)$ is the position of the vehicle at timestep t

Step 1: Acceleration component
If $v_{i-1}(t) < v_\ell$ then $v_i(t) = v_{i-1}(t) + 1$

Step 2: Braking component
If the gap $g_i(t)$ after Step 1 is smaller than $v_{i-1}(t)$ then $v_i(t) = min(v_{i-1}(t), gi(t))$

Step 3: Randomisation component
Using random probability of $p_i(t)$, the velocity $v_i(t)$ is reduced by one unit after Step 2 for all vehicles to which the probability applies, *ie:* $v_i(t) = v_i(t) - 1$

Step 4: Driving component
After Steps 1–3, the new velocity $v_i(t)$ for each vehicle is determined and each vehicle is moved by $v_i(t)$ cells, where $x_i(t) = x_{i-1}(t) + v_i(t)$

5.3 Improving the Stability of the IDM

5.3.1 Instability of the IDM at the Speed Limit

First, we show that the IDM is in fact unstable when vehicles travel at or near the nominal speed limit v_0, and introduce a variant of the IDM that resolves the instability without altering its stable behaviour at lower velocities. This is done by reinterpreting v_0 as an upper bound on velocity and shifting the focus to appropriately setting v_0 as a function of the 'two-second-rule' headway gap and the true speed limit. The resultant speed-limit-stable IDM (SLS-IDM) allows vehicles to converge to the speed limit in a stable manner.

(Treiber *et al.*, 2000a) examined four traffic modes to demonstrate the IDMs suitability for simulating traffic flow, one of which was equilibrium traffic — the velocity and headway pair that would result in the IDM maintaining a constant spacing between vehicles (*ie:* perfect stability). This mode requires constant (but not necessarily equal) headway, and constant velocity (but not specifically the speed limit) between vehicles. They showed that there exists equilibrium headway s_e and equilibrium velocity v_e situations for the IDM, deriving equations for the two on the basis that equilibrium traffic has $dv_i(t)/dt = 0$ and $\Delta v_i = 0$ and, for brevity, setting $s_1 = 0$. The resultant equation for s_e is:

$$s_e(v_i) = (s_0 + v_i T)\left[1 - \left(\frac{v_i(t)}{v_0}\right)^{\delta}\right]^{-\frac{1}{2}} \tag{5.2}$$

In other words, the equilibrium headway mandated by the IDM will grow as actual velocity v_i increases towards v_0, and will allow it to shrink to the minimum distance s_0 when $v_i = 0$. These outcomes reflect real-world driver behaviour in maintaining headway according to velocity. Deriving equilibrium velocity v_e requires assuming that $v_i << v_0$ and the implicit assumption that every vehicle has a leading vehicle, all with a headway of s_i (*ie:* a closed system with uniform spacing). Simple and intuitive equations for v_e can then be produced when the acceleration exponent δ is set to $\delta = 1$, $\delta = 2$ or $\delta = \infty$ (other choices do not so easily lead to closed-form solutions):

$$v_e(s_i) = \frac{s_i^2}{2v_0T^2}\left[-1 + \sqrt{1 + \left(\frac{2v_0T}{s_i}\right)^2}\right], \delta = 1 \tag{5.3}$$

$$v_e(s_i) = \frac{v_0}{\sqrt{1 + \left(\frac{v_0T}{s_i}\right)^2}}, \qquad \text{when } \delta = 2 \tag{5.4}$$

where:

$$v_e(s_i) = \min\left\{v_0, \frac{s_i - s_0}{T}\right\} \qquad \text{when } \delta = \infty \tag{5.5}$$

These are the flip-side of Equation (5.2), showing that as headway s_i increases, the IDM will allow a higher v_e and conversely when s_i shrinks, v_e will be smaller to achieve stability.

(a)

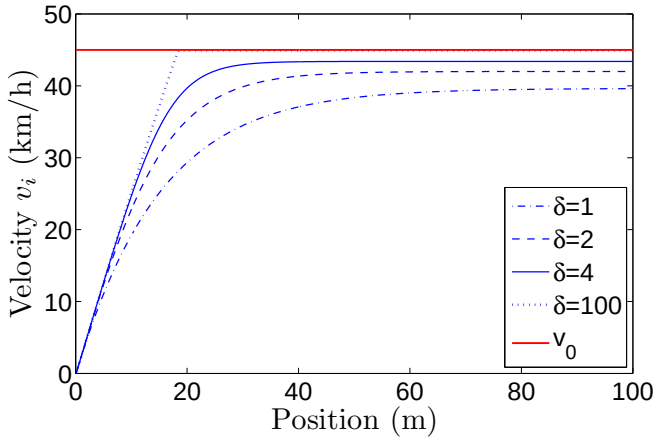

(b)

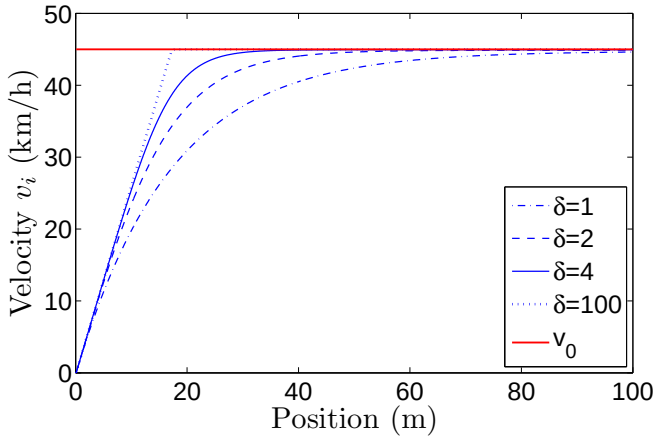

Figure 5.2: Velocity of a vehicle as it accelerates according to the IDM with a fixed headway to the vehicle ahead of it. (a) Headway = $20m$, (b) Headway = $100m$. Note that in (a), velocity converges to well below v_0 unless δ is relatively high, whereas in (b) convergence is closer to v_0 (but not quite reaching) v_0 due to the larger headway.

Again, these are realistic responses, and v_e can be considered the velocity that the IDM 'driver' seeks to reach under free-flowing traffic conditions. When all drivers achieve this v_e (and thus a corresponding s_e), traffic stability is guaranteed.

However, the issue with Equations (5.3), (5.4) and (5.5) is that Treiber *et al.* (2000a) only showed this behaviour for $v_i << v_0$ and in a closed system in which every vehicle has the same headway s_i. The behaviour as $v_i \rightarrow v_0$ was left unexplored. Note that it is natural to interpret v_0 as the speed limit, although this was not explicitly defined in the original paper. In fact it will be shown that the speed limit to which the IDM converges is not v_0 directly but rather a function of v_0.

Consider Figure 5.2, which shows the velocity profiles over time of a vehicle accelerating from $0km/h$ to $45km/h$ ($12.5m/s$) with various values of δ. In order to focus on the behaviour of velocity, the headway is constant and $\Delta v_i = 0$ for all time steps, as if the leading and following vehicles have precisely the same speed. Two mini-simulations of two vehicles along a straight road were run using the IDM for fixed headways of $20m$ and $100m$ (Figures 5.2a and 5.2b respectively, where $v_0 = 12.5m/s$ ($45km/h$) and the vehicles begin at rest (*ie:* $v_i(t = 0) = 0$)). Also, setting $s_0 = 0$ eliminates vehicle length as an issue. Only the fixed headway was changed for each simulation.

The graphs show the follower vehicle's velocity as it converges to a stable value — specifically, as it converges to v_e. They illustrate that for reasonable $\delta \leq 4$, the velocity v_i of a vehicle never actually reaches v_0 (our assumed speed limit) even though the headways are all at least as large as the $v_i T$ minimum safe distance (*ie:* $1.6s \times 12.5m/s = 20m$) where headways should be acceptable given the low v_0. However, every graph shows a gap between v_0 and the velocity to which v_i converges. This is most pronounced at $20m$ headways, with the gap being $3.5km/h$. Even at a headway of $100m$ the IDM will refuse to allow the following vehicle to reach v_0 (allowing only approximately $44km/h$), yet for a speed limit of $45km/h$ this distance is certainly more than sufficient to allow the driver to safely drive at the speed limit.

Note that as δ increases, the gap decreases and largely disappears when setting $\delta = 100$ (approximating $\delta \to \infty$). However, such a high δ means that there is no moderation in acceleration or deceleration: the velocity profile is essentially maximum acceleration until reaching v_0, at which point it abruptly switches to zero acceleration. In effect, the IDM is reduced to a most simplistic driver model when δ is high enough to cause the gap to be eliminated.

In general, the figures show that with reasonable headways for the IDM, v_i approaches v_0 closely only in the cases where the headway $s_i \to \infty$ or where $\delta \to \infty$. Examining Equation (5.2) shows this same result mathematically. Taking the limit $v_i \to v_0$:

$$
\begin{aligned}
s_e(v) &= \lim_{v_i \to v_0} \Big(s_0 + v_i T)\Big) \left\lceil 1 - \left(\frac{v_i}{v_0}\right)^{\delta} \right\rceil^{-\frac{1}{2}} \\
&= \Big(s_0 + v_0 T)\Big) \lim_{v_i \to v_0} \left\lceil 1 - \left(\frac{v_i}{v_0}\right)^{\delta} \right\rceil^{-\frac{1}{2}} \\
&= \Big(s_0 + v_0 T)\Big) \lim_{v_i \to v_0} \frac{1}{\sqrt{1 - \left(\frac{v_i}{v_0}\right)^{\delta}}} \\
&= \Big(s_0 + v_0 T) \times \infty \\
&= \infty
\end{aligned} \tag{5.6}
$$

In other words, the equilibrium headway s_e approaches ∞ when $\delta < \infty$, regardless of v_i. Since the vehicle will never be able to accelerate to v_0, it is clear that v_0 is not the speed limit (particularly since the gap to v_0 can be quite significant, as Figure 5.2 shows), but more of an upper bound on velocity. Moreover, the velocity to which the IDM converges is a function of both v_0 and the headway; in other words, the speed limit does not exist as a parameter of the IDM. However, a contradiction occurs with the following observation: a leading vehicle k of a platoon of vehicles in an open system may have no vehicles ahead of it. Thus $s_k = \infty$, and from Equation (5.4)b, one can show v_e in the limit of $s_i = \infty$

$$
\begin{aligned}
v_e(s_i) &= \lim s_i \to \infty \frac{v_0}{\sqrt{1 + \left(\frac{v_0 T}{s_i}\right)^2}} \\
&= \frac{v_0}{\sqrt{1 + \left(\lim s_i \to \infty \frac{v_0 T}{s_i}\right)^2}} \\
&= \frac{v_0}{\sqrt{1}} \\
&= v_0
\end{aligned} \tag{5.7}
$$

This illustrates that in an open system that defines v_0 as the speed limit, the lead vehicle will accelerate to v_0, but for all other vehicles i their velocity v_i will never reach the upper

bound of v_0, with the gap between v_i and v_0 dependent on the headway. This means that the lead vehicle will slowly pull away from the followers, causing vehicles from the same platoon to become strung out and destroying both local stability and platoon stability.

5.3.2 Speed Limit Stable IDM

As shown, the IDM in its current form suffers from instability in cases where velocity is allowed to approach v_0. Although setting $\delta = \infty$ will allow vehicles to attain the speed limit, this comes at the cost of unrealistic acceleration behaviour, as shown in Figure 5.2. However, it is interesting to note that Figure 5.2 indicates that *some* velocity is being converged to in each case — just not v_0. Hence v_0 is merely a hard upper bound on the velocity that a vehicle uses to achieve convergence to its target equilibrium velocity v_e. The controlling factor in v_e is the headway s_i. Hence we propose to modify the IDM to incorporate an explicitly-defined speed limit by switching emphasis to s_i rather than v_0.

Given a required speed limit v_ℓ, we define s as the 'desired headway' and then calculate the desired (upper bound) velocity v_0 that will result in convergence of v_i to v_ℓ at the desired headway s_α. This will force vehicles to moderate their behaviour to reach s_α and thus v_ℓ. This resonates with real driving experience: a human driver will, under the constraint of the speed limit, attempt to achieve and maintain a specific gap to the vehicle ahead — embodied by the well-known 'two-second rule' that recommends drivers leave at least a two-second interval between them and the vehicle ahead as an adequate safety margin. We dub this the speed limit stable IDM, or SLS-IDM.

In effect, v_0 becomes a variable that indirectly defines the upper bound for v_i, and appropriate manipulation can make this upper bound equal to v_ℓ. In this way, a vehicle's velocity v_i will always be able to attain the speed limit v_ℓ. To determine the value that v_0 should take such that the speed limit v_ℓ will the equilibrium velocity v_e for vehicles travelling at headway $\geqslant s_\alpha$, we follow a similar approach to Treiber *et al.* (2000a) and set $dv/dt = 0$, $\Delta v_i(t) = 0$ and $s_1 = 0$, as in their original derivation for equilibrium headway and velocity. However, as we are interested in calculating the v_0 required for converging to the speed limit v_ℓ, we set $v = v_\ell$:

$$\frac{dv_\ell}{dt} = a\left[1 - \left(\frac{v_\ell}{v_0}\right)^\delta - \left(\frac{s^*(v_{\ell,0})}{s_\alpha}\right)^2\right]$$
$$0 = 1 - \left(\frac{v_\ell}{v_0}\right)^\delta - \left(\frac{s^*(v_{\ell,0})}{s_\alpha}\right)^2$$
$$\left(\frac{v_\ell}{v_0}\right)^\delta = 1 - \left(\frac{s_0 + v_\ell T}{s_\alpha}\right)^2 \tag{5.8}$$

substituting for $s^*()$ with $s_1 = 0$:

$$v_0 = \frac{v_\ell}{\left[1 - \left(\frac{s_0 + v_\ell T}{s_\alpha}\right)^2\right]^{\frac{1}{\delta}}} \tag{5.9}$$

Equation (5.9) thus allows one to calculate the v_0 that will ensure vehicles accelerate such that their velocity converges to v_ℓ. In practice, we use $v_0 + \xi$ (where ξ is a small constant) to ensure v_0 will definitely be reached regardless of computational floating-point rounding errors.

The free variable in Equation (5.9) is s_α, the desired headway. Although this may be any value it is important to note that any $s_\alpha < (s_0 + v_\ell T)$ will result in the root of a negative value being evaluated for the denominator, producing a complex v_0 for even δ and negative v_0 for odd δ. In other words, the IDM will fail if the desired headway is less than the minimum safe headway. Thus we take the approach of defining s_α in terms of a desired gap interval in seconds T_α:

$$s_\alpha = s_0 + v_\ell T_\alpha \qquad \text{where } T_\alpha > T \tag{5.10}$$

To highlight how v_0 will vary with T_α, Figure 5.3 shows the gap between the calculated v_0 and v_ℓ as the desired interval T_α increases ($s_0 = 0$ and $\delta = 2$ for the purposes of the figure). This figure directly relates to Figure 5.2 in that the difference between the calculated v_0 and v_ℓ in Figure 5.3 corresponds to the gap between the constant v_0 and the v_i after convergence in Figure 5.2. The difference is that here v_0 is varying relative to

a fixed v_ℓ (v_ℓ is the constant) whereas in Figure 5.2 v_0 is the constant and v_i converges below it with a gap.

Note that at the minimum safe interval of $T_\alpha = T = 1.6s$ the gap between v_0 and v_ℓ approaches infinity, reinforcing the concept that the IDM cannot tolerate gaps at or below the minimum safe distance. Fortunately, this gap quickly reduces and sensible intervals can be calculated, such as $T_\alpha = 2.0s$ produces $v_0 \approx 1.5 \times v_\ell$. (For the experiments in Section 5.6, a value of $T_\alpha = 2.0s$ is used).

It is important to note that this proposed SLS-IDM only adjusts v_0 for the purposes of facilitating stability at the speed limit. In effect, it re-defines how to set the v_0 parameter of the original IDM for a given stretch of road that is at a specific speed limit. Other road sections that are at different speed limits will have a different v_0 — exactly as the original IDM also requires. Hence the behaviour of the IDM at $v_i << v_0$ is left unchanged, and the analysis of Treiber *et al.* (2000a) that showed the stability of the IDM at these speeds still fully applies.

One final point to note is that the SLS-IDM brings the equilibrium headway s_e down from ∞ to $s_\alpha = v_\ell T_\alpha$. However, the IDM's formulation implicitly means that exceeding s_e will allow the vehicle to exceed the speed limit. This was not a problem for the original IDM since $s_e = \infty$ and the speed limit bound is v_0, but in the SLS-IDM headway can be larger than s_α, and the bound to be enforced is v_ℓ rather than the higher v_0. Fortunately, in practice this is not a significant issue since the approximating nature of a computer simulation already means that the original IDM can cause the speed limit to be overshot simply due to the granularity of the time interval, and so the simulation must heuristically enforce that each vehicle does not exceed the speed limit anyways. Hence when $s_i > s_\alpha$ and the SLS-IDM returns accelerations that would overshoot the speed limit v_ℓ, this heuristic must already be in place to ensure the speed limit is not exceeded. Moreover, this problem only occurs when headway is large, a situation that implies low-density (uncongested) traffic that is of little concern for analysis.

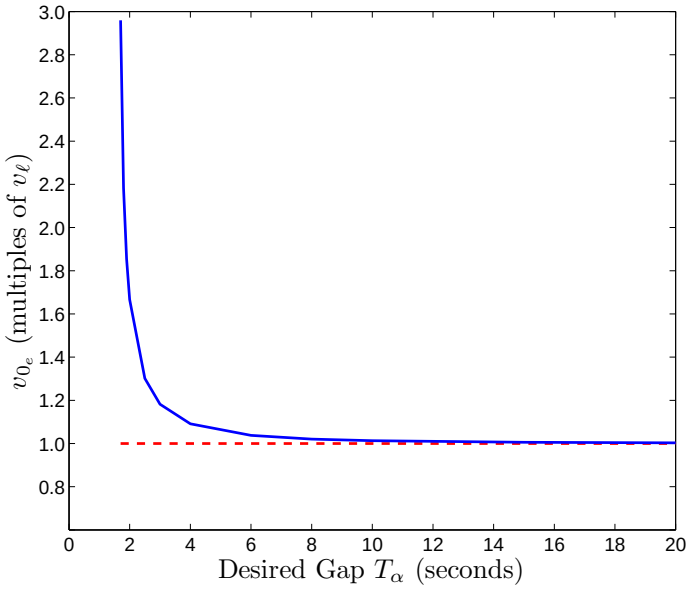

Figure 5.3: This figure plots the multiplying factor that must be applied to v_ℓ to produce an upper bound v_0 that will allow stable convergence to the speed limit v_ℓ at the given stable headway gap T_α (in seconds). v_0 is in solid blue and v_ℓ is the dashed red line. Note that the multiplying factor begins from infinity at the IDM minimum gap $T = 1.6$, and drops very quickly towards 1.0 as T_α grows, meaning that the SLS-IDM does not need to adjust v_0 significantly to effect reasonable stable headways.

5.4 Analysing Stability in a Heterogeneous Network

Since our goal is to investigate the effect of heterogeneous networks on stability, we first verify that the base CF and CA models employed and the proposed SLS-IDM as well as the N-S algorithms are stable on a homogeneous network (*ie:* when only one or the other model is operational along all road segments). Given this verified stability of the base models, we then modify the road network to include heterogeneous links that alternate between the two different models. Any instability in density and headway must then be due to the heterogeneity of the models. If traffic stability is maintained while switching models, we expect no change in traffic density at the transition points. Moreover, the entire network will have uniform density since velocity will be constant for all vehicles (*ie:* at the speed limit). If the assumption is false, however, then density fluctuations will indicate that an instability exists and will also identify where in the network and for how long the density is affected.

5.4.1 Measuring Density

To test the overall stability of our heterogeneous network, each link is divided into a set of bins to enable measurements to be taken at consistent points. Bins are $0.1m$ wide to handle fractional link lengths and detailed granularity. To measure density, a counter associated with each bin is incremented by one every time when a vehicle is either positioned in or passes over that particular bin during the simulation. At the end of the simulation, the counts of each bin are plotted. Fluctuations in the plot indicate instability at those points. The same bin interval and structure is used to measure local stability, but rather than incrementing a counter each time the system detects a vehicle in a specific bin, the system measures the distance between the vehicle in the particular bin and the vehicle ahead of it in the same platoon (*ie:* the headway). Headways between platoons are explicitly ignored as the distribution of headways implicitly indicates the platoon's stability, with the average of the headways of each bin plotted to examine any fluctuations.

5.5 Simulations

5.5.1 Test Networks

5.5.1.1 Control Network

To initially analyse the stability of traffic density in a heterogeneous system, we constructed a simple closed-system network — a four-sided circuit alternating between CF (SLS-IDM) and CA (N-S) links with three vehicles per link to give a total of 12 vehicles. Figure 5.1 shows the network. The speed limit v_ℓ on all links is identical. This *Control Network* consists of four transition nodes linking the alternating CF and CA links, and facilitating a correlation between flow measurements and stability, as described in Section 5.1.1. The group of three vehicles on each link is organised into a platoon in which vehicles follow relatively closely behind one another.

The four points in the system at which instability is expected to potentially happen are at the nodes where the changeover of model occurs. Approaching the CA→CF transition point, no discernible change in flow is expected since the transition is from a coarse-

grained (discrete) calculation to a finer-grained (continuous) calculation, and thus has no loss of modelling accuracy. However, when approaching the CF→CA transitions, some adjustment (*ie:* rounding up or rounding down to the nearest cell) is required when positioning a vehicle in its initial cell on the discrete CA link. This will affect the headway to the following vehicles still on the CF link and likely cause a change in acceleration of the follower(s). The resultant effect on stability, its magnitude and its duration is the focus of the analysis.

5.5.1.2 Model Network

A second network is constructed that reflects a more complex, real-world road network. Figure 5.4 shows this *Model Network*, which is used to examine if the findings from the Control Network also manifest in more realistic networks. In this network, speed limits vary between links and multi-road junctions such as four-way intersections.

5.5.1.3 Simulations

The simulations run as a discrete-time dynamics system in which the initial state of each vehicle (acceleration, velocity and position) is updated at every successive timestep according to the SLS-IDM model or the N-S algorithm, depending on which type of link the vehicle is on. Components of the state that are not directly updated by the models are updated according to the physics of a body in motion (*eg:* for position p of vehicle i, $p_i(t) = p_i(t-1) + v_i(t-1)$, where $v_i(t-1)$ has already been updated to incorporate the acceleration at $t-1$). Timesteps are incremented at intervals of one second, balancing the accuracy of the simulation against processing needs.

At the beginning of the simulation, each platoon is positioned at the start of its link with headway slightly smaller than the desired headway s_α to allow the SLS-IDM to converge to s_α. Velocity and acceleration are initially zero so that the models (SLS-IDM and N-S) must accelerate the vehicles to their equilibrium velocities. However, this initial acceleration means that the final traffic flow will be slightly higher at the beginning of the links (due to the time taken to begin moving). Hence for the purposes of flow and headway measurement, the simulation ignores the first 1000 timesteps. Constants used for the SLS-IDM and for the N-S algorithm are both found in section 5.2.

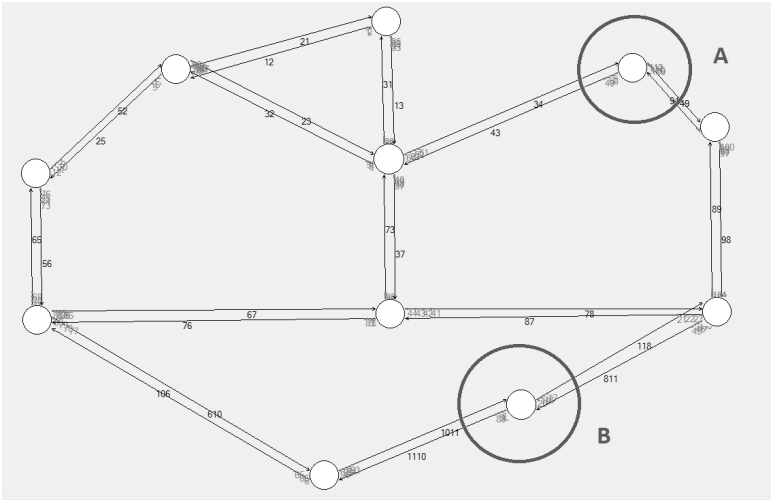

Figure 5.4: Model Network: Heterogeneous simulation with 28 links, 11 nodes and 112 vehicles. CF*rightarrow*CA transitions are circled and marked A and B. Note that grey numbers represent vehicles, and when vehicles are close together the numbers overlap. The darker numbers indicate the name of the links, with the naming convention being from node to node, *eg:* link 12 is from link 1 to link 2.

5.6 Experiments

Three sets of experiments were run. The first was designed to verify that the individual SLS-IDM and N-S algorithms are themselves stable, by adjusting the four-link Control Network to contain only CF links or only CA links.

The second set of experiments was to examine a heterogeneous system under controlled conditions. To this end, experiments were conducted on the Control Network with alternating CF and CA links and varying the parameters of the transition between the link types to investigate the stability behaviour of a microscopic heterogeneous network. Confounding factors related to instability that are eliminated include ensuring that the link lengths are long enough so that the models can re-stabilise after transitioning if necessary, ignoring the first 1000 timesteps to guarantee that no aberrations in density from the initial acceleration will affect the results, setting the same speed limit for all links, initialising the headway between all vehicles in a platoon to be uniform and at a reasonable distance given the speed limit, and placing each platoon of vehicles on a different link.

In these experiments, vehicles moving from a CF link to a CA link are assigned to a cell on the CA link in one of two ways — rounding down or rounding up to the nearest cell. For example, consider a vehicle that is moving on a CF link at a constant speed of $12.5m/s$ and is positioned at $242m$ along the link's $250m$ length. In the next timestep, the SLS-IDM will move the vehicle to $254.5m$, which is in fact $4.5m$ into the discrete link. On a subsequent CA link with a cell size of $2.5m$, the vehicle will fall between the second ($+2.5m$) and third ($+5.0m$) cells. By rounding down, the vehicle will be placed at the $+2.5m$ cell while rounding up would place the vehicle at the $+5.0m$ cell. The effect of both rounding approaches will be explored.

A third experimental group was conducted on the full Model Network to examine whether driver model transitions also produce similar outcomes in more realistic networks.

For the IDM, $s_\alpha = 25$ and v_0 is calculated according to Equation (5.9) based on the speed limit v_ℓ (which varies between experiments). For the N-S algorithm the probability of braking during the randomisation component is 0.0 to avoid introducing instability due to random driver braking. Cell size is either $2.5m$ or $7.5m$, with the only other parameter being v_ℓ (note that the N-S algorithm operates on cell indexes, but this can be converted into m and m/s by multiplying by cell size). The values for other parameters are listed in section 5.2.

5.6.1 Experimental Parameters

5.6.1.1 Control Network Parameters

Given the stability of the individual models, our goal is to examine their stability when executing them in a heterogeneous model network. The basic Control Network of Figure 5.1 was used to produce four variants in parameterisation to explore the effects of these parameters on stability. Table 5.1 lists the configurations of each test case.

The hypothesis behind the parameterisations is as follows. As a vehicle travels through a CF→CA transition point, it will be assigned to a cell on the discrete destination link. If the vehicle is not precisely positioned on a cell this necessitates choosing a cell to place the vehicle in, decided by rounding the vehicle's position either up or down to the nearest cell

position. Such rounding may then have effects on following vehicles in that the follower that is still on the CF link will now detect that the headway has changed and the SLS-IDM will react accordingly. For rounding down, this will likely create an instability as the follower must brake to compensate for the sudden reduction in headway below the desired headway s_α. With larger cell sizes, the potential rounding will also be larger and hence any instability should be more pronounced. However, it is less clear what the outcome will be with rounding up since the headway will remain reasonable and since the vehicles are at the speed limit no acceleration to close the gap can occur. In other words, potential instabilities may be avoided by simply ensuring the CA model rounds positions up to the nearest cell.

In contrast, it is not likely that there will be similar instability effects at the CA→CF transition points since vehicles would be moving from a coarse-grained discrete to a fine-grained continuous model and hence rounding will not be a factor. Thus the parameterisations are split into two groups: Basic for small rounding errors and Large for large rounding errors, further separated into rounding up and rounding down (Basic-U, Basic-D, Large-U, Large-D). The Basic parameterisations represent the situation that would be expected if no particular care would be taken in link length selection and with reasonably small cell sizes, whereas the Large sets are used to explore worst-case behaviour.

		Link Length				
Name	Test Case	Cell Size	CF	CA	v_ℓ	Rounding
Basic-D	Basic simulations, round down	$2.5m$	$256.2m$	$250.0m$	$12.5m/s^2$	Down
Basic-U	Basic simulations, round up	$2.5m$	$256.2m$	$250.0m$	$12.5m/s^2$	Up
Large-D	Significant round down	$7.5m$	$255.1m$	$255.0m$	$15.0m/s^2$	Down
Large-U	Significant round up	$7.5m$	$262.4.2m$	$262.5m$	$15.0m/s^2$	Up

Table 5.1: Parameters for each of the variants explored. Simulation names (first column) also indicate rounding: (U)p or (D)own. Items marked CF imply a parameter for the car-following links; items marked CA imply a parameter for the cellular automata links.

5.6.1.2 Model Network Parameters

The Model Network is the model of real roads, hence different links have different speed limits and lengths. A full listing of the parameters is of little value since the specifics will vary from road network to road network. What is of value is to focus on the CF→CA

transition points (the respective nodes are circled and denoted as A and B in Figure 5.4). This network consists of 28 links (14 roads going in both directions), 11 nodes and 112 vehicles (four vehicles per link at start-up). The nodes are a mixture of throughways and T-junctions, with one four-way junction. The latter two node types allow vehicles to make decisions as to which direction (next link) to take, and this will have an impact on density in the network since not all vehicles will travel the same route. The simulation is run twice, once for rounding down and a second time for rounding up.

5.7 Results and Analysis

5.7.1 Verifying Stability of the SLS-IDM and N-S Models

To show that the SLS-IDM and N-S models are themselves independently stable, a simulation with only CF links (SLS-IDM) and another simulation with only CA links (N-S) were run, using the following parameters: link length = $250m$, $v_\ell = 12.5m/s$ and (for CA) cell size = $2.5m$. Figure 5.5 shows the traffic density at each point in the network, averaged over the duration of the simulation. In the figure, position is defined as metres from the $0m$ position on the first link — effectively the distance along a 'lap' of the circuit. As can be seen, the SLS-IDM and N-S simulations produce uniform flow and constant headway measurements throughout the road network, indicating that both models are stable when operating homogeneously within the network.

The transition point is at the $1000m$ mark in all figures. Note that scale differs from that for the Control Network (Figures 5.5–5.7) as fewer vehicles exist per metre of road.

5.7.2 Control Network Analysis

Figure 5.6 shows the density and average headway fluctuations in the Basic-D and Basic-U simulations. They display some effects of rounding down (Figure 5.6a) or rounding up (Figure 5.6b) for the initial positioning of the vehicle on the discrete link. Figure 5.7 shows similar results for the Large-D and Large-U simulations. The figures show both the density and average headway over the entire simulation. The simulation consists of $256.2m$ link

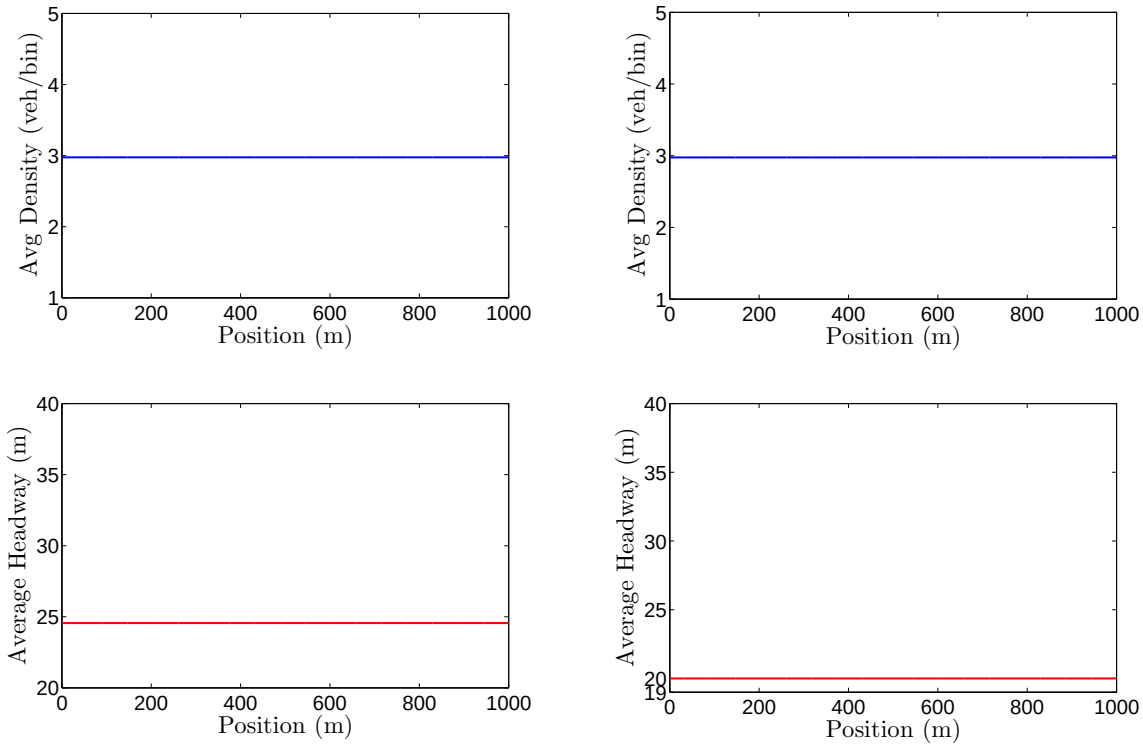

(a) Continuous IDM

(b) Discrete N-S

Figure 5.5: Density and average headway in CF-only and CA-only networks with links = $250m$, velocity = $12.5m/s^2$ and cell size (for discrete) = $2.5m$.

lengths for the continuous portions of the network. This link length was chosen so that the choice between rounding down or rounding up produces a similar rounding error since vehicle transitioning through CF→CA will land approximately in the middle of the cell.

For Figure 5.6a (Basic-D) it can be seen that small density and average headway aberrations start at approximately the $220 - 225m$ mark and the $735 - 740m$ mark (which is approximately on the $220 - 225m$ mark of the second continuous link) — in other words at the end of the two CF links. This is approximately $35m$ before each CF→CA transition point, roughly 1.5 times the desired headway of $25m$. It is at these points when the trailing (last) vehicle in each cluster of vehicles starts to feel the effects of the leading vehicle making the transition. When this happens, the following (middle) vehicle slows down, which in turn generates a cascading effect to the last vehicle in the cluster. The peak of the aberration occurs on the CF link about $15 - 20m$ from the transition point. At this point the middle vehicle has just moved on to the CA link with the last vehicle

still on the CF link and still being affected by the disturbance. However, it is interesting to note that the instability ends within $5m$ after the transition occurs — between $2.5m$ and $7.5m$ on the CA link, or about two cells. This indicates that the discrete CA is very effective in smoothing out the disturbance created by the transitioning of vehicles. This is due the fact that velocities are quantised to the nearest whole multiple of a cell; hence, any instability that falls below this threshold is simply quantised out of existence. Finally, note that as expected no instability exists at the CA→CF transition.

Figure 5.7a shows a more extreme case of rounding down with the Large-D case, where the CF link length of $255.1m$ was chosen to cause vehicles to land near the end of a cell and thus be rounded down nearly a full cell length ($7.4m$). As with Basic-D, density spikes occur in the immediate lead-up to the CF→CA transition point, with the Large-D instability being more significant due to the larger position shift and subsequent increased braking of the following vehicle. Of note is the clear asymmetry of the spike, with a sharp leading 'face' and a trailing 'tail'. This arises due to the non-linear effects of rounding down on the following vehicle. The second vehicle experiences significant 'emergency' braking to compensate for the sudden unexpected proximity of the lead vehicle — as minimum headway is to be avoided at all costs, the IDM reacts strongly. Although this has a cascade effect on the third vehicle, both vehicles are still within the CF link and thus the change in headway between the second and third vehicles is governed by decelerations that are constrained to lie within realistic limits by the IDM.

Rounding up should eliminate the squeezing effect of vehicles having to bunch up, and the subsequent density spike and average headway dip due to rounding down on the discrete CA link. While this is the case and no density spike occurs, Figure 5.6b shows a dip in density and a corresponding spike in average headway. However, the two are slightly offset from one another: the density dip occurs just at the transition point and immediately after it, whereas the headway spike begins about 20 m before the transition juncture. In essence, the density dip minimum occurs at the beginning of the CA link and is due to the transitioning vehicle occasionally being 'jumped' forwards by a cell due to the rounding up. The headway spike that this creates affects the following vehicles that are still on the CF link, hence the headway spike reaches a maximum about $8m$ before the transition point. The symmetry of the fluctuation is also noteworthy in comparison to the 'trailing-off' that occurred when rounding down — this is because the dip occurs in the discrete CA link.

Figure 5.7b shows the Large-U case of rounding up where again the link length forces a very large rounding error. In this case, the dip in density is more pronounced obviously because the larger position shift due to rounding up results in a greater distance 'jumped'. But otherwise the case is similar to the Basic-U experiment, with the headway and density effects again slightly offset from each other.

The results indicate that both rounding up and rounding down produce effects on traffic density and headways around the CF→CA transition points. Rounding down tends to produce more problematic instabilities by causing traffic density to spike immediately prior to the CF→CA transition via reduced headways, and thus inducing braking in the following vehicles. These instabilities propagate upstream quite a distance (between 1 and 2 times the desired headway s_α). Fortunately, the stability of the individual driver models limits the spread of the instability: once vehicles transition onto the discrete CA link the fluctuation is quickly eliminated by the N-S algorithm, and the IDM ensures that its effect on upstream traffic is dampened down by limiting the decelerations to realistic values. Rounding up avoids this braking and associated density spikes and only produces density dips where vehicles are 'jumped' forwards by a cell length due to the rounding. However, it is conceivable that the rounding up may create undesirable cell moves in congested situations, or even a collision with vehicles already on the CA link.

The figures highlight that the driver model transition causes a fairly unique 'fingerprint' of instability in density and headway around the CF→CA transition points. If vehicles are rounded down to the nearest CA cell the consequence is a significant spike in density and a corresponding dip in headway just prior to the transition point. For rounding up, a different situation occurs, with a sudden dip in density immediately following the transition point and a corresponding spike in headway immediately prior to the transition. In both cases, the magnitude of the spikes or dips depends on the magnitude of the rounding error induced by the CA link (which is a function of the cell size and where the vehicles land within the cell). Importantly, the spikes and corresponding dips are very short lived, and hence if such a density or headway fluctuation exists on a CF→CA transition link in a realistic heterogeneous network, it is likely that the fluctuation is due to the model transition and is not a true feature of traffic flow.

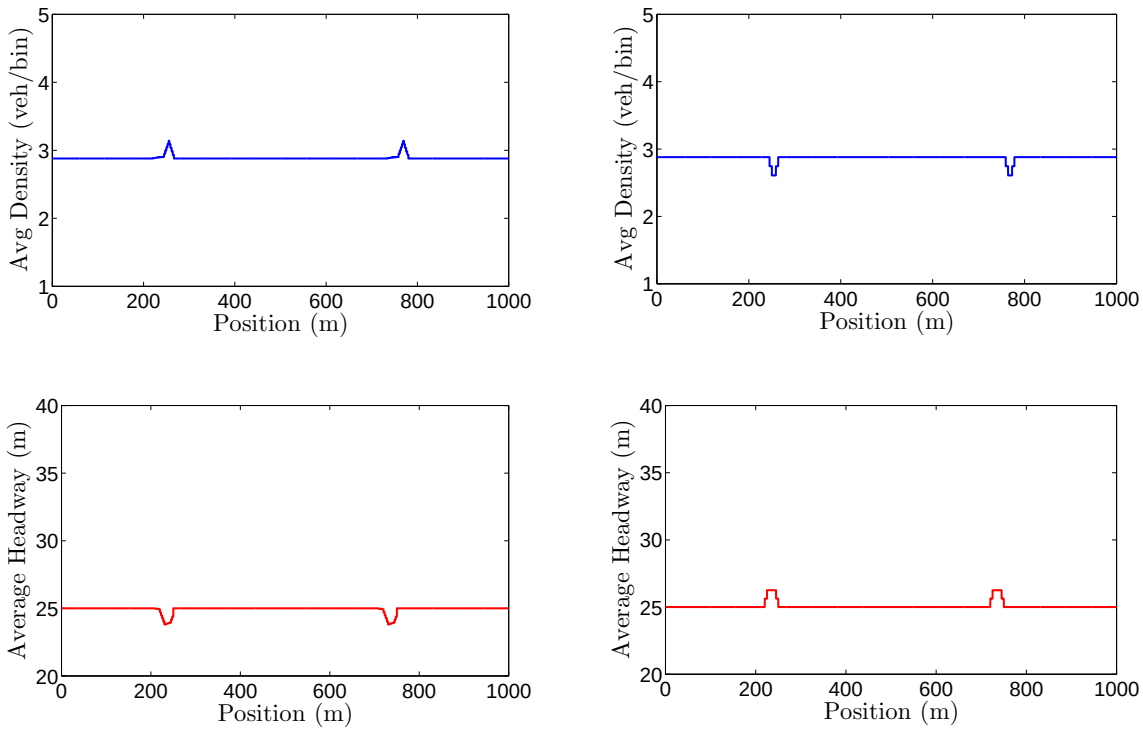

(a) Rounding Down

(b) Rounding Up

Figure 5.6: Density and average headway Basic simulations.

5.7.3 Model Network Analysis

To examine whether such characteristic spikes and dips continue to occur in more realistic settings, a simulation run was performed on the Model Network of Figure 5.4. Although density measurements were taken at every point of the network, the Control Network results have shown that only the transition points from CF→CA links will be expected to exhibit instabilities due to heterogeneous links. Hence attention is focused on the two sets of links that have this transition (circled in Figure 5.4). Figures 5.8a and 5.8b show the density plots for transitions A and B in the network respectively. Note that traffic interactions are far more complex than in the Control Network; hence, density fluctuates due to the traffic itself and so cannot be clearly correlated to the stability of the models. Nevertheless, the distinctive spike-or-dip fingerprint of the driver model instability re-occurs at the transition point similarly to the one observed in the Control Network. This shows that the density analyses on the simpler network actually apply to more re-

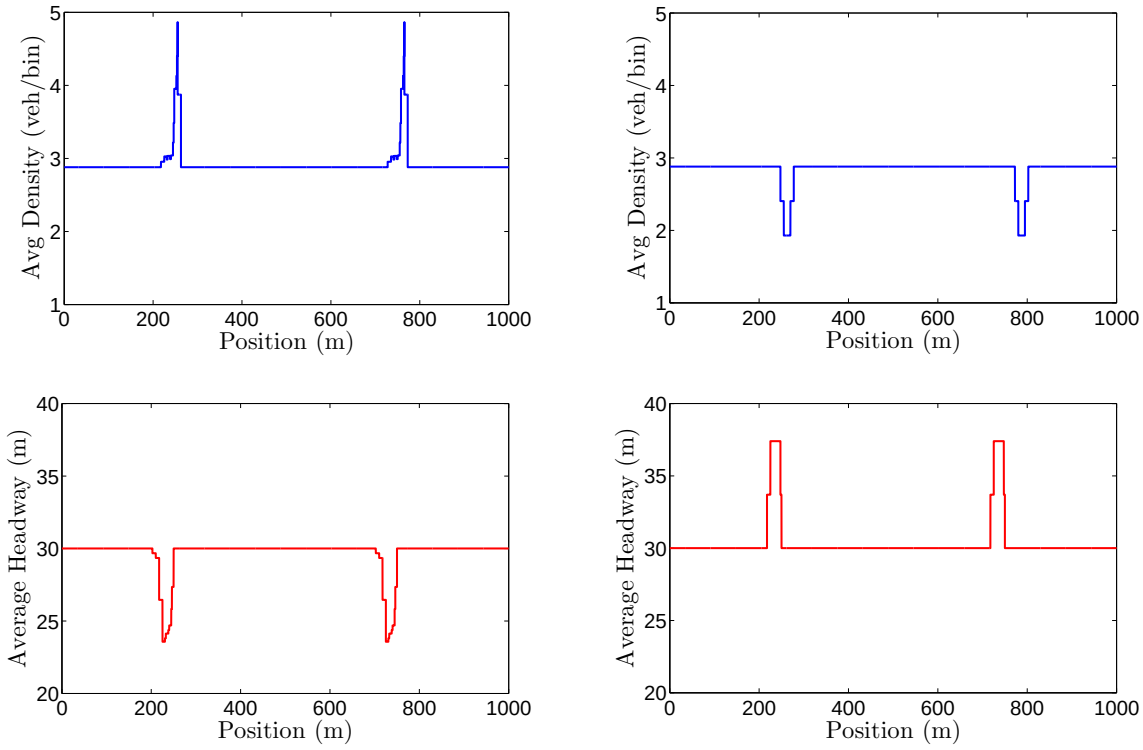

(a) Rounding Down

(b) Rounding Up

Figure 5.7: Density and average headway Large simulations.

alistic simulations. Moreover, it means that instabilities due to heterogeneous links can be identified through simple density measurements, and these spikes could potentially be identified and removed from overall density measurements to avoid contaminating further analyses of traffic flow density.

5.8 Discussion

As a result of the above analysis, a flaw in the stability of the IDM at the speed limit is identified and corrected. Subsequently it is shown that the model switch-over points will experience instabilities despite the stability of the individual driver models and, although careful choice of parameters can reduce the problem, it cannot be completely eliminated in practical road networks. However, the instability produces a significant 'fingerprint' effect on traffic density, and this fingerprint is readily identifiable using simple measures

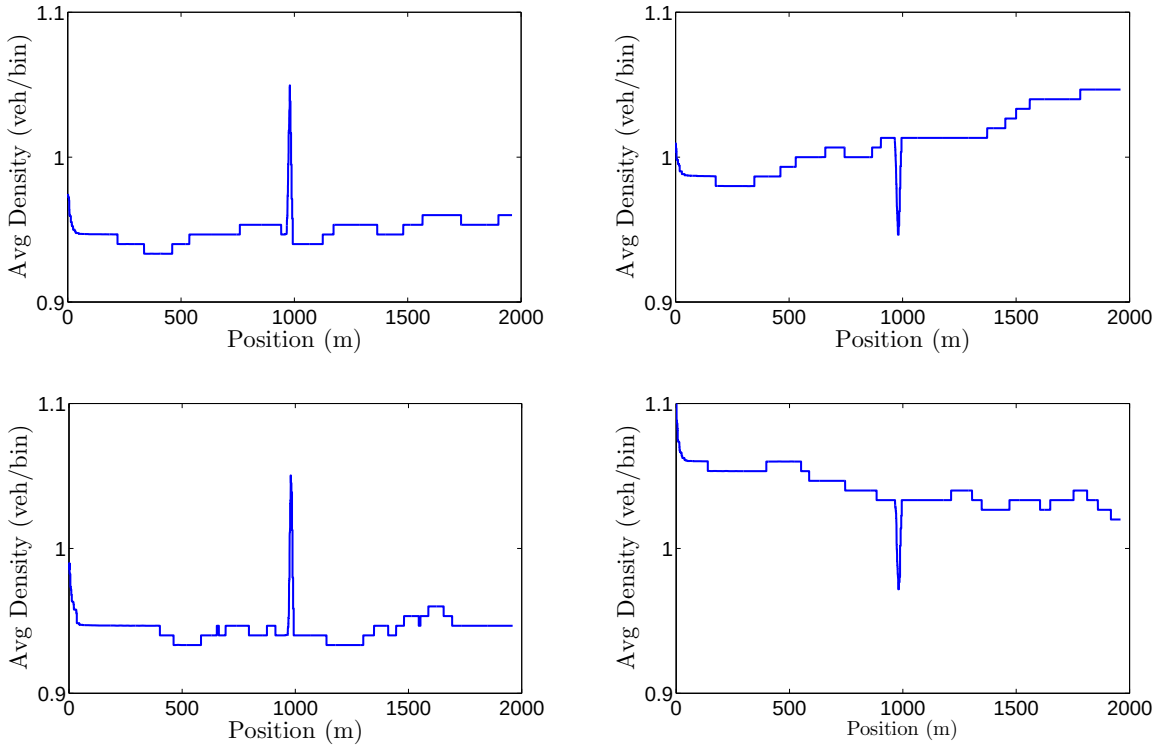

(a) Rounding Down

(b) Rounding Up

Figure 5.8: Density in Model Network simulations for CF→CA transitions.

of traffic flow even in realistic road networks.

As part of this investigation it was discovered that the IDM, whilst defined as a stable model, was actually unstable when vehicle velocities approached the nominal speed limit of v_0, thereby negating the assumption that the individual microscopic models being used are stable under normal driving conditions. To overcome this problem without introducing instabilities for vehicles travelling at lower speeds, a new variant of the IDM is devised. Rather than having v_0 act as a hard speed limit, it is instead re-interpreted to be an upper bound on velocity, and now v_0 has to be re-set correctly so that it is a function of an appropriate headway gap and the actual speed limit. An applicable headway gap usually follows the '2-second-rule', a safety margin generally applied to the road rules in the real world. In this form the IDM is stable at the designated speed limit since it has a buffer zone against v_0 which allows vehicles to converge to the speed limit without becoming unstable. The derived speed-limit-stable IDM is referred to as the SLS-IDM.

Whilst the SLS-IDM and N-S models are both stable individually, when they are put together as part of a heterogeneous network it is possible for instabilities to develop at the transition junctures where the models switch over from one to the other. This is potentially due to rounding issues, since rounding up or down creates different effects at these points. Whether it is better to round up or to round down or whether it makes no difference is investigated.

Instability at the transition points where the model switch over occurs will also produce a clearly identifiable 'fingerprint' which can be used to differentiate the instability caused by a model changeover versus the instability inherent in the models themselves.

5.9 Summary

This chapter has explored the effects on stability by mixing two different microscopic models together in a heterogeneous traffic simulation — the IDM and the N-S cellular automata. The IDM is shown to be unstable near the nominal speed limit v_0 and a variant, the SLS-IDM, is proposed to correct this flaw without affecting the behaviour of the IDM at lower speeds. Using the individually stable SLS-IDM and N-S algorithms, simulations are run on two heterogeneous traffic networks to examine the effects on mixing different microscopic models within the same system. Issues are found to arise due to the rounding errors induced by the transition from the continuous-space SLS-IDM to the discrete-space N-S. Although both rounding up and rounding down cause effects on density and headway, it is concluded that rounding up is the better choice since it avoids causing sudden downstream 'emergency' braking effects on the following vehicles. Fortunately, the individual stability of the models dampens down the instabilities and ensures that they do not propagate far. In addition, it is found that a signature 'fingerprint' of the instability is detectable in simple measures of density, and this fingerprint continues to be evident in a more realistic road network containing multi-way junctions and varying speed limits. Future work in heterogeneous traffic network simulations could use such a signature to identify density changes due to model transitions and potentially remove these spurious fluctuations from the density output.

Chapter 6

Conclusions and Further Study

6.1 Conclusions

This thesis has studied the behaviour of microscopic traffic models under a variety of novel conditions not previously considered in the literature. The overall objective was to investigate how well the models represent real human driver behaviour and whether the density (and thus traffic flow) values produced by mixing different types of microscopic models remains usable. This is important since density and flow measurements derived from simulations form the basis of higher level traffic studies such as congestion analysis and 'what-if' scenarios examining the effects of changes in traffic conditions on traffic flow. Microscopic models that do not behave like human drivers will provide a questionable basis for any conclusions drawn from the traffic flow measurements of simulations that use these models, but little work has been performed in the past to examine the empirical behaviour of such models in urban settings. In addition, whilst mixing different model types in the same road network has the benefit of being able to select the most useful model for each section of road, this mixing is likely to have undesirable anomalies on density measurements, particularly near the transitions between models. It is thus important to isolate these anomalies and characterise them in order to be able to take their effect into account when conducting higher level analyses.

The simulation system supporting this research, described in Chapter 3, has been made flexible so that both continuous and discrete microscopic models can be run, either individually or in tandem, with the network being adaptable to different configurations as required. This is achieved by using simple constructs for the roads and various types of intersections, so that these can easily be interchanged as necessary. Since the driver models do not recognise intersections, the system that was developed also incorporates short-term route plans for each vehicle so that all traffic obeys the road rules at junctions, for example giving way to oncoming vehicles in give-way situations, and collisions are avoided.

In Chapter 4 a detailed empirical comparison of the performance of four common car following microscopic driver models was performed, evaluating each model against the others as well as with respect to GPS data captured from human drivers. The comparison was specifically aimed at examining the behaviour of the driver models in typical everyday urban traffic scenarios, and was concerned with identifying the situations where each model reacts in an unreasonable manner. The poorest performer was the Optimal Velocity Model (OVM), the earliest and also the simplest model of the four models tested. The Full Velocity Difference Model (FVDM) and Full Velocity and Acceleration Difference Model (FVADM) add in factors to consider velocity difference (FVDM and FVADM) as well as acceleration difference (FVADM), and this improves the performance in some instances. Nevertheless, there were other cases where the extra information resulted in over-reactions, especially with the FVADM's inclusion of an acceleration difference term. The final model, the Intelligent Driver Model (IDM), achieved the most realistic results in all of the scenarios studied except for one, where it did not respond as expected. The case highlighted the inclination for the IDM to be quite comfortable with a relatively small headway, and if the headway was larger, it would accelerate accordingly to close the gap before determining its next action, which would be dependant on the leading vehicle.

Given its effective performance, the IDM was chosen for further experiments. Chapter 5 showed that the IDM is in fact an unstable model when vehicles are at or near the speed limit and all vehicles have a finite headway. The issue was traced to the IDM's confusion of the desired velocity with the speed limit, and a solution has been proposed to address this issue by focusing instead on a desired headway based on the well-known 'two second rule' for the distance in following another vehicle. An upper bound is then calculated such that the speed limit is able to be reached at this desired headway, rather than only being approached as headway approaches infinity.

From this basis, density within a mixed continuous microscopic / discrete microscopic hybrid (or heterogeneous) road network was examined, using the IDM and Nagel-Schreckenberg (N-S) algorithms as the respective models. The focus was on detecting any anomalies in the densities (and thus flows) generated by the system. This has been achieved by carefully building a circuit network where all other factors aside from model switch-over are controlled such that density should theoretically be uniform across the entire road network. A clear density fluctuation was then identified that occurs at the transition point where the models meet, with a predictable location and a distinctive 'dip-and-spike' profile, or signature. It is suggested that when analysing the density and flow measurements in these

types of heterogeneous networks, the distinctive signature will need to be recognised and disregarded since it is related to the model switch over point rather than a fundamental feature of the traffic itself.

6.2 Further Studies

There are several directions along which the research in this thesis can be taken forward. One such area is in expanding the empirical analysis of microscopic driver models in Chapter 4 to include a wider variety of scenarios when comparing the model behaviours against GPS data captured from human drivers. The aim would be to instrument two vehicles with GPS devices where one vehicle follows the other whilst performing multiple instances of specific scenarios that involve vehicle interactions. Examples would include the behaviour of the following vehicle when accelerating from a standstill with a lead vehicle in front, or reactions of the following vehicle to fast and slow changes in the leading vehicle's speed. With both vehicles capturing GPS data, the driver models can be provided with all relevant data including the velocity and the acceleration of both vehicles in order to be able to compare the velocity curve produced by the model against those of human drivers. However, several practical difficulties would need to be overcome, including the need to synchronise capture timings of the GPS data, accurately estimate the initial headway (subsequent headways would be a consequence of the measured velocity of the lead vehicle and the velocity decisions made by the driver model for the following vehicle) and to define the start and end times of each test scenario out of the ongoing stream of GPS data.

Other areas of potential further work revolve around the open issues in handling the density fluctuations identified in Chapter 5 caused by the transition from a continuous car-following microscopic model to a discrete cellular automata microscopic driver model in a heterogeneous road network. The density anomaly itself is quite distinctive and follows a clear dip-and-spike characteristic, and this anomaly was shown to manifest even in a realistic road network. Whilst the location of the fluctuation is predictable and thus that position could be disregarded when using density measurements to consider issues such as congestion improvement, better approaches should also be investigated. Specifically, it may be feasible to overlap the two models to cover the area of fluctuation and only use the density measurements of the incoming car-following model in this range. This is a similar approach to that used in macroscopic / microscopic heterogeneous networks,

and would give the succeeding cellular automata model time to 'settle' its density values before becoming the source of density information for higher level analysis. Issues here would be to define precisely how long the overlap range must be in order to provide a smooth handover. Another approach would be to take a signal processing approach and use the density fluctuation's characteristic dip-and-spike signature to suppress its effect on the density 'signal', somewhat similar to noise cancellation. The difficulty with this approach is that the amplitude of the fluctuation depends on the number of vehicles passing through that transition point, hence the precise amount of 'noise' to be cancelled is difficult to determine.

Bibliography

Ahn, S. and Vadlamani, S. (2010). Driver characteristics and their impact on traffic hysteresis and stop-and-go oscillations. In *Presentation at the Summer Meeting of the Transportation Research Board*.

Ahn, S., Cassidy, M., and J, L. (2004). Verification of a simplified car-following theory. *Transportation Research Part B*, **38**(5), 431–440.

Algers, S., Bernauer, E., Boero, M., Breheret, L., Di Taranto, C., Dougherty, M., Fox, K., and Gabard, J. (1997). *Review of micro-simulation models*.

Aw, A. and Rascle, M. (2000). Resurrection of "second order" models of traffic flow. *SIAM Journal of Applied Mathematics*, **60**(3), 916–938.

Aw, A., Klar, A., Rascle, M., and Materne, T. (2002). Derivation of continuum traffic flow models from microscopic follow-the-leader models. *SIAM Journal of Applied Mathematics*, **63**, 259–278.

Bagnerini, P. and Rascle, M. (2003). A multiclass homogenized hyperbolic model of traffic flow. *SIAM Journal on Mathematical Analysis*, **35**, 949–973.

Bando, M., Hasebe, K., Nakayama, A., Shibata, A., and Sugiyama, Y. (1995). Dynamical model of traffic congestion and numerical simulation. *Physical Review E*, **51**(2), 1035–1042.

Bando, M., Hasebe, K., Nakanishi, K., and Nakayama, A. (1998). Analysis of optimal velocity model with explicit delay. *Physical Review E*, **58**(5), 5429–5435.

Barceló, J., Ferrer, L., Garcia, D., Florian, M., and Le Saux, E. (1998). *Parallelization of microscopic traffic simulation for ATT systems*. Kluwer Academic Publishers.

Barceló, J., Casas, J., Garcia, D., and Perarnau, J. (2005). Methodological notes on combining macro, meso and micro models for transportation analysis. In *Traffic Modeling Workshop: Simulation Models from the Labs to the Trenches, Sedona, Arizona*.

Bellemans, T., de Schutter, B., and de Moor, B. (2002). Models for traffic control. Technical report.

Bellemans, T., de Schutter, B., and de Moor, B. (2006). Model predictive control for ramp metering of motorway traffic: A case study. *Control Engineering Practice*, **14**, 757–767.

Bevrani, K. and Chung, E. (2011). Car following model improvement for traffic safety metrics reproduction. In *Proceedings of Australasian Transport Research Forum*.

Bevrani, K., Chung, E., and Miska, M. (2012). Evaluation of the GHR car following model for traffic safety studies. In *Proceedings of the 25th ARRB Conference, ARRB Group Ltd*, pages 1–11.

Biham, O., Middleton, A., and Levine, D. (1992). Self-organization and a dynamical transition in traffic-flow models. *Physical Review A*, **46**(10).

Bloomberg, L. and Dale, J. (2000). Comparison of VISSIM and CORSIM traffic simulation models on a congested network. *Transportation Research Record: Journal of the Transportation Research Board*, **1 727**, 52–60.

Bourrel, E. and Lesort, J. (2003). Mixing microscopic and macroscopic representations of traffic flow: Hybrid model based on Lighthill-Whitham-Richards theory. *Transportation Research Record: Journal of the Transportation Research Board*, **1852**, 193–200.

Brackstone, M. and McDonald, M. (1999). Car-following: A historical review. *Transportation Research Part F: Traffic Psychology and Behaviour*, **2**, 181–196.

Burghout, W. (2004). *Hybrid microscopic-mesoscopic traffic simulation*. Ph.D. thesis, Royal Institute of Technology.

Burghout, W., Kotsopoulos, H., and Andrasson, I. (2005). Hybrid mesoscopic-microscopic traffic simulation. *Transportation Research Record: Journal of the Transportation Research Board*, **1934**, 218–255.

Burzyńsky, M. and Kosińksi, W. (2009). Two-lane discrete traffic flow model for highway traffic. In *Proceedings of XI International PhD Workshop*.

Chakroborty, P. and Kikuchi, S. (1999). Evaluation of the general motors based car-following models and a proposed fuzzy inference model. *Transportation Research Part C: Emerging Technologies*, **7**, 209–235.

Chakroborty, P. and Kikuchi, S. (2003). Calibrating the membership functions of the fuzzy inference system: instantiated by car-following data. *Transportation Research Part C: Emerging Technologies*, **11**, 91–119.

Chen, X., Li, R., Xie, W., and Shi, Q. (2009). Stabilization of traffic flow based on multi-anticipative intelligent driver model. In *Proceedings of the 12th International IEEE Conference on Intelligent Transportation Systems*, pages 1–6.

Chiabaut, N., Buisson, C., and Leclercq, L. (2009). Fundamental diagram estimation through passing rate measurements in congestion. *IEEE Transactions on Intelligent Transportation Systems*, **10**, 355–359.

Chiabaut, N., Leclercq, L., and Buisson, C. (2010). From heterogeneous drivers to macroscopic patterns in congestion. *Transportation Research Part B: Methodological*, **44**, 299–308.

Cristiani, E., Piccoli, B., and Tosin, A. (2012a). A first macroscopic-microscopic pedestrian model: Results in the case of a unidirectional flow. In *Transportation Research Board, Transportation Research Board Annual Meeting 2012*.

Cristiani, E., Piccoli, B., and Tosin, A. (2012b). How can macroscopic models reveal self-organization in traffic flow? In *Proceedings of the 51st IEEE Conference on Decision and Control*, pages 6989–6994.

Daganzo, C. (1995). Requiem for second-order fluid with approximation to traffic flow. *Transportation Research Part B: Methodological*, **29**, 277–286.

Daganzo, C. (2007). Urban gridlock: Macroscopic modeling and mitigation approaches. *Transportation Research Part B: Methodological*, **41**, 49–62.

Daganzo, C., Lin, W., and del Castillo, J. (1997). A simple physical principle for the simulation of freeways with special lanes and priority vehicles. *Transportation Research Part B: Methodological*, **31**, 103–125.

Daganzo, C., Gayah, V., and Gonzales, E. (2011). Macroscopic relations of urban traffic variables: Bifurcations, multivaluedness and instability. *Transportation Research Part B: Methodological*, **45**, 278–288.

Davis, L. (2003). Modifications of the optimal velocity traffic model to include delay due to driver reaction time. *Physica A: Statistical Mechanics and its Applications*, **319**, 557–567.

Davis, L. (2004). Multilane simulations of traffic phases. *Physical Review E*, **69**.

del Castillo, J. (2012). Three new models for the flowdensity relationship: Derivation and testing for freeway and urban data. *Transportmetrica*, **8**, 443–465.

Donat, R. and Mulet, P. (2008). Characteristic-based schemes for multi-class Lighthill-Whitham-Richards traffic models. *Journal of Scientific Computing*, **37**, 233–250.

D'Souza, R. (2005). Coexisting phases and lattice dependence of a cellular automaton model for traffic flow. *Physical Review E*, **71**.

Esser, J. and Schreckenberg, M. (1997). Microscopic simulation of urban traffic based on cellular automata. *International Journal of Modern Physics C*, **8**(5), 1025–1036.

Flötteröd, G. and Rohde, J. (2011). Operational macroscopic modeling of complex urban road intersections. *Transportation Research Part B: Methodological*, **45**, 903–922.

Gaididei, Y., Berkemer, R., Caputo, J., Christiansen, P., Kawamoto, A., Shiga, T., Sorensen, M., and Starke, J. (2009). Analytical solutions of jam pattern formation on a ring for a class of optimal velocity traffic models. *New Journal of Physics*, **11**.

Gao, K., Jiang, R., Hu, S.-X., Wang, B.-H., and Wu, Q.-S. (2007). Perceptual thresholds in car following a recent comparison of recent measurements with earlier results. *Physical Review E*, **76**.

Gao, Y. (2008). *Calibration and comparison of the VISSIM and INTEGRATION microscopic simulation models*. Ph.D. thesis, Faculty of the Virginia Polytechnic Institute and State University, Blacksburg, Virginia.

Gayah, V. and Daganzo, C. (2011). Clockwise hysteresis loops in the macroscopic fundamental diagram: An effect of network instability. *Transportation Research Part B: Methodological*, **45**, 643–655.

Gazis, D., Herman, R., and Potts, R. (1961). Nonlinear follow-the-leader models of traffic flow. *Operations Research*, **9**, 545–567.

Ge, H., Cheng, R., and Li, Z. (2008). Two velocity difference model for a car following theory. *Physica A: Statistical Mechanics and its Applications*, **387**, 5239–5245.

Geroliminis, N. and Sun, J. (2011). Properties of a well-defined macroscopic fundamental diagram for urban traffic. *Transportation Research Part B: Methodological*, **45**, 605–617.

Gipps, P. (1981). A behavioural car-following model for computer simulation. *Transportation Research Part B: Methodological*, **15**, 105–111.

Greenshields, B. (1934). The photographic method of studying traffic behavior. In *Proceedings of the 13th Annual Meeting of the Highway Research Board*, volume 13, pages 382–399.

Habel, L. and Schreckenberg, M. (2014). Asymmetric lane change rules for a microscopic highway traffic model. *Cellular Automata, Lecture Notes in Computer Science*, **8751**, 620–629.

Hae, A. (2009). Examining and improving the limitations of Gazis-Herman-Rothery car following model. In *In Salford Postgraduate Annual Research Conference*.

Hawas, Y. (2007). A microscopic simulation model for incident modeling in urban networks. *Transportation Planning and Technology*, **30**, 289–309.

Hawas, Y. (2009). A multi-stage procedure for validating microscopic traffic simulation models. *Transportation Planning and Technology*, **32**, 71–91.

He, Z. and Sun, W. (2013). A microscopic simulation model for incident modeling in urban networks. *Acta Physica Sinica*, **62**.

Hegyi, A., de Schutter, B., and Hellendoorn, H. (2005). Model predictive control for optimal coordination of ramp metering and variable speed limits. *Transportation Research Part C: Emerging Technologies*, **13**, 185–209.

Helbing, D. (1995). Theoretical foundations of macroscopic traffic models. *Physica A: Statistical Mechanics and its Applications*, **219**, 375–390.

Helbing, D. (1996). Gas-kinetic derivation of Navier-Stokes-like traffic equations. *Physical Review E*, **53**.

Helbing, D. (2001). Traffic and related self-driven many particle systems. *Reviews of Modern Physics*, **73**.

Helbing, D. (2009). Derivation of a fundamental diagram for urban traffic flow. *The European Physical Journal B*, **70**, 229–241.

Helbing, D. and Molnár, P. (1995). Social force model for pedestrian dynamics. *Physical Review E*, **51**.

Helbing, D. and Tilch, B. (1997). Modeling multi-lane traffic flow with queuing effects. *Physica A: Statistical Mechanics and its Applications*, **242**, 175–194.

Helbing, D. and Tilch, B. (1998). Generalized force model of traffic dynamics. *Physical Review E*, **58**, 133–138.

Helbing, D. and Tilch, B. (1999). Cellular automata simulating experimental properties of traffic flow. *Physical Review E*, **59**.

Helbing, D., Hennecke, A., Shvetsov, V., and Treiber, M. (2002). Micro- and macro-simulation of freeway traffic. *Mathematical and Computer Modelling*, **35**, 517–547.

Hennecke, A., Treiber, M., and Helbing, D. (2000). *Macroscopic simulation of open systems and micro-macro link*. Springer.

Herty, M. and Moutari, S. (2009). A macro-kinetic hybrid model for traffic flow on road networks. *Computational Methods in Applied Mathematics*, **9**, 238–252.

Holland, E. (1998). A generalized stability criterion for motorway traffic. *Transportation Research Part B: Methodological*, **32**, 141–154.

Hoogendoorn, R., Hoogendoorn, S., van Arem, B., and Brookhuis, K. (2013). Microscopic traffic flow properties in emergency situations. *Transportation Research Board*, **2391**, 124–132.

Hoogendoorn, S. (1999). *Multiclass continuum modelling of multilane traffic flow*. Ph.D. thesis, Delft University of Technology, TRAIL Research School, Delft, The Netherlands.

Hoogendoorn, S. and Bovy, P. (2001). State-of-the-art vehicular traffic flow modelling. *Journal of Systems and Control Engineering*, **215**, 283–303.

Hoogendoorn, S. and Hoogendoorn, R. (2010). Calibration of microscopic traffic-flow models using multiple data sources. *Philosophical Transactions of the Royal Society A, Mathematical Physical and Engineering Sciences*, **368**, 4497–4517.

Hoogendoorn, S., Ossen, S., and Gorte, B. (2006). Inter-driver differences in car following: A vehicle trajectory based study. *Transportation Research Board*, **1965**, 121–129.

Hoogendoorn, S., van Lint, J., and Knoop, V. (2009). *Dynamic first-order modeling of phase-transition probabilities*. Springer Berlin Heidelberg.

Horni, A., Scott, D., Balmer, M., and Axhausen, K. (2009). Location choice modeling for shopping and leisure activities with MATSim. *Transportation Research Board*, **2135**, 87–95.

Jabari, S. and HX, L. (2012). A stochastic model of traffic flow: Theoretical foundations. *Transportation Research Part B: Methodological*, **46**, 156–174.

Jabari, S. and HX, L. (2013). A stochastic model of traffic flow: Gaussian approximation and estimation. *Transportation Research Part B: Methodological*, **47**, 15–41.

Jia, N. and Ma, S. (2009). Analytical investigation of the open boundary conditions in the Nagel-Schreckenberg model. *Physical Review E*, **79**.

Jiang, R., Wu, Q., and Zhu, Z. (2001). Full velocity difference model for a car-following theory. *Physical Review E*, **64**.

Jin, W. (2010). A kinematic wave theory of lane-changing traffic flow. *Transportation Research Part B: Methodological*, **44**, 1001–1021.

Jin, W. (2013). A multi-commodity Lighthill-Whitham-Richards model of lane-changing traffic flow. *Transportation Research Part B: Methodological*, **57**, 361–377.

Kari, J. (2005). Theory of cellular automata: A survey. *Theoretical Computer Science*, **334**, 3–33.

Kerner, B. (2009). *Introduction to modern traffic flow theory and control: The long road to three-phase traffic theory*. Springer Berlin Heidelberg.

Kerner, B. (2013). Criticism of generally accepted fundamentals and methodologies of traffic and transportation theory: A brief review. *Physica A: Statistical Mechanics and its Applications*, **392**, 5261–5282.

Kerner, B. and Klenov, S. (2002). A microscopic model for phase transitions in traffic flow. *Journal of Physics A: Mathematical and General*, **35**.

Kerner, B. and Klenov, S. (2006). Deterministic microscopic three-phase traffic flow models. *Journal of Physics A: Mathematical and General*, **39**.

Kerner, B. and Rehborn, H. (1996). Experimental features and characteristics of traffic jams. *Physical Review E*, **53**, 1297–1300.

Kerner, B., Klenov, S., and Wolf, D. (2002). Cellular automata approach to three-phase traffic theory. *Journal of Physics A: Mathematical and General*, **35**.

Kerner, B., Klenov, S., and Schreckenberg, M. (2011). Simple cellular automaton model for traffic breakdown, highway capacity, and synchronized flow. *Physical Review E*, **84**.

Kesting, A. and Treiber, M. (2008). How reaction time, update time, and adaptation time influence the stability of traffic flow. *Computer-Aided Civil and Infrastructure Engineering*, **23**, 125–137.

Kesting, A., Treiber, M., Schnhof, M., and Helbing, D. (2008). Adaptive cruise control design for active congestion avoidance. *Transportation Research Part C: Emerging Technologies*, **16**, 668–683.

Keyvan-Ekbatani, M., Kouvelas, A., Papamichail, I., and Papageourgiou, M. (2012). Exploiting the fundamental diagram of urban networks for feedback-based gating. *Transportation Research Part B: Methodological*, **46**, 1393–1403.

Khodayari, A., Kazemi, R., Ghaffari, A., and Braunsting, R. (2011). Design of an improved fuzzy logic based model for prediction of car following behavior. In *Proceedings of IEEE International Conference on Mechatronics (ICM)*, pages 200–205.

Kikuchi, S. and Chakroborty, P. (1992). Car-following model based on fuzzy inference system. *Transportation Research Board*, **1365**, 82–91.

Klar, A., Greenberg, J., and Rascle, M. (20003). Routing strategies based on macroscopic fundamental diagram. *SIAM Journal on Applied Mathematics*, **63**, 818–833.

Knoop, V., Hoogendoorn, S., and van Lint, J. (2012). Routing strategies based on macroscopic fundamental diagram. *Transportation Research Record: Journal of the Transportation Research Board*, **2315**, 1–10.

Knospe, W., Santen, L., Schadschneider, A., and Schreckenberg, M. (2000). Towards a realistic microscopic description of highway traffic. *Journal of Physics A: Mathematical and General*, **33**.

Knospe, W., Santen, L., Schadschneider, A., and Schreckenberg, M. (2004). Empirical test for cellular automaton models of traffic flow. *Physical Review E*, **70**.

Kokubo, S., Tanimoto, J., and Hagishima, A. (2011). A new cellular automata model including a decelerating damping effect to reproduce Kerners three-phase theory. *Physica A: Statistical Mechanics and its Applications*, **390**, 561–568.

Kometani, E. and Sasaki, T. (1959). Dynamic behaviour of traffic with a non-linear spacing-speed relationship. In *Proceedings of the Symposium on Theory of Traffic Flow, Research Laboratories, General Motors*, pages 105–119.

Kotsialos, A., Papageorgiou, M., Diakaki, C., and Pavlis, Y. (2002). Traffic flow modeling of large-scale motorway networks using the macroscopic modeling tool METANET. *IEEE Transactions on Intelligent Transportation Systems*, **4**, 282–292.

Kumamoto, H., Nishi, K., Tenmoku, K., and Shimoura, H. (1995). Rule based cognitive animation simulator for current lane and lane change drivers. In *Proceedings of the Second World Congress on ATT*, volume 4, pages 1746–1752.

Laagland, J. (2005). How to model aggressive behavior in traffic simulation. In *3rd Twente Student Conference on IT*.

Lattanzio, C. and Piccoli, B. (2010). Coupling of microscopic and macroscopic traffic models at boundaries. *Mathematical Models and Methods Applied Sciences*, **20**, 2349–2370.

Laval, J. and C, D. (2006). Lane-changing in traffic streams. *Transportation Research Part B: Methodological*, **40**, 251–264.

Laval, J. and Leclercq, L. (2010). A mechanism to describe the formation and propagation of stop-and-go waves in congested freeway traffic. *Philisophical Transactions A*, **1928**, 4519–4541.

Lebacque, J. (2002). A two phase extension of the lwr model based on the boundedness of traffic acceleration. In *Proceedings of the 15th International Symposium on Transportation and Traffic Theory*, pages 697–718.

Leclercq, L. (2007). A new numerical scheme for bounding acceleration in the LWR model. In *Proceedings of the 4th IMA International Conference on Mathematics in Transport*, pages 279–292.

Leclercq, L., Laval, J., and Chevallier, E. (2007). The lagrangian coordinates and what it means for first order traffic flow models. In *Transportation and Traffic Theory 2007*, pages 735–753.

Leisch, J. (1979). A new technique for design and analysis of weaving sections on freeways. *Insitute of Transportation Engineers Journal*, **49**, 26–29.

Lenz, H., Wagner, C., and Sollacher, R. (1999). Multi-anticipative car-following model. *The European Physical Journal B - Condensed Matter and Complex Systems*, **7**, 331–335.

Li, J., Chen, Q., Wang, H., and Ni, D. (2012). Analysis of LWR model with fundamental diagram subject to uncertainties. *Transportmetrica*, **8**, 387–405.

Li, Z. and Zang, R. (2013). An extended non-lane-based optimal velocity model with dynamic collaboration. *Mathematical Problems in Engineering*, **2013**.

Lighthill, M. and Whitham, G. (1955). On kinematic waves. II. A theory of traffic flow on long crowded roads. *Proceedings of the Royal Society of London, Series A*, **229**, 317–345.

Lu, Y., Wong, S., Zhang, M., Shu, C., and Chen, W. (2008). Explicit construction of entropy solutions for the Lighthill-Whitham-Richards traffic flow model with a piecewise quadratic flowdensity relationship. *Transportation Research Part B: Methodological*, **42**, 355–372.

Marsden, G., McDonald, M., and Brackstone, M. (2001). Towards an understanding of adaptive cruise control. *Transportation Research Part C: Emerging Technologies*, **9**, 33–51.

Mathew, T. and Radhakrishnan, P. (2010). Calibration of microsimulation models for nonlane-based heterogeneous traffic at signalized intersections. *Journal of Urban Planning and Development, Special Issue: Challenges in Transportation Planning for Asian Cities*, **136**, 59–66.

Meng, Q. and Weng, J. (2011). An improved cellular automata model for heterogeneous work zone traffic. *Transportation Research Part C: Emerging Technologies*, **19**, 1263–1275.

Messmer, A. and Papageorgiou, M. (1990). Metanet: A macroscopic simulation program for motorway networks. *Traffic Engineering and Control*, **31**, 466–470.

Mo, Y., He, H., and Xue, Y. (2008). Effect of multi-velocity-difference in traffic flow. *Chinese Physics B*, **17**, 4446–4450.

Moutari, S. and Rascle, M. (2007). A hybrid Lagrangian model based on the Aw-Rascle traffic flow model. *SIAM Journal of Applied Mathematics*, **68**(2), 413–436.

Nagel, K. and Schreckenberg, M. (1992). A cellular automaton model for freeway traffic. *Journal de Physique I*, **2**, 2221–2229.

Nagel, K., Stretz, P., Pieck, M., Donnelly, R., and Barrett, C. (1997). TRANSIMS traffic flow characteristics. *Los Alamos Unclassified Report (LA-UR) 97-3530, Los Alamos National Laboratory*.

Nagel, K., Wolf, D., Wagner, P., and P, S. (1998). Two-lane traffic rules for cellular automata: A systematic approach. *Physical Review E*, **58**.

Newell, G. (1961). Nonlinear effects in the dynamics of car following. *Operations Research*, **9**, 209–229.

Newell, G. (1993). A simplified theory of kinematic waves in highway traffic, part I: General theory. *Transportation Research Part B: Methodological*, **27**, 281–287.

Newell, G. (2002). A simplified car-following theory: a lower order model. *Transportation Research Part B: Methodological*, **36**, 195–205.

Newell, G. (2011). Multiscale modeling of traffic flow. *Mathematica Aeterna*, **1**, 27–54.

Olstam, J. (2004). Comparison of car-following models. *Swedish National Road and Transport Research Institute*.

Olstam, J. (2005). *A model for simulation and generation of surrounding vehicles in driving simulators*. Ph.D. thesis, Department of Science and Technology, Linköpings Universiteit, Norrköping, Sweden.

Ossen, S. and Hoogendoorn, S. (2006). Multi-anticipation and heterogeneity in car-following empirics and a first exploration of their implications. In *Proceedings of IEEE Intelligent Transportation Systems (ITSC 2006)*, pages 1615–1620.

Pandey, G., Rao, K., and Mohan, D. (2014). *A review of cellular automata model for heterogeneous traffic conditions*. Springer International Publishing.

Panwai, S. and Dia, H. (2005). Comparative evaluation of microscopic car-following behavior. *IEEE Transactions on Intelligent Transportation Systems*, **6**, 314–325.

Papageorgiou, G. (2007). Computer simulation for transportation planning and traffic management: A case study systems approach. In *Proceedings of the 6th WSEAS International Conference on Signal Processing, Robotics and Automation*, pages 236–241.

Papageorgiou, M. (1998). Some remarks on macroscopic traffic flow modelling. *Transportation Research A: Policy and Practice*, **32**, 323–329.

Papageorgiou, M., Posch, B., and Schmidt, G. (1983). Comparison of macroscopic models for control of freeway traffic. *Transportation Research B: Methodological*, **17**, 107–116.

Papageorgiou, M., Blosseville, J., and Hadj-Salem, H. (1990a). Modelling and real-time control of traffic flow on the southern part of Boulevard Peripherique in Paris: Part I: Modelling. *Transportation Research A: General*, **24**, 345–359.

Papageorgiou, M., Blosseville, J., and Hadj-Salem, H. (1990b). Modelling and real-time control of traffic flow on the southern part of Boulevard Peripherique in Paris: Part II: Coordinated on-ramp metering. *Transportation Research A: General*, **24**, 361–370.

Papageorgiou, M., Diakaki, C., Dinopoulou, V., and Kotsialos, A. (2003). Review of road traffic control strategies. In *Proceedings of IEEE*, volume 91, pages 2043–2067.

Papageorgiou, M., Kosmatopoulos, E., and Papamichail, I. (2008). Effects of variable speed limits on motorway traffic flow. *Transportation Research Record: Journal of the Transportation Research Board*, **2047**, 37–48.

Peng, G., Sun, D., and He, H. (1971). Models of freeway traffic and control. *Mathematical Models of Public Systems*, **1**, 51–61.

Peng, G., Sun, D., and He, H. (2008). Two-car following model of traffic flow and numerical simulation. *Acta Physica Sinica*, **57**, 7541–7546.

Prevedouros, P. and Wang, Y. (1999). Simulation of large freeway and arterial network with CORSIM, INTEGRATION, and WATSim. *Transportation Research Record: Journal of the Transportation Research Board*, **1678**, 197–207.

Prigogine, I. and Andrews, F. (1960). A Boltzmann-like approach for traffic flow. *Operations Research*, **8**, 789–797.

Prigogine, I. and Andrews, F. (1961). A Boltzmann-like approach to the statistical theory of traffic flow. In R. Herman, editor, *Proceedings of Theory of Traffic Flow 1959*, pages 158–164. Elsevier.

Pueboobpaphan, R. and van Arem, B. (2010). Driver and vehicle characteristics and platoon and traffic flow stability. *Transportation Research Record: Journal of the Transportation Research Board*, **2189**, 89–97.

Rakha, H. (2003). Comparison and calibration of FRESIM and INTEGRATION steady-state car-following behavior. *Transportation Research Part A: Policy and Practice*, **37**, 1–27.

Rakha, H. and Crowther, B. (2002). Comparison of Greenshields, Pipes, and van Aerde car-following and traffic stream models. *Transportation Research Record: Journal of the Transportation Research Board*, **1802**, 248–262.

Ranjitkar, P., Nakatsuji, T., and Kawamura, A. (2005a). Car-following models: An experiment based benchmarking. *Journal of Eastern Asia Society for Transport Studies*, **6**, 1582–1596.

Ranjitkar, P., Nakatsuji, T., and Kawamura, A. (2005b). Experimental analysis of car-following dynamics and traffic stability. *Transportation Research Record: Journal of the Transportation Research Board*, **1934**, 22–32.

Richards, P. (1956). Shock waves on the highway. *Operations Research*, **4**, 42–51.

Roess, R. and Ulerio, J. (2000). Weaving area analysis in year 2000 highway capacity manual. *Transportation Research Record: Journal of the Transportation Research Board*, **1710**, 145–153.

Sawada, S. (2006). Optimal velocity model with relative velocity. *International Journal of Modern Physics C*, **17**, 65–73.

Schakel, W., van Arem, B., and Netten, B. (2010). Effects of Cooperative Adaptive Cruise Control on traffic flow stability. In *Proceedings of the 13th International IEEE Conference on Intelligent Transportation Systems (ITSC)*, pages 759–764.

Senin, P. (2008). Dynamic time warping algorithm review. Technical report.

Singh, A. (2006). Optimization and control of traffic flow networks. Master's thesis, Technischen Universität Kaiserslautern, Kaiserslautern.

Skabardonis, A. and Christofa, E. (2011). Evaluation of methodologies for the design and analysis of freeway weaving sections. In *Proceedings of the 1st International Conference on Access Management*.

Soria, I., Elefteriadou, L., and Kondyli, A. (2014). Assessment of car-following models by driver type and under different traffic, weather conditions using data from an instrumented vehicle. *Simulation Modelling Practice and Theory*, **40**, 208–220.

Stevanovic, J., Stevanovic, A., Martin, P., and Bauer, T. (2008). Stochastic optimization of traffic control and transit priority settings in VISSIM. *Transportation Research Part C: Emerging Technologies*, **16**, 332–349.

Tampere, C., van Arems, B., and Hoogendoor, S. (2003). Gas-kinetic traffic flow modeling including continuous driver behavior models. *Transportation Research Record: Journal of the Transportation Research Board*, **1852**, 231–238.

Tang, T., Huang, H., and Gao, Z. (2005). Stability of the car-following model on two lanes. *Physical Review E*, **72**.

Tang, T., Wang, Y., Yu, G., and Huang, H. (2012). A stochastic LWR model with consideration of the driver's individual property. *Communications in Theoretical Physics*, **58**.

Treiber, M. and Helbing, D. (1999). Macroscopic simulation of widely scattered synchronized traffic states. *Journal of Physics A: Mathematical and General*, **32**.

Treiber, M. and Kesting, A. (2012). Validation of traffic flow models with respect to the spatiotemporal evolution of congested traffic patterns. *Transportation Research Part C: Emerging Technologies*, **21**.

Treiber, M., Hennecke, A., and Helbing, D. (2000a). Congested traffic states in empirical observations and microscopic simulations. *Physical Review E*, **62**.

Treiber, M., Hennecke, A., and Helbing, D. (2000b). *Microscopic simulation of congested traffic*. Springer.

Treiber, M., Kesting, A., and Helbing, D. (2004). Multi-anticipative driving in microscopic traffic models. *arXiv:cond-mat/0404736v1 [cond-mat.soft]*.

Treiber, M., Kesting, A., and Helbing, D. (2006). Delays, inaccuracies and anticipation in microscopic traffic models. *Physica A: Statistical Mechanics and its Applications*, **360**, 71–88.

Treiber, M., Kesting, A., and Helbing, D. (2007). Influence of reaction times and anticipation on stability of vehicular traffic flow. *Transportation Research Record: Journal of the Transportation Research Board*, **1999**, 23–29.

Treiber, M., Kesting, A., and Helbing, D. (2010). Three-phase traffic theory and two-phase models with a fundamental diagram in the light of empirical stylized facts. *Transportation Research Part B: Methodological*, **44**, 983–1000.

van Aerde, M., Hellinga, B., Baker, M., and Rakha, H. (1996). INTEGRATION: An overview of traffic simulation features. In *Presentation at 1996 Transportation Research Board Anuual Meeting*.

van Arem, B., van Driel, C., and Visser, R. (2006). The impact of Cooperative Adaptive Cruise Control on traffic-flow characteristics. *IEEE Transactions on Intelligent Transportation Systems*, **7**.

van den Berg, M., Hegyi, A., De Schutter, B., and Hellendoorn, J. (2003). A macroscopic traffic flow model for integrated control of freeway and urban traffic networks. In *Proceedings of the 42nd IEEE Conference on Decision and Control*, volume 3, pages 2774–2779.

van den Berg, M., de Schutter, B., Hegyi, A., and Hellendoorn, J. (2004). Model predictive control for mixed urban and freeway networks. In *Proceedings of the 83rd Annual Meeting of the Transportation Research Board*.

van Wageningen-Kessels, F. (2013). *Multi-class continuum traffic flow models: Analysis and simulation methods*. Ph.D. thesis, Delft University of Technology, The Netherlands.

van Wageningen-Kessels, F., van Lint, H., Vuik, K., and Hoogendoorn, S. (2014). Genealogy of traffic flow models. *EURO Journal on Transporation and Logistics*.

Wang, Y., Papageorgiou, M., and Messmer, A. (2006). RENAISSANCE - A unified macroscopic model-based approach to real-time freeway network traffic surveillance. *Transportation Research Part C: Emerging Technologies*, **14**, 190–212.

Wiedemann, R. (1974). Simulation des strassenverkehrsflusses. In *Institute for Traffic Engineering*.

Wiedemann, R. and Reiter, U. (1992). Microscopic traffic simulation: The simulation system MISSION, background and actual state. In *Project ICARUS (V1052) Final Report*, volume 2.

Wilson, R. (2001). An analysis of Gipps's car-following model of highway traffic. *IMA Journal of Applied Mathematics*, **66**, 509–537.

Windover, J. and May, A. (1994). Revisions to level D methodology of analyzing freeway ramp weaving sections. *Transportation Research Record: Journal of the Transportation Research Board*, **1457**, 43–49.

Wolfram, S. (1986). *Theory and applications of cellular automata*. World Scientific.

Wong, G. and Wong, S. (2002). A multi-class traffic flow model an extension of LWR model with heterogeneous drivers. *Transportation Research Part A: Policy and Practice*, **36**, 827–841.

Xue, Y. (2003). A car-following model with stochastically considering the relative velocity in a traffic flow. *Acta Physica Sinica*, **52**, 2750–2756.

Yeldan, O., Colorni, A., Lue, A., and Rodaro, E. (2012). A stochastic continuous cellular automata traffic flow model with a multi-agent fuzzy system. *Procedia - Social and Behavioral Sciences, Special Issue: Proceedings of EWGT2012 - 15th Meeting of the EURO Working Group on Transportation, September 2012, Paris*, **54**, 1350–1359.

Yiaki, K., Satoh, J., Itakura, N., Honda, N., and Satoh, A. (1993). A fuzzy model for behavior of vehicles to analyze traffic congestion. In *Proceedings of the International Congress on Modelling and Simulation*.

Zegeer, J., Blogg, M., Nguyen, K., and Vandehey, M. (2008). Default values for highway capacity and level-of-service analyses. *Transportation Research Record: Journal of the Transportation Research Board*, **2071**, 35–43.

Zhan, B. (1997). Three fastest shortest path algorithms on real road networks: Data structures and procedures. *Procedia - Social and Behavioral Sciences, Special Issue: Proceedings of EWGT2012 - 15th Meeting of the EURO Working Group on Transportation, September 2012, Paris*, **1**, 70–82.

Zhang, Y. (2004). Systematic validation of a microscopic traffic simulation program. *Transportation Research Record: Journal of the Transportation Research Board*, **1876**, 112–120.

Zhao, X. and Gao, Z. (2005). A new car-following model: Full velocity and acceleration difference model. *The European Physical Journal B - Condensed Matter and Complex Systems*, **47**, 145–150.

Every reasonable effort has been made to acknowledge the owners of copyright material. I would be pleased to hear from any copyright owner who has been omitted or incorrectly acknowledged.